2017

Determination of Novel Metabolites of Therapeutic Agents used in the Treatment of Castration-Resistant Prostate Cancer

Mohammad Alyamani

DETERMINATION OF NOVEL METABOLITES OF THERAPEUTIC AGENTS USED IN THE TREATMENT OF CASTRATION-RESISTANT PROSTATE CANCER

MOHAMMAD ALYAMANI

Bachelor of Science in Chemistry

The University of Jordan

June 2000

Masters of Science in Chemistry

The University of Jordan

August 2004

Submitted in partial fulfillment of requirements for the degree

DOCTOR OF PHILOSOPHY IN CLINICAL AND BIOANALYTICAL CHEMISTRY

WITH SPECIALIZATION IN CELLULAR AND MOLECULAR MEDICINE

at the

CLEVELAND STATE UNIVERSITY

MARCH 2017

We hereby approve this dissertation for

Mohammad Mosleh Alyamani

Candidate for the Doctor of Philosophy in Clinical-Bioanalytical Chemistry degree for

the

Department of Chemistry

and the CLEVELAND STATE UNIVERSITY

College of Graduate Studies

_____

Dissertation Co-Chairperson, Dr. Nima Sharifi

_____

Department & Date

_____

Dissertation Co-Chairperson, Dr. David Anderson

_____

Department & Date

_____

Dissertation Committee Member, Dr. Yan Xu

_____

Department & Date

_____

Dissertation Committee Member, Dr. Baochuan Guo

_____

Department & Date

_____

Dissertation Committee Member, Dr. Girish Shukla

_____

Department & Date

Student's Date of Defense: March 9th 2017

DEDICATION

This work is dedicated to the memory of my parents. They believed that there would be a day when I achieve my dreams, and they supported me until their last day. This work is also dedicated to my siblings in Jordan. I also want to dedicate this work to my lovely wife, Dana and my four children, Yumna, Sultan, Alma, and Saif. You all motivated me and nothing would be accomplished without your support, patience, and encouragement.

I love you all.

ACKNOWLEDGMENTS

I would like to express my sincerest gratitude to all who have helped me throughout my magnificent journey.

First and foremost, this project was made possible because of the patients who decided to help humanity through participating in the clinical trials. So, our prayers and thoughts are with all cancer patients and their families.

No words can express how thankful and grateful I am to my mentor, Dr. Nima Sharifi. He was very kind to accept me as his graduate student and to be part of his great team. He introduced me to the cancer field that I dreamed of being part of, and was so supportive in helping me to attain my accomplishments and achievements. He gave me the space to think independently and encouraged me to do more. He was generous in his time to advise and guide me when I needed him. Thank you for your support and for all the efforts you made to make my journey a wonderful experience and memory.

A special thanks goes to my academic advisor, Dr. David Anderson, for his support and guidance. He introduced me to the clinical chemistry field through supporting my application to the AACC annual meeting. I wish to thank the members of my dissertation committee for their valuable time and suggestions to improve my research, Dr. Yan Xu, Dr. Baochun Guo, and Dr. Girish Shukla. I also want to thank the Department of Chemistry graduate advisor Dr. Michael Kalafatis for his efforts in helping me and supporting my graduation application. Many thanks go to the faculty, staff, and my colleagues in the chemistry department and in the Cellular and Molecular Specialization Program at CSU.

I wish to acknowledge the current and former members of the Sharifi lab, especially Dr. Zhenfei Li, with whom I worked closely and who taught me lot of techniques that helped me through my research. I also want to thank our lab managers, Marianne Petro and Michael Berk, for their efforts. Marianne provided all the logistics for this project. Michael helped and trained me in the mice experiments. I also want to thank the administrative staff in the Cancer Biology department at the Lerner Research Institute. Special thanks go to Cassandra Talerico for critical evaluation and helping in preparing my manuscripts.

I would like to thank our collaborators, Dr. Richard Auchus and Dr. Sunil Upadhyay, from University of Michigan Medical School for providing the metabolites. I also wish to acknowledge Dr. Mary-Ellen Taplin from Dana Farber Cancer Institute/ Harvard Medical School, Dr. Terence Friedlander from the University of California San Francisco Medical Center, and Dr. Caly Chien from Janssen Research & Development for providing the clinical samples. I would also acknowledge Dr. Paul Elson and Xuefei Jia who helped in the statistical analysis for the clinical data.

Finally, I wish to acknowledge Dr. Mohammad B. Zughul, Dr. Abeer Al-Bawab, and Dr. Suhair Al-Nimry from Jordan who provided the recommendation letters and supported my application to CSU.

DETERMINATION OF NOVEL METABOLITES OF THERAPEUTIC AGENTS USED IN THE TREATMENT OF CASTRATION-RESISTANT PROSTATE CANCER

MOHAMMAD ALYAMANI

ABSTRACT

Despite an array of improved treatment options over the past decade, prostate cancer remains the second leading cause of cancer mortality for men in the United States. Abiraterone and galeterone are oral steroidal compounds that are used to treat metastatic castration-resistant prostate cancer (CRPC). Abiraterone blocks 17α-hydroxylase/17,20-lyase (CYP17A1), an enzyme required for androgen synthesis. Galeterone inhibits CYP17A1, blocks the androgen receptor (AR), and decreases AR protein levels. Both drugs share the same structure with endogenous androgens such as dehydroepiandrosterone, which are substrates for the enzyme, 3β-hydroxysteroid dehydrogenase (3βHSD). Metabolites of 3βHSD undergo further metabolism to produce the AR ligand, testosterone and dihydrotestosterone.

Overall this project aimed to investigate the steroidogenic metabolism of abiraterone and galeterone and evaluate the metabolites' role in prostate cancer. The background on prostate cancer, steroid biosynthesis, and treatment options is described in Chapter I. Chapter II describes the development and validation of a liquid chromatography mass spectrometry method LC-MS/MS to determine abiraterone metabolites. My method distinguished between all the diastereoisomers with conventional chromatographic

conditions. In chapter III and IV my validated LC-MS/MS method was utilized to study the metabolism of abiraterone *in vitro* using prostate cancer cell lines and *in vivo* using mice. It also helped in determining abiraterone metabolites in a pharmacokinetic trial in healthy human subjects and in prostate cancer patients enrolled in several clinical trials. The trials aimed to evaluate the standard dose of abiraterone acetate, combining abiraterone acetate with androgen deprivation therapy (ADT), adding dutasteride (an SRD5A inhibitor), or increasing the frequency of the standard dose of abiraterone acetate. In chapter V, galeterone metabolism was studied *in vitro* and *in vivo* and the metabolites' activities were evaluated for their roles in prostate cancer. Chapter VI discusses the overall conclusions and future directions.

This project identified a new subset of abiraterone and galeterone metabolites that are generated by steroidogenic enzyme conversion. These metabolites had opposing effects on prostate cancer. These findings suggest a common pathway for steroidal drugs with a Δ^5, 3β-hydroxyl structure. This project also provides new strategies in prostate cancer treatment that will make the current treatment options more beneficial.

TABLE OF CONTENTS

LIST OF TABLES

LIST OF FIGURES

CHAPTER I

PROSTATE CANCER: AN OVERVIEW

1.1. Background

"A very rare disease" is how J. Adams, the surgeon at The London Hospital, described the first case of prostate cancer, which he discovered by histological examination in 1853[1]. After more than 160 years, prostate cancer is the most frequently diagnosed cancer and the third leading cause of cancer death in men in the United States. One out of seven American men will be diagnosed with prostate cancer during their lifetime. In 2017, it is estimated that 160,000 American men will be diagnosed with prostate cancer and 26,000 will lose their lives to the disease[2].

The prostate gland is part of the male reproductive system. It is a walnut size and shaped organ. It sits below the bladder just in front of the rectum and surrounds part of the urethra. The role of the prostate is to help make the semen. Even though researchers do

not know exactly what causes prostate cancer, several factors can be linked to it: age, ethnicity, heredity, and geographic region[3]. The older the man is, the higher the possibility of being diagnosed with prostate cancer. According to recent statistics from the Prostate Cancer Foundation, 65% of prostate cancer patients are older than 65 years old. Compared with Caucasian and Asian men, African American men are more likely to develop prostate cancer and are more likely to die from the disease. The chance of being diagnosed with prostate cancer will double if a man has a father or brother who developed prostate cancer. Those who live in the northern part of the United States are at higher risk to develop and die from the disease. Although why this pattern exists is unclear, it may be that low exposure to sun light and vitamin D deficiency can increase the disease rates[4]. Other factors that can be linked to prostate cancer include diet, obesity, and smoking[5].

1.2. The Androgen Receptor

Prostate cancer is a hormone-dependent malignancy; tumor progression depends on androgen receptor AR presence and function[6,7]. AR belongs to the steroid hormone group of nuclear receptors, along with the estrogen receptor (ER), glucocorticoid receptor (GR), progesterone receptor (PR) and mineralocorticoid receptor (MR)[8]. Testosterone (T) and its more potent metabolite, 5α-dihydrotestosterone (DHT), are the ligands for activating the AR. Therefore, these two steroids are the endogenous ligands fueling the growth of malignant prostate cells. DHT is 10 times more potent than T in activating the AR[9]. AR protein is encoded by the AR gene located on the X chromosome at Xq11-12 and spans ~180 kb of DNA containing 8 canonical exons. The AR contains four domains: (I) the amino terminal activation domain (NTD); (II) the DNA-binding domain (DBD); (III) the hinge region (HR) and (IV), the carboxyl ligand-binding domain (LBD). NTD, which

is encoded by exon 1, is the transcriptional regulatory region of the AR containing activation function-1 (AF-1). The DBD, composed of two zinc finger motifs, is encoded by exons 2 and 3, respectively. The hinge region is encoded by exon 4. The LBD is encoded by exons 5–8 and contains activation function-2 (AF-2) that allows the recruitment of co-activators and co-repressors (**Fig 1**). The transcriptional activity of the AR requires AF-1 in its NTD with negligible activity being attributed to AF-2 region in the LBD[10,11].

When androgens such as DHT diffuse through the plasma membrane of the cell and bind to the LBD of AR, they will initiate cellular events involving conformational changes, receptor stabilization, and nuclear translocation. It will also result in binding of AR dimer to androgen response elements (AREs) located in the promoter and enhancer sequences of target genes. AR binds target AREs via its DBD; a portion of the DBD together with the hinge region encode for a nuclear localization signal (NLS)[12,13] (**Fig. 2**).

1.3. Regulation of Testosterone Synthesis by the Endocrine Axis

The major source of circulating testosterone are the testes; however the adrenal gland can also produce T by regulating androgen biosynthesis. The endocrine axis contributes to the growth of prostate cancer by regulating T synthesis in these two sources: (i) the hypothalamus-pituitary-gonadal axis (HPG axis) and (ii) the hypothalamus-pituitary-adrenal axis (HPA axis)[14,15]. In the hypothalamus, gonadotropin-releasing hormone (GnRH), also known as luteinizing hormone (LH)-releasing hormone (LHRH), is produced and travels to the anterior pituitary and interacts with LHRH receptors (LHRH-Rs). Due to this interaction, LH will be released into the blood stream. In the testes, the released LH binds to its receptors (LH-R), inducing T production. The hypothalamus also produces corticotropin-releasing hormone (CRH). CRH stimulates the secretion of

adrenocorticotropic hormone (ACTH) from the pituitary into the blood stream where it interacts with the adrenal cortex portion of the adrenal gland and stimulates the synthesis of adrenal androgens, including T (**Fig 3**). T synthesized and released from both sites enters the prostate cells, where it is converted to 5α-dihydrotestosterone (DHT) by the enzyme 5α-reductase SRD5A. DHT binds tightly to AR, enters the cytoplasm, and the complex translocates to the nucleus, where it activates transcription of genes that regulate cell growth and survival.

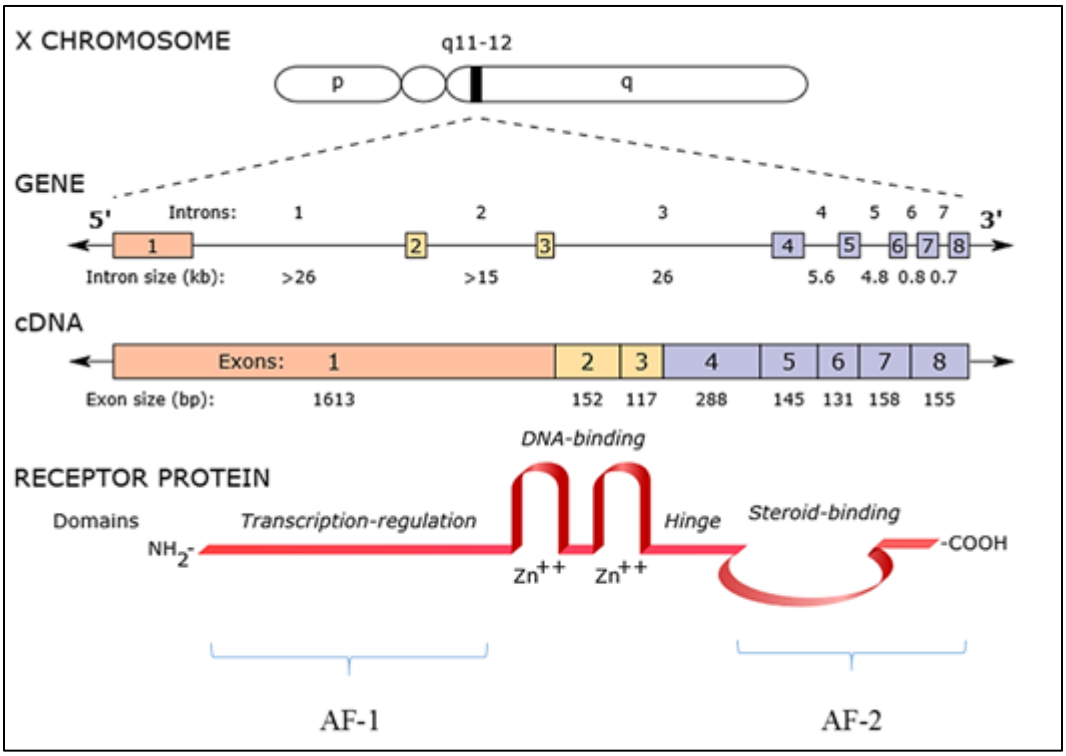

Figure 1. Genomic organization of the AR gene.
(Source: Quigley, C. A,1995)[11]

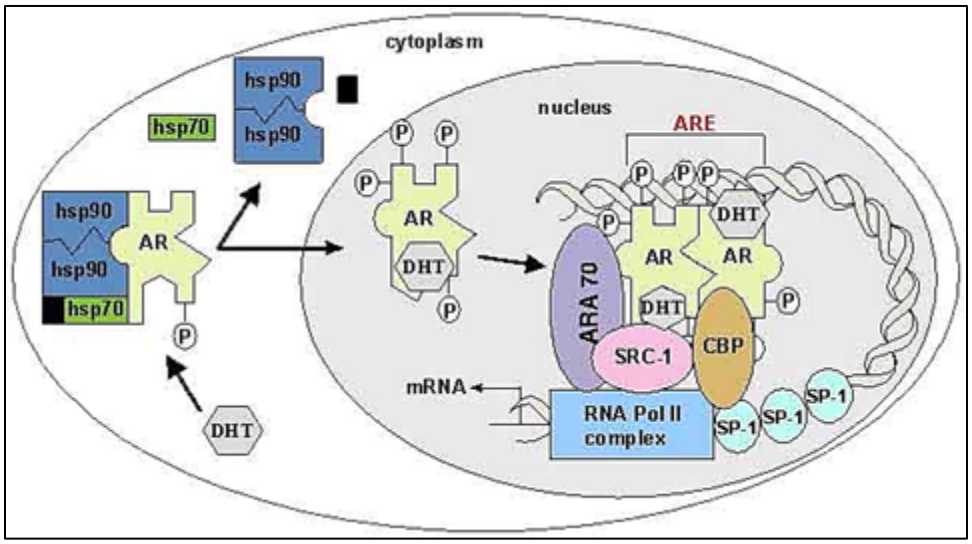

Figure 2. Ligand-dependent activation of the AR.

CBP (CREB-binding protein); hsp (heat shock protein); SRC-1 (steroid receptor coactivator 1) (Source: *Meehan, K. L; 2003*)[12].

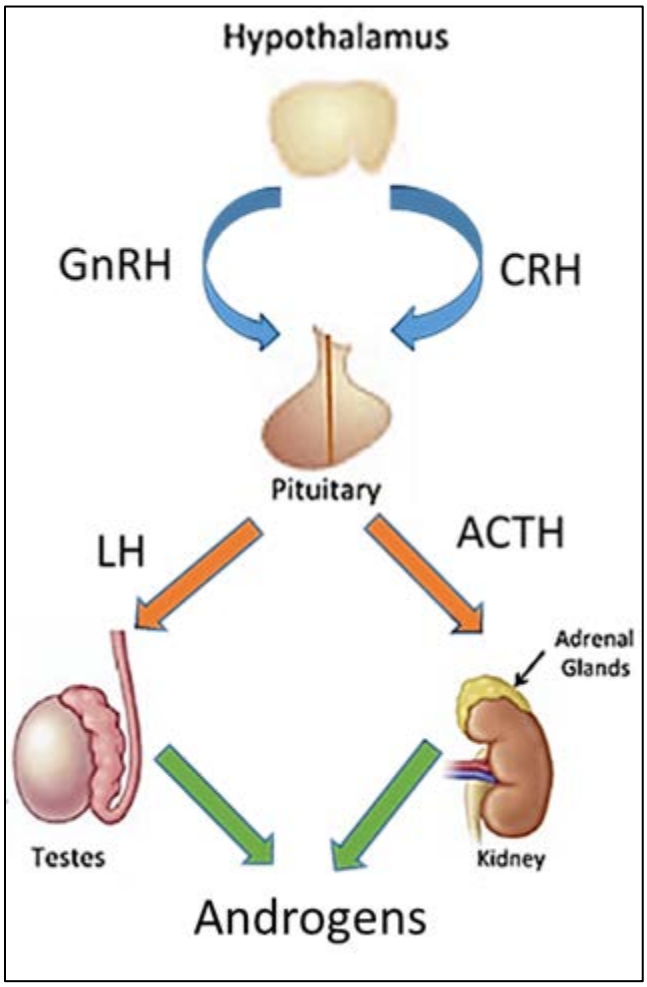

Figure 3. The regulation of androgen synthesis by the HPA and HPG axes.

1.4. Steroid Biosynthesis (Steroidogenesis)

Cholesterol is the precursor for steroid biosynthesis[16,17]. This 27-carbon compound can be oxidized to 21-carbon steroids (progestins, glucocorticoids, and mineralocorticoids) that then can form 19-carbon androgens. As discussed in section 1.3, the two primary sources of androgens are the adrenal cortex and the Leydig cells. Enzymes involved in steroidogenesis are either part of the cytochrome P450 (CYP) system, which is a group of oxidative enzymes that contain a single heme group and almost 500 amino acids[18], or hydroxysteroid dehydrogenases (HSDs), which contain heme groups and require nicotinamide adenine dinucleotide as a cofactor for their activity. Structurally, HSDs belong to two groups of enzymes: the short-chain dehydrogenase reductase (SDR) family or the aldo-keto reductase (AKR) family[19]. CYP reactions are irreversible, meaning that the accumulation of product will not drive flux to its precursor. On the other hand, some HSD reactions are reversible. The first step of steroidogenesis is catalyzed by CYP11A1, which results in side chain cleavage of cholesterol to pregnenolone (**Fig. 4**). CYP17A1 (17α-hydroxylase and 17,20 lyase) converts pregnenolone to 17 hydroxy-pregnenolone and then to dehydroepiandrosterone (DHEA). 3β-hydroxysteroid dehydrogenase/Δ^5-Δ^4 isomerase (3βHSD) irreversibly converts 3β-OH, Δ^5 steroids to 3-keto, Δ^4 steroids. Two isoforms of 3βHSD are present in human, with 3βHSD1 being the isoenzyme dominantly expressed in peripheral tissue. This enzyme converts pregnenolone to progesterone, 17-hydroxypregnenolone to 17-hydroxyprogesterone, DHEA to androstendione (AD), and Δ^5-Androstenediol (A5diol) to T.

The Sharifi lab reported that in CRPC a mutation in the gene coding for 3βHSD results in increased DHT levels[20]. Steroid-5α-reductase (SRD5A) converts 3-keto, Δ^4

steroids to 5α-reduced steroids. Two isoforms of SRD5A are present in human. This enzyme converts AD to 5α-androstanedione (5α-dione) and T to DHT. It has been reported that in CRPC, conversion of AD to T is less favored and DHT synthesis requires conversion of AD to 5α-dione, where AD is the favored 5α-reductase substrate[21]. 17β-hydroxysteroid dehydrogenase (17βHSD) reversibly converts 17 keto-androgens to 17 hydroxy-androgens. Fourteen 17βHSD isoenzymes are present in humans; some have a preference for the reductive reaction (17-keto to 17-hydroxyl) and some prefer the reverse reaction. In males, 17βHSD3 is the isoenzyme responsible for T synthesis in the testes. However, in CRPC, 17βHSD5, also known as the aldo-keto reductase 1C3, another reductive enzyme and converts AD to T, is up-regulated[22,23]. 3α-hydroxysteroid dehydrogenase (3αHSD) is also an aldo-keto reductase; it has four isoenzymes and although it is required for converting active steroids to inactive steroids, it can be involved in the backdoor DHT synthesis pathway[24,25].

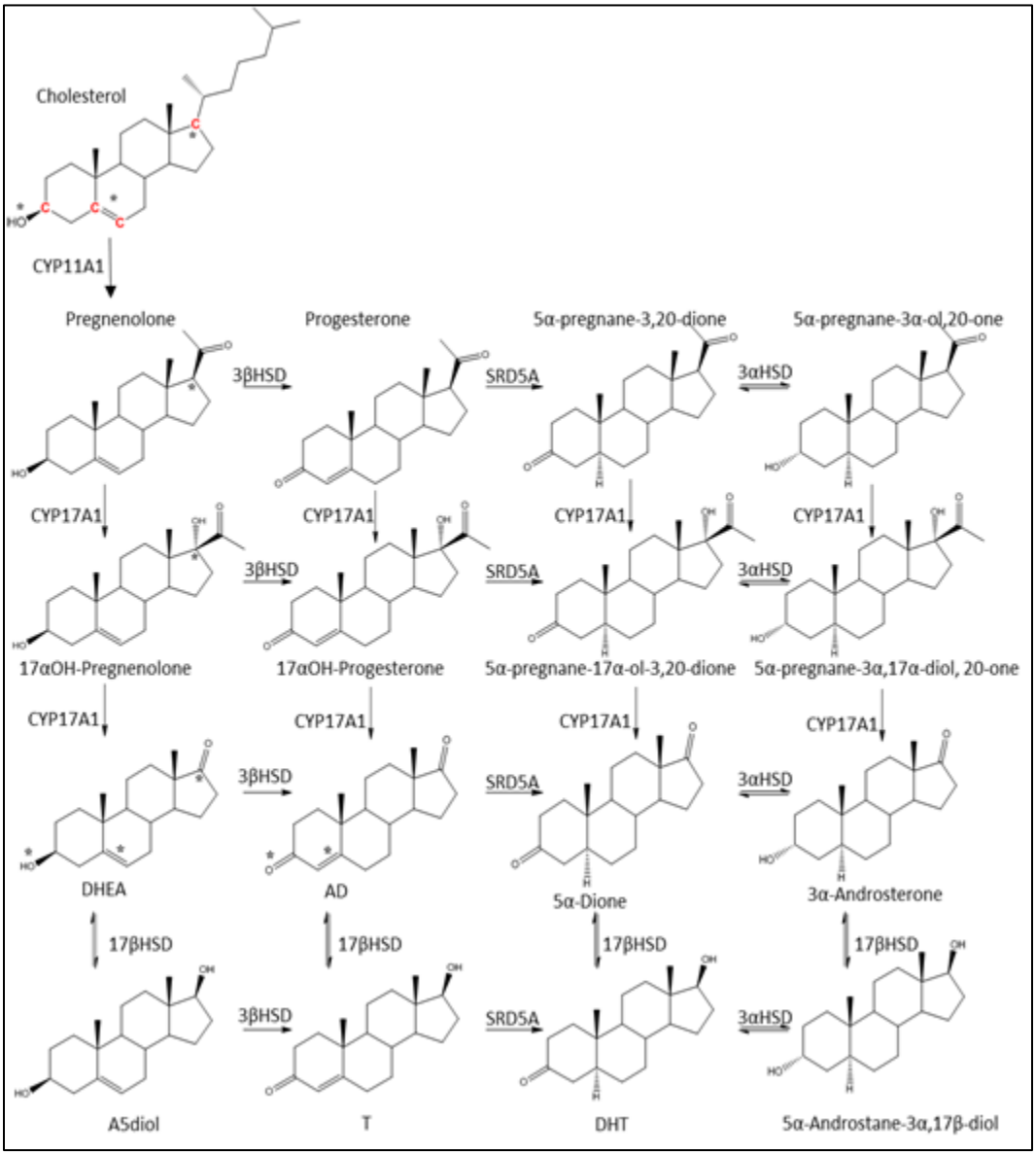

Figure 4. DHT synthesis pathways.

1.5. The Development of Castration-Resistant Prostate Cancer

Prostate cancer develops in stages. In its early stages the tumor is found in the prostate only. In this stage, prostate cancer is microscopic; it cannot be felt on a digital rectal exam (DRE), and it is not seen on imaging of the prostate. The tumor then spreads but still inside the prostate and does not extend beyond it. After that the tumor will spread outside the prostate but only barely, and may involve the nearby tissues like the seminal vesicles. In its latest stages the tumor will spread (metastasize) outside the prostate to other tissues (lymph nodes, the bones, liver, or lungs). The treatment option will depend on the stage: active surveillance, radical prostatectomy, or radiation therapy (external beam or brachytherapy) are the options for localized disease. In the advanced stages, chemotherapy and hormonal therapy are the options. Hormonal therapy is the gold standard for treating patients with prostate cancer[26-28]. The discoveries of Charles Huggins concerning hormonal therapy to treat prostate cancer led him to win Nobel Prize in 1966. In his early research, Huggins found that castration or estrogen administration shrinks the tissue[29,30]. His discoveries led to what is known now as androgen deprivation therapy, or ADT, which can be achieved either by surgical castration (orchiectomy) or medical castration using a GnRH agonist or antagonist. ADT will lower serum T levels and it initially works in many cases; however, the tissue can still find its fuel which leads it to resist this treatment and the tumor will develop to the castration-resistant prostate cancer CRPC stage[22,31,32]. Second-generation hormone therapies such as abiraterone acetate and enzalutamide are treatment options at the CRPC stage[33-36] (**Fig 5A&B**).

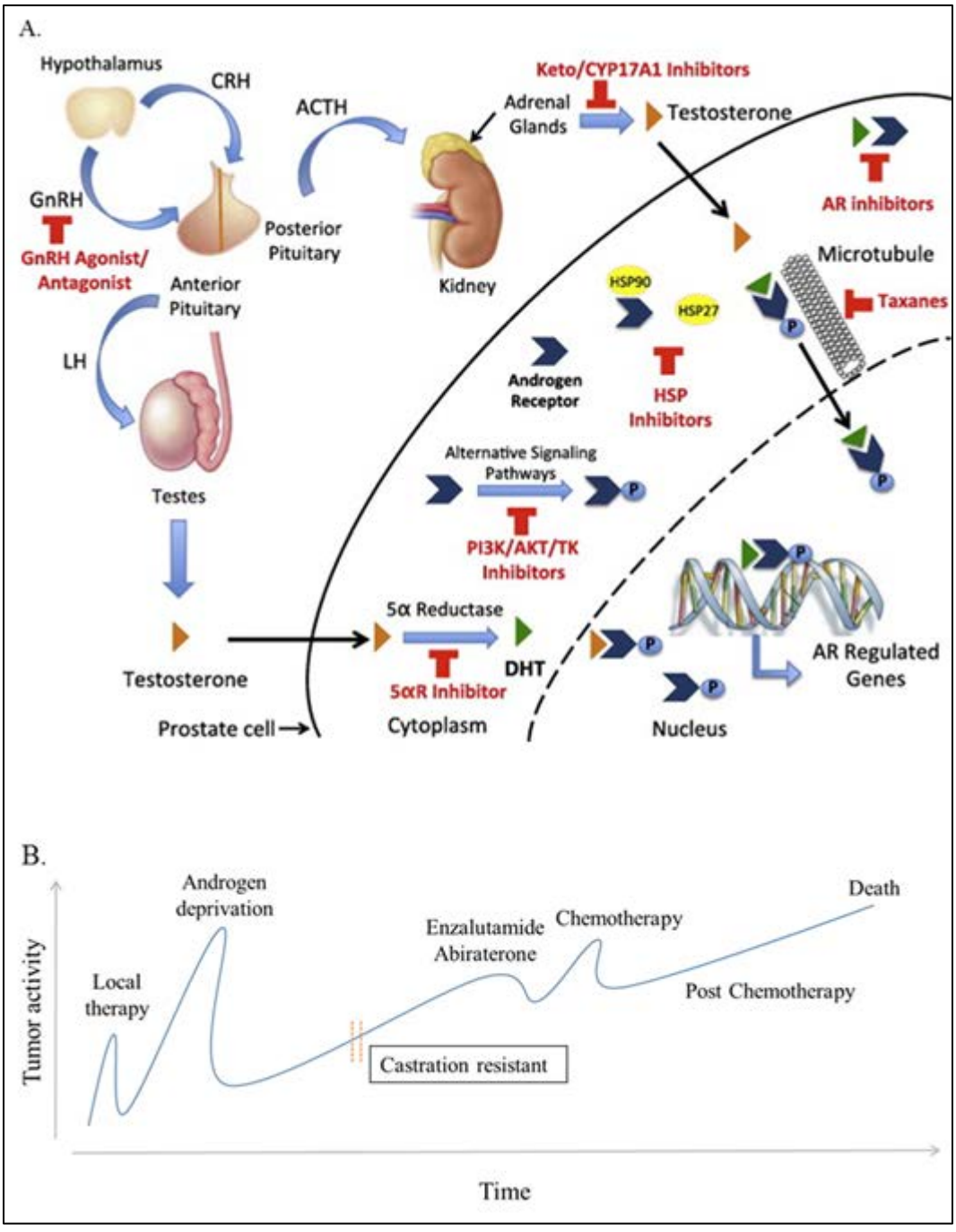

Figure 5. Treatment options for prostate cancer

(Source; *Gomez, L. 2015*)[28]

1.6. Abiraterone

Abiraterone [abi; 17-(3-pyridyl)-androsta-5,16-dien-3β-ol] is a 17-heteroazole steroidal compound and a potent inhibitor of steroid 17α-hydroxylase/17,20-lyase (CYP17A1), an enzyme required for androgen synthesis[37]. Abiraterone's structure makes it a potent CYP17A1 inhibitor, and the double bond at C16 is necessary for functionally irreversible inhibition of the enzyme[38-40]. Abiraterone is administered as the prodrug, abiraterone acetate (AA), for the treatment of CRPC and prolongs survival for these patients[34,41,42]. In 2011, the United States Food and Drug Administration (FDA) approved AA in the post-chemotherapy setting, and in December 2012 it approved the use of AA for patients with chemotherapy-naïve CRPC[43]. Prednisone is administered with AA to block mineralocorticoid excess that occurs with the simultaneous inhibition of cortisol synthesis[27,44]. The major recognized metabolites of abiraterone result from hepatic CYP3A4 and SULT2A1 processing, forming the N-oxide of abiraterone and abiraterone sulfate[45], respectively. Neither of these modifications affect the Δ^5, 3β-hydroxyl-structure of the steroid backbone.

1.7. Galeterone

Galeterone (Gal), 17-(1H-benzimidazol-1-yl) androsta-5,16-dien-3β-ol, is a steroidal 17-azole compound that inhibits CYP17A1[46-49], directly competes with androgens to bind and antagonize AR[50], promotes AR protein degradation, and has clinical activity as reported in a phase I/II clinical trial[51-55]. Galeterone's structure enables interaction with the steroid binding site of CYP17 in addition to coordination with the enzyme's heme iron, resulting in a highly specific and tightly binding inhibitor. The x-ray crystal structure of CYP17A1 binding to abiraterone or galeterone shows that they bind to heme iron[56].

Galeterone shares its Δ^5, 3β-hydroxyl structure with abiraterone. The two drugs are distinguished by their C17 moieties – the benzamidazole ring of galeterone and the 3-pyridyl structure of abiraterone. These differences may explain why galeterone has been reported to have more direct effects on AR.

1.8. Hypothesis

Δ^5, 3β-hydroxyl steroids are substrates of the enzyme 3βHSD, which irreversibly converts them to 3-keto, Δ^4 steroids. An example of this is the conversion of DHEA to AD and A5diol to T. The next step is then 5α reduction of 3-keto, Δ^4 steroids by SRD5A to form 3-keto-5α reduced steroids, as present in T conversion to DHT. AKR1C2 will then reduce the 3-keto-5α steroids to the 3α-OH-5α steroids. This last step is one mechanism of DHT elimination. DHT is converted to 5α-androstan-3α,17β-diol (3α-diol) (**Fig. 4**).

Both abiraterone and galeterone are Δ^5, 3β-hydroxyl steroids. Therefore, they can be possible substrates of 3βHSD and converted to their 3-keto, Δ^4 structures, which may follow the downstream mechanism and be converted to the 5α-reduced form. The main aim of this project is to study abiraterone and galeterone metabolism by steroidogenic enzymes and study the activity of the resultant metabolites. The metabolism was studied *in vitro* using prostate cancer cell lines and *in vivo* using NSG mice. **I hypothesized that the enzymes present in prostate cancer cell lines and in mice will convert abiraterone and galeterone to their steroidogenic enzyme metabolites and this conversion is irreversible.** Galeterone metabolite activity was studied *in vitro* and *in vivo*. **I hypothesized that galeterone metabolites will show activity toward the AR signaling pathway in prostate cancer cell lines, and in mouse models, the metabolites will have activity directed against tumors in mouse xenograft models.** Abiraterone metabolism

was investigated in patients with CRPC who are treated with abiraterone acetate in clinical trials. **I hypothesized that inhibiting steroidogenic enzymes or increasing the frequency of abiraterone dose will affect abiraterone metabolite levels in CRPC patients which may correlate with clinical outcomes.**

1.9. References

1 Denmeade, S. R. & Isaacs, J. T. A history of prostate cancer treatment. *Nature reviews. Cancer* **2**, 389-396, doi:10.1038/nrc801 (2002).

2 Siegel, R. L., Miller, K. D. & Jemal, A. Cancer Statistics, 2017. *CA: A Cancer Journal for Clinicians* **67**, 7-30, doi:10.3322/caac.21387 (2017).

3 Patel, A. R. & Klein, E. A. Risk factors for prostate cancer. *Nature clinical practice. Urology* **6**, 87-95, doi:10.1038/ncpuro1290 (2009).

4 Chen, T. C. & Holick, M. F. Vitamin D and prostate cancer prevention and treatment. *Trends in endocrinology and metabolism: TEM* **14**, 423-430 (2003).

5 Bostwick, D. G. *et al.* Human prostate cancer risk factors. *Cancer* **101**, 2371-2490, doi:10.1002/cncr.20408 (2004).

6 Attard, G. *et al.* Prostate cancer. *Lancet (London, England)* **387**, 70-82, doi:10.1016/s0140-6736(14)61947-4 (2016).

7 Miyamoto, D. T. *et al.* Androgen receptor signaling in circulating tumor cells as a marker of hormonally responsive prostate cancer. *Cancer Discov* **2**, 995-1003, doi:10.1158/2159-8290.CD-12-0222 (2012).

8 Tan, M. H. E., Li, J., Xu, H. E., Melcher, K. & Yong, E.-l. Androgen receptor: structure, role in prostate cancer and drug discovery. *Acta Pharmacol Sin* **36**, 3-23, doi:10.1038/aps.2014.18 (2015).

9 Deslypere, J. P., Young, M., Wilson, J. D. & McPhaul, M. J. Testosterone and 5 alpha-dihydrotestosterone interact differently with the androgen receptor to enhance transcription of the MMTV-CAT reporter gene. *Molecular and cellular endocrinology* **88**, 15-22 (1992).

10 Haile, S. & Sadar, M. D. Androgen receptor and its splice variants in prostate cancer. *Cellular and molecular life sciences : CMLS* **68**, 3971-3981, doi:10.1007/s00018-011-0766-7 (2011).

11 Quigley, C. A. *et al.* Androgen Receptor Defects: Historical, Clinical, and Molecular Perspectives*. *Endocrine Reviews* **16**, 271-321, doi:10.1210/edrv-16-3-271 (1995).

12 Meehan, K. L. & Sadar, M. D. Androgens and androgen receptor in prostate and ovarian malignancies. *Frontiers in bioscience : a journal and virtual library* **8**, d780-800 (2003).

13 Galani, A., Kitsiou-Tzeli, S., Sofokleous, C., Kanavakis, E. & Kalpini-Mavrou, A. Androgen insensitivity syndrome: clinical features and molecular defects. *Hormones (Athens)* **7**, 217-229 (2008).

14 Kluth, L. A. *et al.* The hypothalamic-pituitary-gonadal axis and prostate cancer: implications for androgen deprivation therapy. *World journal of urology* **32**, 669-676, doi:10.1007/s00345-013-1157-5 (2014).

15 Montgomery, R. B. *et al.* Maintenance of intratumoral androgens in metastatic prostate cancer: a mechanism for castration-resistant tumor growth. *Cancer research* **68**, 4447-4454, doi:10.1158/0008-5472.can-08-0249 (2008).

16 Miller, W. L. & Auchus, R. J. The Molecular Biology, Biochemistry, and Physiology of Human Steroidogenesis and Its Disorders. *Endocrine Reviews* **32**, 81-151, doi:10.1210/er.2010-0013 (2011).

17 Sharifi, N. & Auchus, R. J. Steroid biosynthesis and prostate cancer. *Steroids* **77**, 719-726, doi:10.1016/j.steroids.2012.03.015 (2012).

18 Gonzalez, F. J. The molecular biology of cytochrome P450s. *Pharmacological reviews* **40**, 243-288 (1988).

19 Agarwal, A. K. & Auchus, R. J. Minireview: cellular redox state regulates hydroxysteroid dehydrogenase activity and intracellular hormone potency. *Endocrinology* **146**, 2531-2538, doi:10.1210/en.2005-0061 (2005).

20 Chang, K. H. *et al.* A gain-of-function mutation in DHT synthesis in castration-resistant prostate cancer. *Cell* **154**, 1074-1084, doi:10.1016/j.cell.2013.07.029 (2013).

21 Chang, K. H. *et al.* Dihydrotestosterone synthesis bypasses testosterone to drive castration-resistant prostate cancer. *Proc Natl Acad Sci U S A* **108**, 13728-13733, doi:1107898108 [pii]

10.1073/pnas.1107898108 (2011).

22 Sharifi, N. Minireview: Androgen metabolism in castration-resistant prostate cancer. *Molecular endocrinology (Baltimore, Md.)* **27**, 708-714, doi:10.1210/me.2013-1007 (2013).

23 Ferraldeschi, R., Sharifi, N., Auchus, R. J. & Attard, G. Molecular pathways: Inhibiting steroid biosynthesis in prostate cancer. *Clinical cancer research : an*

official journal of the American Association for Cancer Research **19**, 3353-3359, doi:10.1158/1078-0432.ccr-12-0931 (2013).

24 Fukami, M., Homma, K., Hasegawa, T. & Ogata, T. Backdoor pathway for dihydrotestosterone biosynthesis: Implications for normal and abnormal human sex development. *Developmental Dynamics* **242**, 320-329, doi:10.1002/dvdy.23892 (2013).

25 Auchus, R. J. The backdoor pathway to dihydrotestosterone. *Trends in endocrinology and metabolism: TEM* **15**, 432-438, doi:10.1016/j.tem.2004.09.004 (2004).

26 O'Donnell, A. *et al.* Hormonal impact of the 17alpha-hydroxylase/C(17,20)-lyase inhibitor abiraterone acetate (CB7630) in patients with prostate cancer. *British journal of cancer* **90**, 2317-2325, doi:10.1038/sj.bjc.6601879 (2004).

27 Attard, G. *et al.* Clinical and biochemical consequences of CYP17A1 inhibition with abiraterone given with and without exogenous glucocorticoids in castrate men with advanced prostate cancer. *The Journal of clinical endocrinology and metabolism* **97**, 507-516, doi:10.1210/jc.2011-2189 (2012).

28 Gomez, L., Kovac, J. R. & Lamb, D. J. CYP17A1 inhibitors in castration-resistant prostate cancer. *Steroids* **95**, 80-87, doi:10.1016/j.steroids.2014.12.021 (2015).

29 Huggins, C., Stevens, R. E., Jr & Hodges, C. V. Studies on prostatic cancer: Ii. the effects of castration on advanced carcinoma of the prostate gland. *Archives of Surgery* **43**, 209-223, doi:10.1001/archsurg.1941.01210140043004 (1941).

30 Huggins, C. Prostatic cancer treated by orchiectomy: The five year results. *Journal of the American Medical Association* **131**, 576-581, doi:10.1001/jama.1946.02870240008003 (1946).

31 Scher, H. I. *et al.* Design and end points of clinical trials for patients with progressive prostate cancer and castrate levels of testosterone: recommendations of the Prostate Cancer Clinical Trials Working Group. *J Clin Oncol* **26**, 1148-1159, doi:26/7/1148 [pii]

10.1200/JCO.2007.12.4487 (2008).

32 Scher, H. I. & Sawyers, C. L. Biology of progressive, castration-resistant prostate cancer: directed therapies targeting the androgen-receptor signaling axis. *J Clin Oncol* **23**, 8253-8261, doi:23/32/8253 [pii]

10.1200/JCO.2005.03.4777 (2005).

33 Ryan, C. J. *et al.* Abiraterone in Metastatic Prostate Cancer without Previous Chemotherapy. *The New England journal of medicine*, doi:10.1056/NEJMoa1209096 (2012).

34 de Bono, J. S. *et al.* Abiraterone and increased survival in metastatic prostate cancer. *The New England journal of medicine* **364**, 1995-2005, doi:10.1056/NEJMoa1014618 (2011).

35 Scher, H. I. *et al.* Increased survival with enzalutamide in prostate cancer after chemotherapy. *The New England journal of medicine* **367**, 1187-1197, doi:10.1056/NEJMoa1207506 (2012).

36 Beer, T. M. *et al.* Enzalutamide in metastatic prostate cancer before chemotherapy. *The New England journal of medicine* **371**, 424-433, doi:10.1056/NEJMoa1405095 (2014).

37 Potter, G. A., Barrie, S. E., Jarman, M. & Rowlands, M. G. Novel steroidal inhibitors of human cytochrome P45017 alpha (17 alpha-hydroxylase-C17,20-lyase): potential agents for the treatment of prostatic cancer. *Journal of medicinal chemistry* **38**, 2463-2471 (1995).

38 Jarman, M., Barrie, S. E. & Llera, J. M. The 16,17-double bond is needed for irreversible inhibition of human cytochrome p45017alpha by abiraterone (17-(3-pyridyl)androsta-5, 16-dien-3beta-ol) and related steroidal inhibitors. *Journal of medicinal chemistry* **41**, 5375-5381, doi:10.1021/jm981017j (1998).

39 Salvador, J. A., Pinto, R. M. & Silvestre, S. M. Steroidal 5alpha-reductase and 17alpha-hydroxylase/17,20-lyase (CYP17) inhibitors useful in the treatment of prostatic diseases. *The Journal of steroid biochemistry and molecular biology* **137**, 199-222, doi:10.1016/j.jsbmb.2013.04.006 (2013).

40 Garrido, M. *et al.* A-ring modified steroidal azoles retaining similar potent and slowly reversible CYP17A1 inhibition as abiraterone. *The Journal of steroid biochemistry and molecular biology* **143**, 1-10, doi:10.1016/j.jsbmb.2014.01.013 (2014).

41 Grist, E. & Attard, G. The development of abiraterone acetate for castration-resistant prostate cancer. *Urologic oncology* **33**, 289-294, doi:10.1016/j.urolonc.2015.03.021 (2015).

42 Ryan, C. J. *et al.* Abiraterone in metastatic prostate cancer without previous chemotherapy. *The New England journal of medicine* **368**, 138-148, doi:10.1056/NEJMoa1209096 (2013).

43 Kluetz, P. G. *et al.* Abiraterone acetate in combination with prednisone for the treatment of patients with metastatic castration-resistant prostate cancer: U.S. Food and Drug Administration drug approval summary. *Clinical cancer research : an official journal of the American Association for Cancer Research* **19**, 6650-6656, doi:10.1158/1078-0432.ccr-13-2134 (2013).

44 Auchus, R. J., Yu, M. K., Nguyen, S. & Mundle, S. D. Use of prednisone with abiraterone acetate in metastatic castration-resistant prostate cancer. *The oncologist* **19**, 1231-1240, doi:10.1634/theoncologist.2014-0167 (2014).

45 Acharya, M. *et al.* A phase I, open-label, single-dose, mass balance study of 14C-labeled abiraterone acetate in healthy male subjects. *Xenobiotica; the fate of foreign compounds in biological systems* **43**, 379-389, doi:10.3109/00498254.2012.721022 (2013).

46 Njar, V. C., Hector, M. & Hartmann, R. W. 20-amino and 20,21-aziridinyl pregnene steroids: development of potent inhibitors of 17 alpha-hydroxylase/C17,20-lyase (P450 17). *Bioorganic & medicinal chemistry* **4**, 1447-1453 (1996).

47 Njar, V. C. & Brodie, A. M. Inhibitors of 17alpha-hydroxylase/17,20-lyase (CYP17): potential agents for the treatment of prostate cancer. *Current pharmaceutical design* **5**, 163-180 (1999).

48 Njar, V. C. *et al.* Novel 17-azolyl steroids, potent inhibitors of human cytochrome 17 alpha-hydroxylase-C17,20-lyase (P450(17) alpha): potential agents for the treatment of prostate cancer. *Journal of medicinal chemistry* **41**, 902-912, doi:10.1021/jm970568r (1998).

49 Handratta, V. D. *et al.* Novel C-17-heteroaryl steroidal CYP17 inhibitors/antiandrogens: synthesis, in vitro biological activity, pharmacokinetics, and antitumor activity in the LAPC4 human prostate cancer xenograft model. *Journal of medicinal chemistry* **48**, 2972-2984, doi:10.1021/jm040202w (2005).

50 Vasaitis, T. *et al.* Androgen receptor inactivation contributes to antitumor efficacy of 17{alpha}-hydroxylase/17,20-lyase inhibitor 3beta-hydroxy-17-(1H-benzimidazole-1-yl)androsta-5,16-diene in prostate cancer. *Molecular cancer therapeutics* **7**, 2348-2357, doi:10.1158/1535-7163.mct-08-0230 (2008).

51 Njar, V. C. & Brodie, A. M. Discovery and development of Galeterone (TOK-001 or VN/124-1) for the treatment of all stages of prostate cancer. *J Med Chem* **58**, 2077-2087, doi:10.1021/jm501239f (2015).

52 Purushottamachar, P. *et al.* Systematic structure modifications of multitarget prostate cancer drug candidate galeterone to produce novel androgen receptor down-regulating agents as an approach to treatment of advanced prostate cancer. *Journal of medicinal chemistry* **56**, 4880-4898, doi:10.1021/jm400048v (2013).

53 Kwegyir-Afful, A. K., Ramalingam, S., Purushottamachar, P., Ramamurthy, V. P. & Njar, V. C. Galeterone and VNPT55 induce proteasomal degradation of AR/AR-V7, induce significant apoptosis via cytochrome c release and suppress growth of

castration resistant prostate cancer xenografts *in vivo*. *Oncotarget* **6**, 27440-27460, doi:10.18632/oncotarget.4578 (2015).

54 Yu, Z. *et al.* Galeterone prevents androgen receptor binding to chromatin and enhances degradation of mutant androgen receptor. *Clinical cancer research : an official journal of the American Association for Cancer Research* **20**, 4075-4085, doi:10.1158/1078-0432.ccr-14-0292 (2014).

55 Montgomery, B. *et al.* Androgen Receptor Modulation Optimized for Response (ARMOR) Phase I and II Studies: Galeterone for the Treatment of Castration-Resistant Prostate Cancer. *Clinical cancer research : an official journal of the American Association for Cancer Research* **22**, 1356-1363, doi:10.1158/1078-0432.CCR-15-1432 (2016).

56 DeVore, N. M. & Scott, E. E. Structures of cytochrome P450 17A1 with prostate cancer drugs abiraterone and TOK-001. *Nature* **482**, 116-119, doi:10.1038/nature10743 (2012).

CHAPTER II

DEVELOPMENT AND VALIDATION OF A NOVEL LC-MS/MS METHOD FOR SIMULTANEOUS DETERMINATION OF ABIRATERONE AND ITS SEVEN STEROIDAL METABOLITES IN HUMAN SERUM

2.1. Introduction to Liquid Chromatography Mass Spectrometry

Due to its sensitivity and selectivity, mass spectrometry-based analysis has been widely used in different types of research. It can be used to detect both small and large molecules. Mass spec applications include basic research, clinical research, drug discovery, forensics, food quality, and environmental protection. Several designs of mass spectrometers are available: linear ion trap, quadrupole based, time of flight (TOF). Also, there are hybrid designs: the quadrupole time of flight QTOF and quadrupole ion trap QTrap[1]. Mass spec analysis allows one to answer numerous questions, including what is in the samples and how much of it is there. To be analyzed, the analyte should be charged,

because mass spec detects mass /charge ratio (m/z). The ionization techniques are electro spray ionization (ESI), atmospheric pressure chemical ionization, and atmospheric pressure photo ionization. The selection of the ionization type depends on the nature of the analyte. Multiple reaction monitoring is the technique that assures that only the analyte of interest is selected: First, analyzer quadrupole Q1 selects the precursor mass of interest from ions only of exactly the selected m/z pass to the collision cell Q2; all other ions are removed. Collision cell Q2 fragments precursor ions. Fragmented ions pass to analyzer quadrupole Q3. Analyzer quadrupole Q3 selects the most sensitive ion for quantitation (**Fig. 6**). Mass spectrometry can be used as a technique by itself or it can be coupled to liquid chromatography (LC-MS) or gas chromatography (GC-MS). Both techniques are widely used for metabolism studies; however the advantages of LC-MS over GC-MS includes simple sample preparation, shorter run times, and high throughput.

Applying LC-MS analysis to detect analytes in human fluids (saliva, blood, serum, plasma, or urine) requires sample purification. Three methods can be applied to extract the analyte of interest from different matrices: direct protein precipitation, liquid-liquid extraction, or solid-phase extraction.

LC-MS methods can be applied to prostate cancer research. As described in chapter I, prostate cancer depends on steroid synthesis. Therefore, using an LC-MS method that accurately detects these steroids and quantifies their levels in patient tissue or serum, may identify potential specific biomarkers[2,3]. LC-MS methods are useful in detecting drug metabolites; therefore it may also give a clue to which patients respond to treatment.

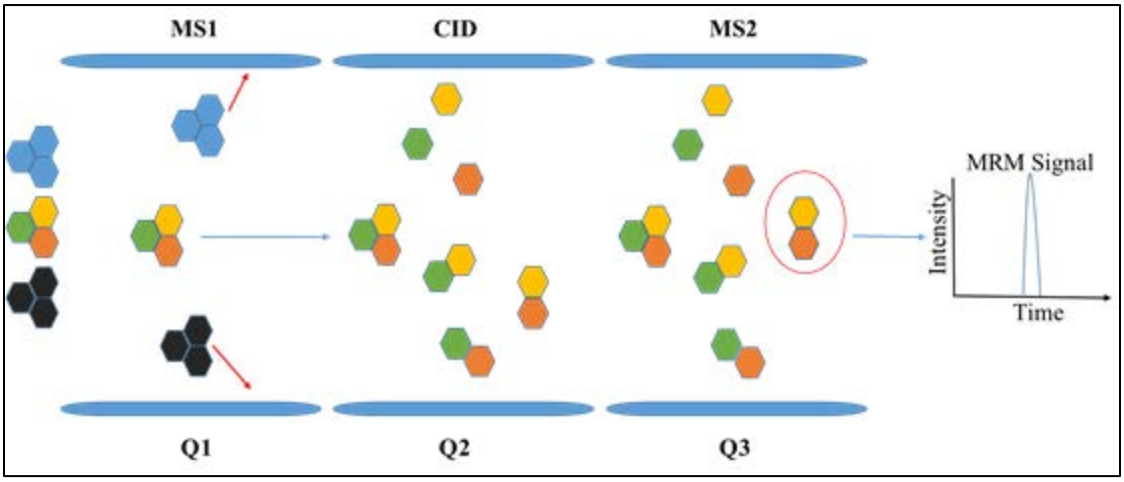

Figure 6. Multiple reaction monitoring principle.

2.2. Method Development and Validation

Although mass spec is a useful technique, operating the instrument and developing the methods requires knowledge and qualifications in separation and ionization. The first step in developing LC-MS methods is to optimize mass spec parameters, which include selecting the appropriate ionization technique, selecting m/z for the parent analyte and the fragment, and selecting the declustering potential, collision energy, and the source temperature. After optimizing source parameters, the next step is to select suitable chromatographic conditions, which include type of analytical column, mobile phase composition, flow rate, and injection volume. Then as a last step, the best method of extraction is selected that leads to high recovery and minimizes the matrix effect. Depending on the purpose of analysis the development may also include selecting the linear range. After testing the developed method for linearity and accuracy, the next stage is validating the method per the guidelines depending on the type of analysis. The purpose of the validation is to make sure that the method is accurate and precise and the analytes are stable at different conditions. Once the validation is completed, the method is ready to be used for analysis. The development and validation steps are described in **Figure 7**.

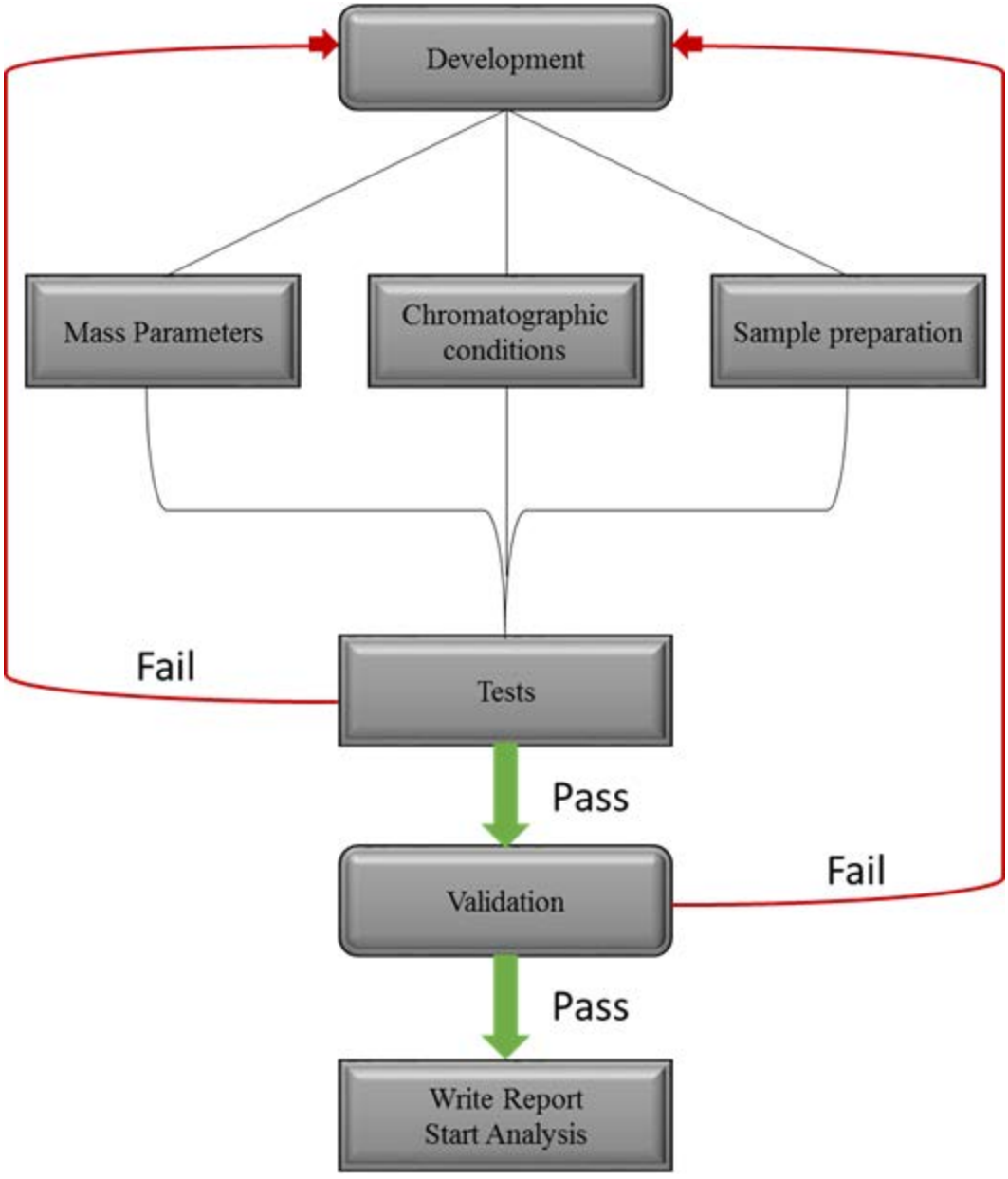

Figure 7. The approach of developing LC-MS methods

2.3. Abiraterone Metabolism by Steroidogenic Enzymes

Abiraterone design was based on its similarity in structure with pregnenolone which is a CYP17A1 substrate[4,5]. Since its FDA approval, abiraterone acetate, the prodrug of abiraterone, became the choice of treatment for patients with CRPC[6,7]. Abiraterone sulfate and N-oxide abiraterone sulfate are the reported abiraterone metabolites[8]. We studied the effect of steroidogenic enzymes on abiraterone both *in vitro* and *in vivo* and found that 3β-hydroxysteroid dehydrogenase (3βHSD) converts abiraterone to its Δ^4, 3-keto congener (Δ^4-abiraterone; D4A)[9]. D4A is similar in structure to T which might enable further metabolism of D4A. D4A undergoes metabolism by two possible pathways: via steroid 5α-reductase (SRD5A) or steroid 5β-reductase. The resultant metabolites can also be metabolized by two enzymes: 3α-hydroxysteroid dehydrogenase (3αHSD) or 3βHSD. The 5α-reduced metabolites are 3-keto-5α-Abi, 3α-OH-5α-Abi and 3β-OH-5α-Abi, while the corresponding 5β-reduced metabolites are 3-keto-5β-Abi, 3α-OH-5β-Abi and 3β-OH-5β-Abi[10] (**Fig 8**).

This chapter describes the development and validation of the LC-MS method that was used to detect abiraterone and its seven steroidal metabolites in human serum. In this validated method, the separation of the structurally identical metabolites was achieved using a reversed-phase chromatographic technique, not requiring a chiral column[11]. All these metabolites were also detected in serum samples from patients with CRPC undergoing treatment with abiraterone acetate.

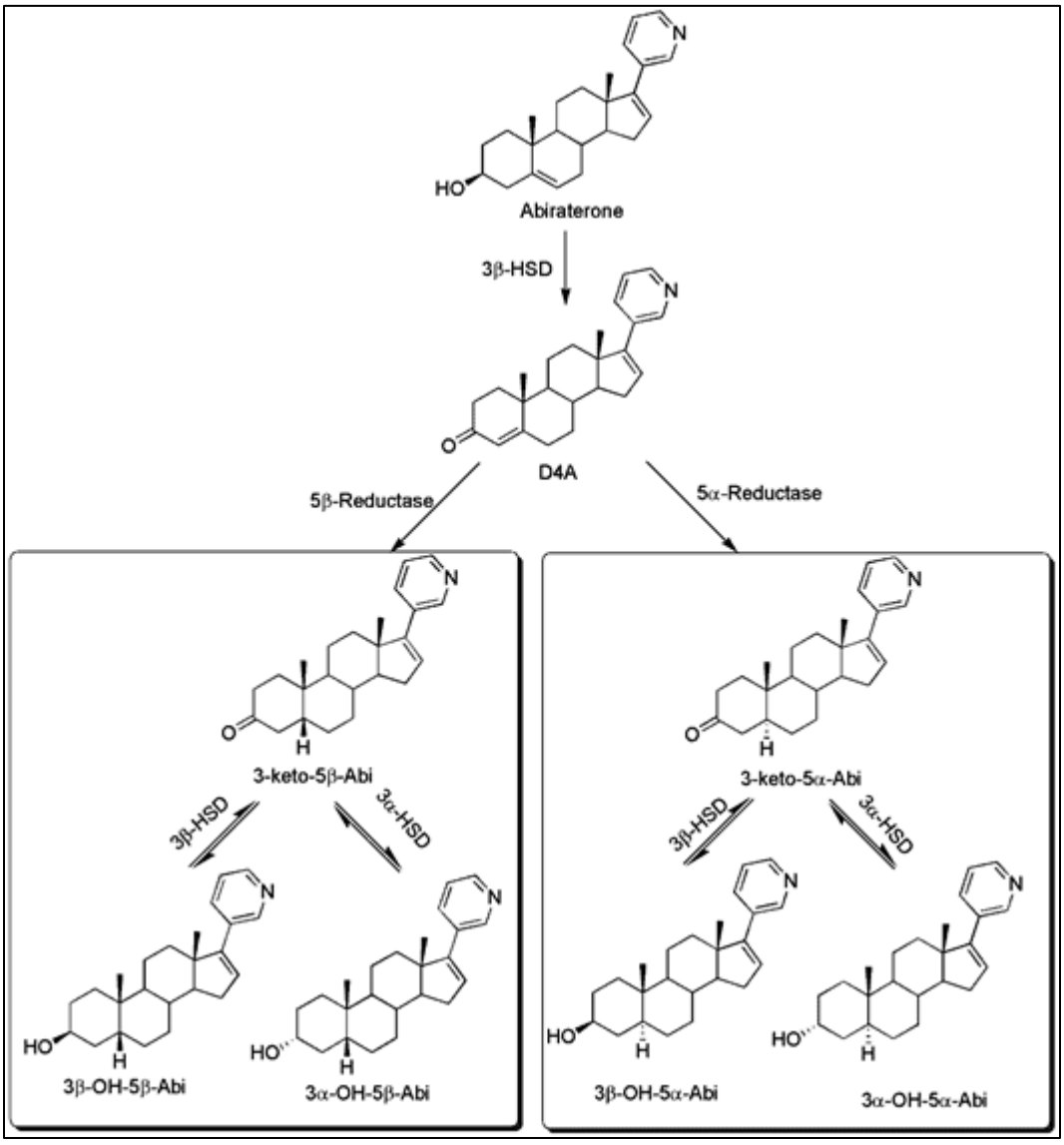

Figure 8. Steroidogenic enzyme metabolism of abiraterone.

2.4. Experimental Section

2.4.1. Materials

Abiraterone and its seven metabolites 3-keto-Δ^4-Abi, 3-keto-5α-Abi, 3α-OH-5α-Abi, 3β-OH-5α-Abi, 3-keto-5β-Abi, 3α-OH-5β-Abi and 3β-OH-5β-Abi were synthesized in the lab as described previously[10]. The internal standard (abiraterone-d4) was purchased from Toronto Research Chemicals, (Toronto, Canada). LC-MS grade methanol, acetonitrile, water, and formic acid were used to prepare the mobile phase and were purchased from Fisher Scientific (Fair Lawn, NJ); methyl tertiary butyl ether (MTBE) was used as the extraction solvent was HPLC grade and was purchased from Acros (Pittsburgh, PA). The control calibrators and all validation samples were prepared by spiking a known concentration of all analytes in double charcoal-stripped human serum from Golden West Biological Inc. (Temecula, CA).

2.4.2. Method development

In this section the development of LC-MS based bioanalytical method is described. The approaches to develop the LC-MS method involve optimizing the mass conditions and the chromatographic conditions, selecting linear range, and the procedure to prepare the sample, all of which are described in detail.

2.4.2.1. Instrumentation and data analysis

To analyze the samples, ultra-pressure liquid chromatography coupled to a mass spectrometer UPLC-MS system was used. The UPLC system (Shimadzu Corporation, Japan), consisted of an LC-30AD solvent delivery system, a DGU-20A5R vacuum degasser, a CTO-30A thermostated column oven, SIL-30AC auto-sampler, and a system CBM-20A controller. The UPLC system was coupled with a Qtrap 5500 mass spectrometer

(AB Sciex, Redwood City, CA). Data acquisition and processing were performed using Analyst software (version 1.6.2) from AB Sciex. The peak area ratio of the analyte over the internal standard was used for quantification purposes.

2.4.2.2. Optimizing mass spectrometer conditions

The mass spectrometer was operated in positive ion mode using an electrospray ionization (ESI) source, and applying multiple reaction monitoring (MRM). Tuning parameters were optimized for the abiraterone metabolites and internal standard by infusing a solution containing 200 ng/mL of each analyte. After infusing the solution and selecting the parent ion in Q1, the optimum value of the ion spray voltage, the source temperature, and the declustering potential were selected. Then the parent ion was fragmented in Q2 and the fragment ion (daughter ion) was selected along with the collision energy, entrance potential, and collision exit potential. The mass spectrometer parameters were optimized to ensure that the highest sensitivity possible would be achieved. Nitrogen was used as the nebulizing and drying gas.

2.4.2.3. Optimizing chromatographic conditions

Selecting an appropriate analytical column and a suitable mobile phase are the main factors in optimizing the chromatographic conditions. This will lead to an enhanced peak shape, increase in the intensity, and most importantly avoid overlap between analytes. In the case of diaseteoisomers, distinguishing between the metabolites based on their mass transition is very difficult because they share the same mass transition. Therefore, the chromatographic conditions are key in distinguishing between the metabolites. Chiral columns are the choice in dealing with diasterioisomers; however, these types of columns are not universal and require lot of trial and error experimentation. The challenge here was

to separate the metabolites using a regular C18 analytical column. Several mobile phases were evaluated with different compositions of organic modifiers or additives. The separation also depends on the column temperature, so this factor was also evaluated.

2.4.2.4. Optimization of sample preparation

When dealing with biological samples, the major factor in selecting the extraction protocol is the recovery of the analyte and also avoiding the matrix effect. Although direct protein precipitation is fastest and the cheapest, the matrix effect can be an issue and can lead to ion suppression during the analysis. Solid phase extraction is a useful technique but it is expensive and requires a long sample processing time. Therefore, here, liquid-liquid extraction procedure was considered from the beginning and optimized to obtain a high recovery and clean samples. Methyl tert butyl ether was selected as the organic solvent. The other solvent that was tested during the extraction was the reconstitution solvent.

2.4.3. Method validation

The developed method was then validated to check its accuracy, precision, robustness and rigidity. The method was validated per US FDA guidance for bioanalytical method validation. The validation parameters evaluated were linearity, accuracy and precision, selectivity, recovery, matrix effect, and stability.

2.4.3.1. Linearity

To ensure that the selected range is suitable for analysis, six calibration curves were constructed in same serum matrix for each analyte. The calibration curve is the plot of the ratio of the analyte peak area over the internal standard peak area versus the nominal concentration. Linear regression was selected applying a weighting factor of 1/x. The FDA guidelines state that for lower limit of quantitation LLOQ the acceptable deviation from

the nominal concentration is < 20% and < 15% for the other calibration points and that 67% of the calibrators, including LLOQ and upper limit of quantitation ULOQ, being within these acceptance criteria.

2.4.3.2. Accuracy, precision, and sensitivity

Five quality control (QC) samples from each level and LLOQ were run to determine intra-day accuracy and precision. To study the inter-day accuracy and precision, five QC samples from each level were prepared on 3 separate days and run immediately on the instrument after preparation. Accuracy was determined by how close the mean of the intra-day QC sample results were to the nominal value. The method is considered accurate if the measured concentration is within 85%-115% (80%-120% for LLOQ) of the expected value. The acceptable precision criterion is a coefficient of variation (CV%) of the QC sample analyte concentration being no more than 15% (LLOQ not more than 20%).

2.4.3.3. Selectivity

A selectivity test was done to ensure that the samples were free of interference. Six different serum batches were used to prepare blank and LLOQ samples. The LLOQ peak height (or peak area) must be at least 5 times of any peak detected in the corresponding blank samples at the same retention time of the analyte in order to be considered free from interference.

2.4.3.4. Recovery

The efficiency of the extraction protocol was evaluated through the recovery test. Three QC samples (low, mid, and high) were prepared pre- and post-extraction in triplicate. The analyte/internal standard peak area in spiked samples before extraction over the

analyte/internal standard peak area in spiked samples after extraction was used to calculate the relative recovery. There is no limit for the recovery; however, the results need to be consistent, precise and reproducible, as assessed by the coefficient of variation for each QC sample type being no more than 15%. The CV% was calculated as CV % = $[(DX/X)^2+(DY/Y)^2)]^{1/2}$, where DX is the standard deviation for the pre-extraction samples, X is the mean area ratio of pre-extraction samples, DY is the standard deviation for the post-extraction samples, and Y is the mean area ratio of post-extraction samples.

2.4.3.5. Matrix effect

The matrix effect is the variability in analyte response due to the sample matrix. To evaluate the matrix effect, QC low was prepared in triplicate in six different serum batches. Matrix effect, calculated as a matrix factor percent (MF%), was calculated as follows: ratio of peak area ratio of spiked analyte/internal standard for the QC low samples after extraction (n=18) over the peak area ratio of the spiked analyte/internal standard in methanol: H_2O, 1:1 (n=3). CV% was calculated as described in section 2.4.3.4.

2.4.3.6. Stability

The stability test was done to ensure that the analytes were stable in solution and in the matrix under different conditions. To study the stability in solution (methanol: H2O), LLOQ, ULOQ, and the internal standard were prepared and kept at room temperature for 6 hours or at 4ºC for 9 days. The prepared samples were compared with freshly prepared samples from stock stored at -20ºC. The peak area was used to compare the samples and the test was performed in triplicate.

In many cases the analytical run will last for more than 24 hours. To ensure that the processed samples were stable during the analytical run, post-preparative stability was

studied by keeping 5 samples of each of the three QC levels for 43 hours at 4ºC. Six samples of each QC low and high were used to evaluate the stability in serum under different conditions -- keeping the samples on the bench at room temperature for 21 hours ("bench top stability"); subjecting the samples to three freeze-thaw cycles (24 h at -80ºC with thaw at room temperature; "freeze thaw stability"); storing the samples at -80ºC for 28 weeks ("long-term stability"). To evaluate the stability, the concentrations in these samples were compared to the nominal values by running freshly prepared calibration curves. The accuracy had to fall within the 85-115% acceptance criteria and the relative standard deviation RSD could not exceed 15%.

2.4.4. Standards and quality control (QC)

Abiraterone and its metabolites were dissolved in methanol to prepare the stock solution of each at a concentration of 1 mg/mL. The working standard was prepared by mixing the stock solutions in one flask and diluted using methanol:H_2O at 1:1; the final concentration of abiraterone was 5.0 µg/mL and 0.25 µg/mL for the other metabolites. Freshly prepared working standard was used to prepare the serum calibrators and serum QC samples, all of which contained appropriate concentrations of all the analytes. Quality control samples were prepared at three levels, QC Low (3x LLOQ), QC Mid (half ULOQ), and QC High, which is 80% of ULOQ. The final concentrations of the calibrators and serum QC samples are listed in **Table 1**. The internal standard stock (2 mg/mL) was prepared by dissolving the stock powder in 100% methanol and further diluting it with methanol:H_2O at 1:1 to a final concentration of 2.5 µg/mL. Stock and working standard solutions were stored at -20°C, and the calibrators with QC samples were freshly prepared through the validation.

Table 1. Calibrators and quality control samples.

Sample	Volume of Working Standard (µL)	Final Volume (mL)	Final Concentration in Serum ng/mL	
			Abiraterone	Metabolites
Calibrator 1	20	10	2	0.1
Calibrator 2	40	10	4	0.2
Calibrator 3	120	10	12	0.6
Calibrator 4	300	5	60	3
Calibrator 5	600	5	120	6
Calibrator 6	1400	5	280	14
Calibrator 7	2000	5	400	20
QC Low	60	10	6	0.3
QC Mid	1000	5	200	10
QC High	1600	5	320	16

2.5. Results and Discussion

2.5.1. Method development

The challenge in the development of a comprehensive pharmacokinetic (PK) technique to determine parent drug and metabolites is to separate these compounds without compromising sensitivity and linearity. The goal here was to develop an LC-MS/MS method with an available column and reagents so the method can be adopted easily by anyone performing the same type of stereoisomer analysis. Several mobile phases were evaluated, including different organic modifiers (methanol, acetonitrile and methanol/acetonitrile mixtures) at various concentrations in water, as well mobile phases containing ammonium formate and/or formic acid without organic modifier. The Prodigy Phenomenix C_{18} analytical columns were also evaluated. Optimization of sample preparation according to recovery was also performed, various volumes of MTBE, as well as evaluating acidic and neutral reconstitution solutions. The best method was then selected based on the separation of all metabolites as well as based on the analytical qualities of linearity and sensitivity.

2.5.1.1. Optimization of the mass analyzer

Because of the steroidal nature of these metabolites and the presence of a pyridyl moiety, the mass analyzer was operated with electrospray ionization in the positive mode. The mass spectrometric parameters were optimized to ensure that the highest sensitivity possible would be achieved. Nitrogen was used as the nebulizing (40 L/min) agent and drying gas (30 L/min). Ion spray voltage and the source temperature were regulated at 2500 V and 500°C, respectively. All the analytes have the same declustering potential (120

V), collision energy (60 V), entrance potential (10 V) and collision exit potential (13 V). The metabolites mass transitions are given in **Table 2**.

2.5.1.2. Optimization of the chromatographic conditions

Due to the difficulty in distinguishing between the metabolites based on their MRM transition, we separated the metabolites (as well as the parent compound) by chromatography. Isocratic chromatographic conditions were optimized, investigating the effect of various mobile phase components at different concentrations. Separation of drug metabolites was achieved using a Zorbax Eclipse Plus C18 column 150 mm x 2.1 mm, 3.5 µm (Agilent, Santa Clara, CA) at 40ºC with an isocratic mobile phase consisting of 35% A (0.1% formic acid in water) and 65% B (0.1% formic acid in methanol:acetonitrile (60:40), at a flow rate of 0.2 mL/min. Sample injection volume was 10 µL, and analytical run time was 13 minutes. Using the optimized chromatographic conditions resulted in separating the parent compound and metabolites, as shown in **Figure 9**. It should be noted that the method was able to resolve diastereomeric metabolites with a C_{18} column -- chiral columns were not required for separation of these stereoisomers. The employment of a methanol/acetonitrile mixture was critical to achieve this separation, as methanol or acetonitrile as the sole organic modifier in the mobile phase did not resolve the chiral compounds.

2.5.1.3. Optimizing the sample preparation

The metabolites were extracted from serum following liquid-liquid extraction. Different volumes of MTBE and various reconstitution solvents to achieve higher recovery and cleaner samples were tested. Each calibrator and QC sample was taken through the following sample preparation steps. Serum, 100 µL, with spiked analytes was placed in a

glass tube, and 20 µL 2.5 µg/mL internal standard working solution was added. The samples were vortexed for 30 seconds. After addition of 2 mL MTBE, the samples were vortexed for 1 minute. The samples were then centrifuged for 5 min at 4000 rpm at 4ºC. The organic layer was transferred to another tube and evaporated to dryness under nitrogen at 40ºC. 300 µL 1:1 methanol: H_2O was used to reconstitute the dried extract and 200 µL was transferred to an HPLC vial.

2.5.2. Method validation

The method was validated according to FDA guidelines. As discussed below, all guideline criteria were met. All the analytes were stable in solution and serum, meeting the stability criterion. The criteria for linearity, accuracy and precision fell within the acceptance criteria. The method gave excellent recovery without matrix effects or interference.

2.5.2.1. Linearity

To evaluate the linearity for each analyte six calibration plots were generated. Seven non-zero points were used to generate the calibration curve. The plot of the response ratio (analyte peak area over internal standard peak area) versus the analyte concentration was linear. The mean values for slope, intercept and R^2 values for each analyte are listed in **Table 3**.

Table 2. Mass transition of abiraterone metabolites.

Analyte	**Q1** (m/z)	**Q3** (m/z)
Abiraterone	350.5	156.1
D4A	348.3	156.1
3-keto-5α-Abi	350.3	156.2
3α-OH-5α-Abi	352.4	156.2
3β-OH-5α-Abi	352.3	156.1
3-keto-5β-Abi	350.4	156.1
3α-OH-5β-Abi	352.4	156.4
3β-OH-5β-Abi	352.1	156.1
Abiraterone-d4 (IS)	354.4	160.1

IS = internal standard

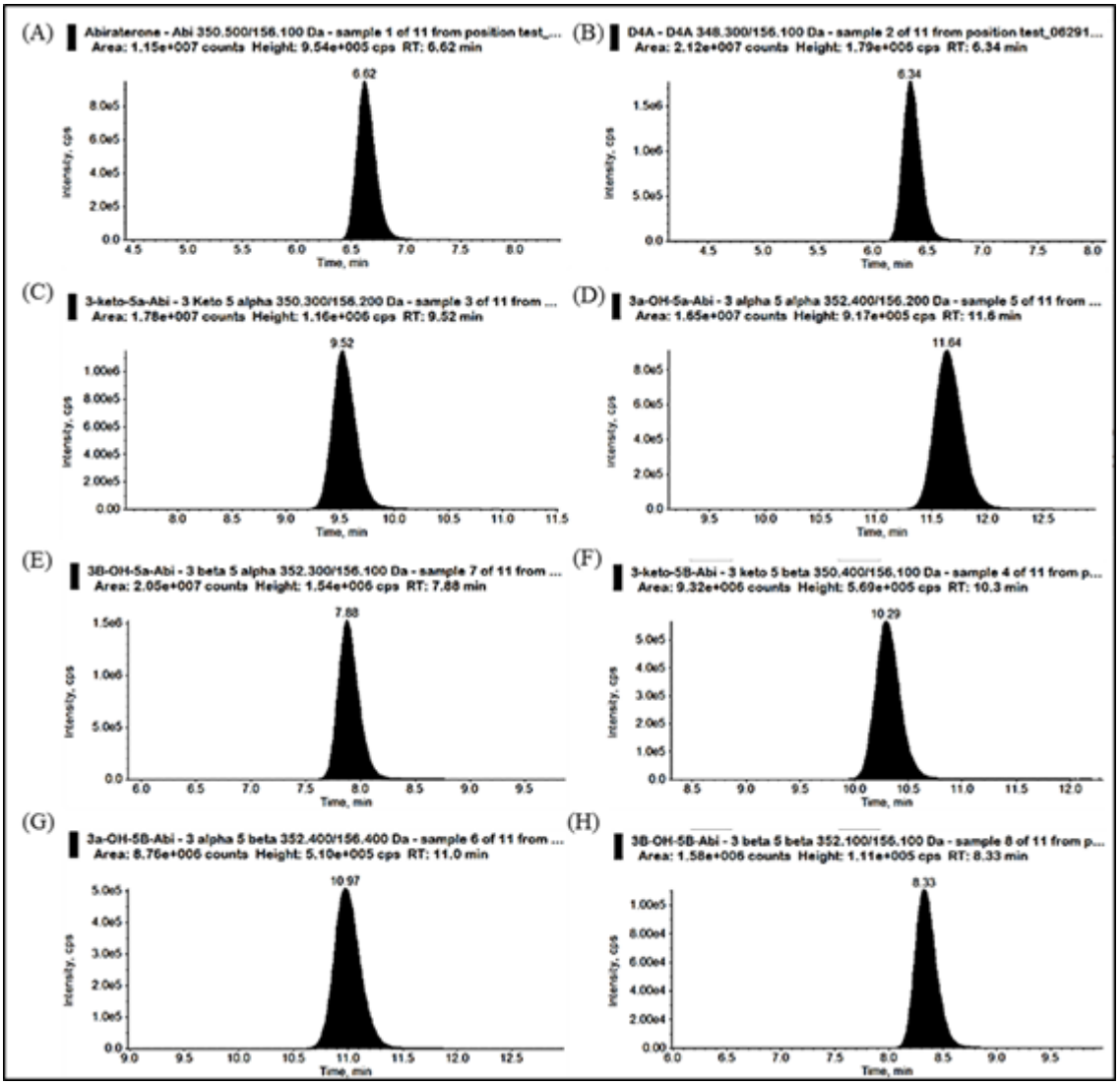

Figure 9. Chromatogram for abiraterone and its metabolites. The results were obtained by injecting 10 µL of 50 ng/mL standard solutions for A, Abi; B, D4A; C, 3-keto-5α-Abi; D, 3α-OH-5α-Abi; E, 3β-OH-5α-Abi; F, 3-keto-5β-Abi; G, 3α-OH-5β-Abi; and H, 3β-OH-5β-Abi.

Table 3. Mean values for slope, intercept and R^2

Analyte	Slope	Intercept	R^2
Abiraterone	1.80E-02	8.17E-03	0.9990
D4A	2.47E-02	3.00E-06	0.9996
3-keto-5α-Abi	2.00E-02	1.04E-04	0.9995
3α-OH-5α-Abi	2.16E-02	-6.33E-05	0.9995
3β-OH-5α-Abi	2.56E-02	1.21E-04	0.9996
3-keto-5β-Abi	1.15E-02	3.80E-05	0.9995
3α-OH-5β-Abi	1.26E-02	-3.67E-05	0.9995
3β-OH-5β-Abi	2.03E-03	5.00E-06	0.9991

2.5.2.2. Accuracy and precision

To test the method's accuracy and precision, five replicates of each QC sample were prepared on three different days. Five LLOQ samples were prepared in the first batch, and the intraday accuracy mean values were 85.3-111.2 %. All the results fall within the FDA acceptance criteria. The measured concentrations (in ng/mL) and the results for inter- and intra-day precision and accuracy determination are given in **Table 4**. Nominal concentrations for abiraterone (LLOQ = 2, QC low = 6, mid = 200, and high = 320 ng/mL); and the nominal concentrations for the metabolites (LLOQ = 0.1, QC low = 0.3, mid=10, and high=16 ng/mL).

2.5.2.3. Selectivity

Testing of six LLOQ samples, each prepared from different serum batches, were compared to their blank samples showed that the serum was free from interference. The MRM chromatograms for the six representative blank samples compared to the MRM chromatograms of LLOQ samples of abiraterone and its 7 steroidal metabolites are shown in **Figure 10**.

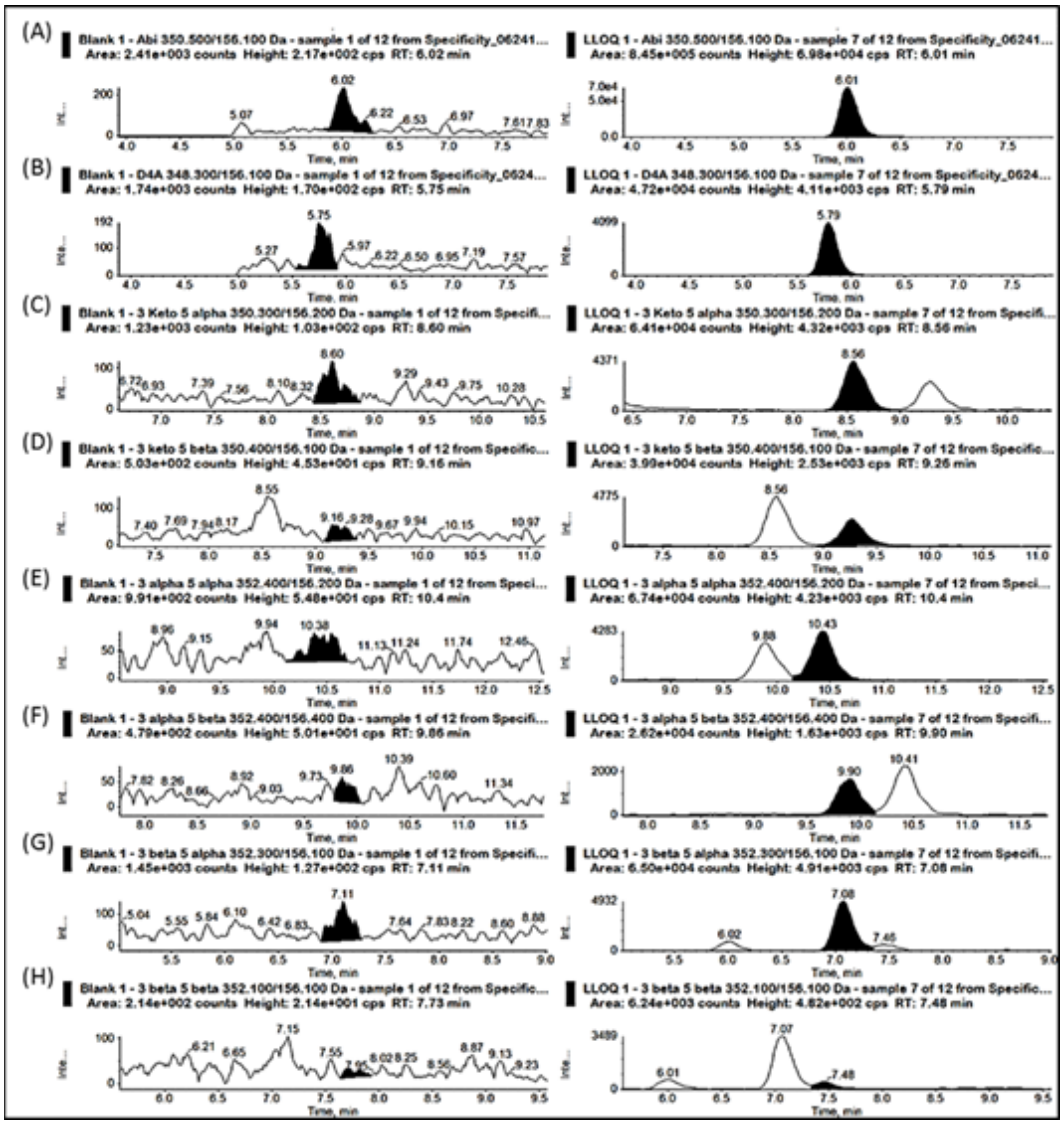

Figure 10. Representative chromatogram of selectivity studies comparing blank samples (left chromatograms) matched to LLOQ (right chromatograms) for A, Abi; B, D4A; C, 3-keto-5α-Abi; D, 3-keto-5β-Abi; E, 3α-OH-5α-Abi; F, 3α-OH-5β-Abi; G, 3β-OH-5α-Abi; and H, 3β-OH-5β-Abi.

Table 4. Intra- and inter-day accuracy and precision.

Analyte	Intra-day (n=5)			Inter-day (n=15)		
	Measured Concentration	**Accuracy %**	**RSD %**	**Measured Concentration**	**Accuracy %**	**RSD %**
Abiraterone	2.05	102.7	2.89	n.a	n.a	n.a
	6.4	106.8	2.65	6.21	103.5	4.95
	203.8	102	2.06	206.3	103.3	2.84
	316	98.7	3.86	317	99.1	6.8
D4A	0.111	111.2	3.89	n.a	n.a	n.a
	0.307	102.3	7.76	0.297	98.9	6.68
	10.02	100.2	1.86	9.74	97.4	3.94
	16.4	102.3	3.02	16	100.1	6.35
3-keto-5α-Abi	0.111	111	3.43	n.a	n.a	n.a
	0.322	107.4	1.56	0.301	100.1	7.86
	10.32	103.2	2.86	9.87	98.7	5.03
	16.8	104.9	4.68	16.5	103.1	7.56
3α-OH-5α-Abi	0.106	106.2	9.23	n.a	n.a	n.a
	0.314	104.6	5.96	0.304	101.5	9.45
	9.91	99.1	4.41	9.39	93.9	6.33
	14.8	92.6	4.97	15.1	94.5	7.61
3β-OH-5α-Abi	0.103	103	2.63	n.a	n.a	n.a
	0.305	101.5	4.21	0.301	100.3	4.66
	9.92	99.2	2.07	9.86	98.6	3.99
	16.0	99.9	4.63	16.1	100.6	6.51
3-keto-5β-Abi	0.106	106.4	4.13	n.a	n.a	n.a
	0.316	105.4	2.56	0.303	101	8.77
	9.95	99.5	2.7	9.56	95.6	4.61
	15.1	94.2	3.61	15.5	96.5	7.8
3α-OH-5β-Abi	0.108	108.4	4.26	n.a	n.a	n.a
	0.308	102.6	6.74	0.301	100.4	7.55
	9.74	97.4	2.98	9.37	93.8	4.26
	15.0	93.8	4.65	15.3	95.8	7.46
3β-OH-5β-Abi	0.085	85.3	16.8	n.a	n.a	n.a
	0.275	91.7	10.7	0.29	97.6	12.1
	9.68	96.8	0.99	9.76	97.6	3.67
	14.9	93.3	5.6	16	99.7	9.66

2.5.2.4. Recovery

The three QC levels were used to study the relative recovery, which is determined by the percent ratio of the analyte/internal standard peak area of a spiked sample before extraction over the analyte/internal standard peak area of a spiked sample after extraction. The results should be consistent, precise, and reproducible. The recovery was calculated as the mean of three triplicates for each analyte at each QC level. Recovery results and the CV% were good and are given in **Table 5**. The results met the 15% CV% criterion for acceptable recovery.

2.5.2.5. Matrix effect

The matrix effect is quantified as a matrix factor percent (MF%) by calculating the peak area ratio of analyte/internal standard of a QC low sample (post-extraction addition of analyte) over the peak area ratio of analyte/internal standard in a methanol/water solution. Matrix effect results are given in **Table 5**, showing that the technique is essentially free from interference.

2.5.2.6. Stability

Analytes were stable in the diluted solution stored at room temperature for 6 hours and at 4ºC for 9 days as given in **Table 6**. Results of serum-based stability studies employing QC samples are given in **Table 7**. The samples were found stable when stored at the autosampler temperature at 4ºC for 43 h. The analytes were stable in serum when the samples were left on the bench for 21 h. Even though all analytes did show a decrease in concentration when subjected to three freeze-thaw cycles or when stored at -80ºC for 28 weeks, the results were less than 15%, which is within the criteria for accuracy.

Table 5. Matrix effect and recovery.

Analyte	MF % (n=18)		Recovery % (n=3)					
	QC low		QC low		QC Mid		QC High	
	Mean (%)	RSD (%)	Mean (%)	RSD (%)	Mean (%)	RSD (%)	Mean (%)	RSD (%)
Abiraterone	114.7	5.04	95.7	6.54	91.7	1.49	93.4	4.65
D4A	88.5	5.99	105.2	4.78	99.0	3.39	94.6	7.81
3-keto-5α-Abi	96.1	5.22	91.6	7.47	89.1	7.62	97.7	9.12
3α-OH-5α-Abi	92.0	5.05	91.2	7.48	85.1	4.51	95.1	5.61
3β-OH-5α-Abi	99.4	4.57	88.5	6.87	86.9	2.12	92.1	5.78
3-keto-5β-Abi	93.2	8.31	91.0	13.47	87.1	6.33	96.3	6.39
3α-OH-5β-Abi	92.0	6.74	86.0	8.47	85.1	1.09	91.1	5.64
3β-OH-5β-Abi	100.0	11.13	96.6	11.50	86.3	4.28	91.4	8.16

RSD% – relative standard deviation percent which is the same as CV%

Table 6. Stock stability and post preparative stability.

Analyte	6 Hours at RT (n=3)		9 Days at 4^{0}C (n=3)		Post-Preparative 42 Hr (n=5)		
	LLOQ (%)	ULOQ (%)	LLOQ (%)	ULOQ (%)	QC Low	QC Mid	QC High
Abiraterone	98.5	103.5	109.5	98.4	97.8	101.7	98.3
D4A	100.2	102.4	91.1	86.9	96.7	96.1	100.3
3-keto-5α-Abi	112.1	103.7	101.6	88.4	100.0	100.2	101.6
3α-OH-5α-Abi	103.8	102.7	97.9	85.7	103.3	100.7	102
3β-OH-5α-Abi	105.2	102.1	101.7	89.3	100.0	98.7	98.1
3-keto-5β-Abi	107.6	103.7	97.5	83.2	103.3	101.7	102
3α-OH-5β-Abi	104.1	103.3	105.0	85.4	100.0	96.2	97.5
3β-OH-5β-Abi	115.0	104.6	95.4	89.7	103.3	98.2	100.4

RT – Room temperature

Table 7. Stability in serum.

Analyte		Short-term 21 hr		Freeze- thaw 3 cycles		Long-term 28 weeks	
		QC Low	QC High	QC Low	QC High	QC Low	QC High
Abiraterone	Concentration	5.3	293.8	5.4	284.9	5.7	290.7
	Accuracy %	88.2	91.8	89.5	89	95.5	90.8
	% RSD	6.03	1.97	11.38	9.45	0.82	2.28
D4A	Concentration	0.3	18.4	0.3	15.3	0.3	14.2
	Accuracy %	100	114.8	86.7	95.8	90	88.6
	% RSD	3.03	1.86	8.82	11.71	3.64	1.42
3-keto-5α-Abi	Concentration	0.3	15.7	0.3	14.7	0.3	14.4
	Accuracy %	93.3	98.1	86.7	91.6	86.7	90.1
	% RSD	8.04	2.57	12.84	14.11	5.9	5.59
3α-OH-5α-Abi	Concentration	0.3	15.8	0.3	14.1	0.3	14.2
	Accuracy %	96.7	98.7	86.7	88.2	86.7	88.6
	% RSD	7.16	3.4	9.82	14.26	7.32	4.34
3β-OH-5α-Abi	Concentration	0.3	15.2	0.3	13.9	0.3	14.1
	Accuracy %	90	95.1	86.7	86.7	86.7	87.9
	% RSD	10.28	2.22	14.55	11.27	4.58	2.5
3-keto-5β-Abi	Concentration	0.3	16.3	0.3	14.2	0.3	14.4
	Accuracy %	100	101.8	93.3	88.9	86.7	90.1
	% RSD	7.58	3.66	14.57	13.44	4.92	4.26
3α-OH-5β-Abi	Concentration	0.3	16.1	0.3	13.8	0.3	15
	Accuracy %	96.7	100.8	86.7	86.3	90	93.5
	% RSD	7.77	2.29	10.66	12.19	3.65	3.53
3β-OH-5β-Abi	Concentration	0.3	16.5	0.3	14.4	0.3	14.7
	Accuracy %	93.3	103	96.7	89.8	93.3	91.9
	% RSD	10.44	5.3	14.41	13.84	5.21	3.56

RSD% = relative standard deviation % is the same as CV%;

2.6. Conclusions

In this chapter an LC-MS/MS MRM method for the determination and accurate quantification of abiraterone and its metabolites in human serum was developed and validated. This is the first report of a method to determine abiraterone metabolites that result from steroidogenic metabolism. The validated LC-MS/MS method resolved and quantitated all the metabolites despite the similarity in their structures, including resolving diastereomers, a situation that precludes analysis of co-eluting isomers based solely on their MRM transitions. Reversed-phase chromatographic conditions were identified to accomplish the separation of all metabolites and their subsequent accurate quantification. This validated method can be applied to determine abiraterone and the aforementioned metabolites in human serum in clinical trials in which patients are treated with abiraterone acetate.

2.7. References

1 Pitt, J. J. Principles and Applications of Liquid Chromatography-Mass Spectrometry in Clinical Biochemistry. *The Clinical Biochemist Reviews* **30**, 19-34 (2009).

2 McDonald, J. G., Matthew, S. & Auchus, R. J. Steroid profiling by gas chromatography-mass spectrometry and high performance liquid chromatography-mass spectrometry for adrenal diseases. *Hormones & cancer* **2**, 324-332, doi:10.1007/s12672-011-0099-x (2011).

3 Wooding, K. M. & Auchus, R. J. Mass spectrometry theory and application to adrenal diseases. *Molecular and cellular endocrinology* **371**, 201-207, doi:10.1016/j.mce.2012.12.026 (2013).

4 Potter, G. A., Barrie, S. E., Jarman, M. & Rowlands, M. G. Novel steroidal inhibitors of human cytochrome P45017 alpha (17 alpha-hydroxylase-C17,20-lyase): potential agents for the treatment of prostatic cancer. *Journal of medicinal chemistry* **38**, 2463-2471 (1995).

5 Rowlands, M. G. *et al.* Esters of 3-pyridylacetic acid that combine potent inhibition of 17 alpha-hydroxylase/C17,20-lyase (cytochrome P45017 alpha) with resistance to esterase hydrolysis. *Journal of medicinal chemistry* **38**, 4191-4197 (1995).

6 Sternberg, C. N. *et al.* Abiraterone acetate for patients with metastatic castration-resistant prostate cancer progressing after chemotherapy: final analysis of a multicentre, open-label, early-access protocol trial. *The Lancet. Oncology* **15**, 1263-1268, doi:10.1016/s1470-2045(14)70417-6 (2014).

7 Ryan, C. J. *et al.* Abiraterone acetate plus prednisone versus placebo plus prednisone in chemotherapy-naive men with metastatic castration-resistant prostate cancer (COU-AA-302): final overall survival analysis of a randomised, double-blind, placebo-controlled phase 3 study. *The Lancet. Oncology* **16**, 152-160, doi:10.1016/s1470-2045(14)71205-7 (2015).

8 Acharya, M. *et al.* A phase I, open-label, single-dose, mass balance study of 14C-labeled abiraterone acetate in healthy male subjects. *Xenobiotica; the fate of foreign compounds in biological systems* **43**, 379-389, doi:10.3109/00498254.2012.721022 (2013).

9 Li, Z. *et al.* Conversion of abiraterone to D4A drives anti-tumour activity in prostate cancer. *Nature* **523**, 347-351, doi:10.1038/nature14406 (2015).

10 Li, Z. *et al.* Redirecting abiraterone metabolism to fine-tune prostate cancer anti-androgen therapy. *Nature* **533**, 547-551, doi:10.1038/nature17954 (2016).

11 Alyamani, M. *et al.* Development and validation of a novel LC-MS/MS method for simultaneous determination of abiraterone and its seven steroidal metabolites in human serum: Innovation in separation of diastereoisomers without use of a chiral column. *J Steroid Biochem Mol Biol*, doi:10.1016/j.jsbmb.2016.04.002 (2016).

CHAPTER III

DETERMINATION OF ABIRATERONE METABOLITES *IN VITRO* AND *IN VIVO*

3.1. Development of Abiraterone

When abiraterone was first studied in 1994[1], it decreased circulating testosterone levels and reduced the weights of androgen-dependent organs in mice. It was designed based on the structure of pregnenolone, which is a substrate of CYP17A1. In the early stages of abiraterone development, several structurally related compounds were studied and compared with ketoconazole which was widely used as a CYP17A1 inhibitor. The 3β-hydroxy, Δ^5 steroidal structure with a 3 pyridyl ring at C17 and the 16, 17 double bond was 10 times more potent than ketoconazole in inhibiting CYP17A1[2]. The 16, 17 double bond was reported to be necessary for the irreversible inhibition of CYP17A1[3]. The x-ray crystal structure of CYP17A1 binding to abiraterone shows that abiraterone binds to heme iron.[4]

Abiraterone was reported to inhibit 3βHSD either at high concentration or when administered with food [5,6]. Abiraterone is administered in patients as the prodrug abiraterone acetate (AA) in combination with prednisone [7-9].

Until recently, the main reported abiraterone metabolites were abiraterone sulfate and N-oxide abiraterone sulfate.[10] Recently, Li et al[11,12] reported a new pathway of abiraterone metabolism by steroidogenic enzymes. They studied the metabolism both *in vitro* and *in vivo* and were able to identify seven steroidal metabolites that were generated from abiraterone[13]. They studied the effect of the generated metabolites and showed that some of the abiraterone steroidal metabolites are biochemically active and had a crucial function in prostate cancer.

3.2. Experimental Section

3.2.1. Materials

Iscove's Modified Dulbecco's (IMDM), Roswell Park Memorial Institute (RPMI) 1640 and Dulbecco's Modified Eagle's (DMEM) media were all purchased from (Sigma-Aldrich, St. Louis, MO). Fetal Bovine Serum (FBS) from Gemini (West Sacramento, CA). VCaP cells were purchased from the American Type Culture Collection (Manassas, VA). C4-2 cells were kindly provided by Dr. Leland Chung (Cedars-Sinai Medical Center, Los Angeles, CA) and maintained in RPMI-1640 with 10% FBS. The LAPC4 cell line was kindly provided by Dr. Charles Sawyers (Memorial Sloan Kettering Cancer Center, New York, NY) and grown in IMDM with 10% FBS. All experiments done with VCaP cells were done in plates coated with poly-DL-ornithine (Sigma-Aldrich, St. Louis, MO). Cell lines were authenticated by DDC Medical (Fairfield, OH) and determined to be mycoplasma-free with primers 5'-ACACCATGGGAGCTGGTAAT-3' and 5'-

GTTCATCGACTTTCAGACCCAAGGCAT3'. All reagents used to run the LC-MS are listed in section 2.4.1.

3.2.2. *In vitro* metabolism of abiraterone

To test the hypothesis that steroidogenic enzymes present in prostate cancer cell lines can convert abiraterone to its steroidal metabolites, LC-MS analyses were performed to analyze samples obtained from *in vitro* assays using prostate cancer cell lines with known enzymatic activity: C4-2 with high 3βHSD enzymatic activity and VCaP and LAPC4 which have a robust SRD5A1 activity and a low 3βHSD enzymatic activity. Cells were seeded and incubated in 12-well plates with 0.2 million cells/well for ~24 h and then incubated with 1μM of abiraterone, D4A, 3-keto-5α-Abi, 3α-OH-5α-Abi, 3β-OH-5α-Abi, 3-keto-5β-Abi, 3α-OH-5β-Abi or 3β-OH-5β-Abi, for 24 and 48 hr. Media was collected at the two time points and were subjected to LC-MS analysis. This experiment was performed in triplicate for each drug and was repeated for three biological repeats.

3.2.3. Abiraterone metabolism in mice

To confirm that abiraterone is metabolized by steroidogenic enzymes, LC-MS analysis was utilized to confirm the metabolism in mice. Male NSG mice, 6 to 8 weeks of age were obtained from the Cleveland Clinic Biological Resources Unit facility. All mouse studies were conducted under a protocol approved by the Cleveland Clinic Institutional Animal Care and Use Committee. Mice were injected intraperitoneally with 100 μL solution containing 0.15 mmol/kg of either abiraterone (n=5), D4A (n=5), 3-keto-5α-Abi (n=4), 3α-OH-5α-Abi (n=4), or 3β-OH-5α-Abi (n = 4 mice/group). Blood was collected 2 and 4 hrs after injection, centrifuged at 10,000 rpm, and the sera were stored at -80ºC for LC-MS analysis.

3.2.4. Pharmacokinetics of abiraterone and its steroidal metabolites in human

The activities conferred by steroidal metabolites of abiraterone may make them biomarkers of clinical response or treatment resistance. To study the pharmacokinetics (PK) of abiraterone and its seven steroidal metabolites in humans, plasma samples from a clinical trial led by Janssen Pharmaceuticals were analyzed. In this pharmacokinetics study, 15 healthy male volunteers received a single oral dose of 1000 mg abiraterone acetate plus 240 mg of the AR antagonist apalutamide under fasting conditions. Serial plasma samples were collected from each volunteer to cover the period from 0-96 hours post-dose as follows: pre-dose, 0.5, 1, 1.5, 2, 4, 6, 8, 12, 24, 48, 72, and 96 hours. Aliquots of the plasma samples were subjected to LC-MS analysis to quantify the concentrations of abiraterone and its seven structurally related steroidal metabolites and to assess the pharmacokinetics parameters for each of the metabolites.

3.2.5. LC-MS analysis

All samples collected from cell metabolism, mouse metabolism, and the pharmacokinetics studies were subjected to LC-MS analysis. All the analyses were performed using the same mass spectrometer conditions and chromatographic conditions; the only difference was the sample preparation procedure. The cell metabolism sample preparation was as follows: To 200 µL media 40 µL internal standard (abiraterone-d4) was added and then the analytes were extracted with 2 ml TMBE, the TMBE was evaporated, and the remaining sample was reconstituted with 200 µL methanol:H_2O; 1:1. The standard curves were prepared in media. Samples obtained from mice were subjected to direct protein precipitation as follows: To 20 µL mouse serum, 180 µL methanol containing the IS was added; the sample was centrifuged at 10,000 g for 10 min, and then 120 µL

supernatant was transferred to HPLC vials. The standard curves were prepared in drug-free mouse sera. The pharmacokinetic samples were prepared as follows: 100 µL of human plasma was spiked with 20 µL IS, 2 ml of TBME was added, the samples were then vortexed and centrifuged. The organic layer was evaporated and the samples were reconstituted with 300 µL methanol:H_2O; 1:1.

3.3. Results and Discussion

3.3.1. Cell metabolism

3βHSD enzymatic activity is present in the C4-2 cell line; therefore treating the cells with abiraterone resulted in detection of the abiraterone downstream metabolites as shown in **Figure 11A**. When the cells were treated with D4A, the downstream metabolites also were detected but not abiraterone itself (**Fig 11B**). This indicates that 3βHSD activity is not reversible and D4A was fully consumed and metabolized after 48 hours. Treating the cells with any of the 5α-reduced metabolites resulted in detecting the other two 5α-reduced metabolites (**Fig. 11C-E**). This behavior was not observed with 5β-reduced metabolite. Only when the cells were treated with 3-keto-5β-Abi all three 5β reduced metabolites were detected (**Fig. 11F**). However, treating the cells with either 3α-OH-5β-Abi or 3β-OH-5β-Abi did not result in detecting all 5β-reduced metabolites (**Fig. 11G&H**). In the C4-2 cell line as well as VCaP and LAPC4 cells, 5β-reductase enzymatic activity is absent. Therefore, only 5α-reduced metabolites were detected when cells were treated with abiraterone or D4A. In contrast to C4-2, LAPC4 and VCaP cell line have low 3βHSD activity. Therefore, treating the cells with abiraterone resulted in low yield of the downstream metabolites (**Fig. 12A &13A**). D4A treatment in the two cell lines resulted in high yield of the 5α-reduced metabolites which substantiates their robust SRD5A1 activity

(**Fig. 12B &13B**). In VCaP and LAPC4 cells, the conversion of the 5α reduced metabolites was not interchangeable (**Fig. 12C-E &13C-E**) due to low 3βHSD activity, which is responsible for converting 3β-OH-5α-Abi back to 3-keto-5α-Abi. 3-keto-5β-Abi conversion was fast, with only 20% and 30% of the metabolites left in the media after 24 hours and almost nothing left after 48 hours (**Fig. 12F&13F**). Treating the cells with 3α-OH-5β-Abi did not result in detecting any of the other 5β-reduced metabolites (**Fig 12G&13G**). In VCaP cells within 24 hours, 20% of 3β-OH-5β-Abi was converted to 3α-OH-5β-Abi. However, in LAPC4 cells it took 48 hours to reach this percentage (**Fig 12H&13H**). Together all these results suggest that steroidogenic enzymes are responsible for the metabolism and formation of abiraterone steroidal metabolites and that once the metabolites are formed, they cannot be converted back to abiraterone.

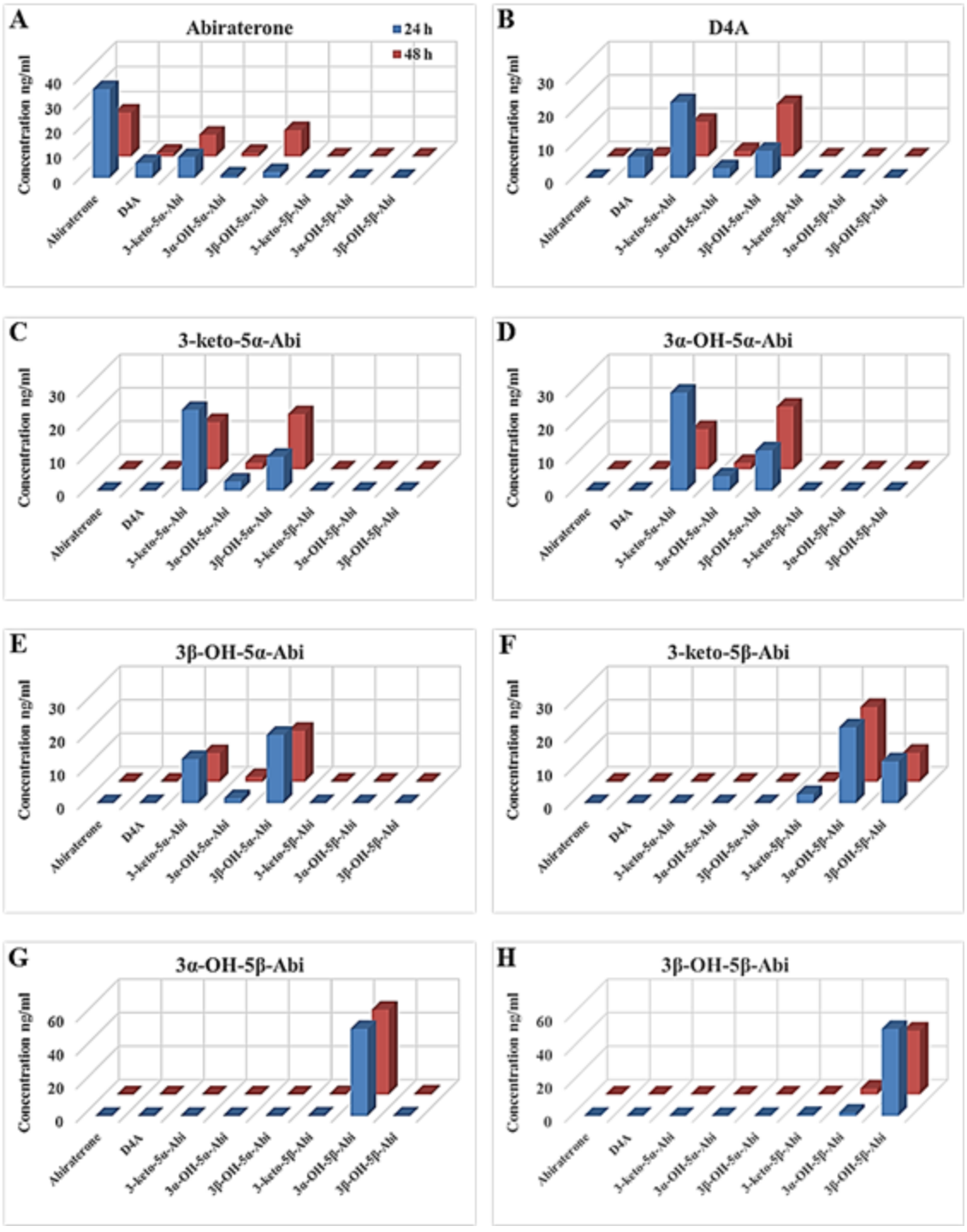

Figure 11. Metabolism of abiraterone and its metabolites in C4-2 cells. A, Abi; B, D4A; C, 3-keto-5α-Abi; D, 3α-OH-5α-Abi; E, 3β-OH-5α-Abi; F, 3-keto-5β-Abi; G, 3α-OH-5β-Abi; and H, 3β-OH-5β-Abi.

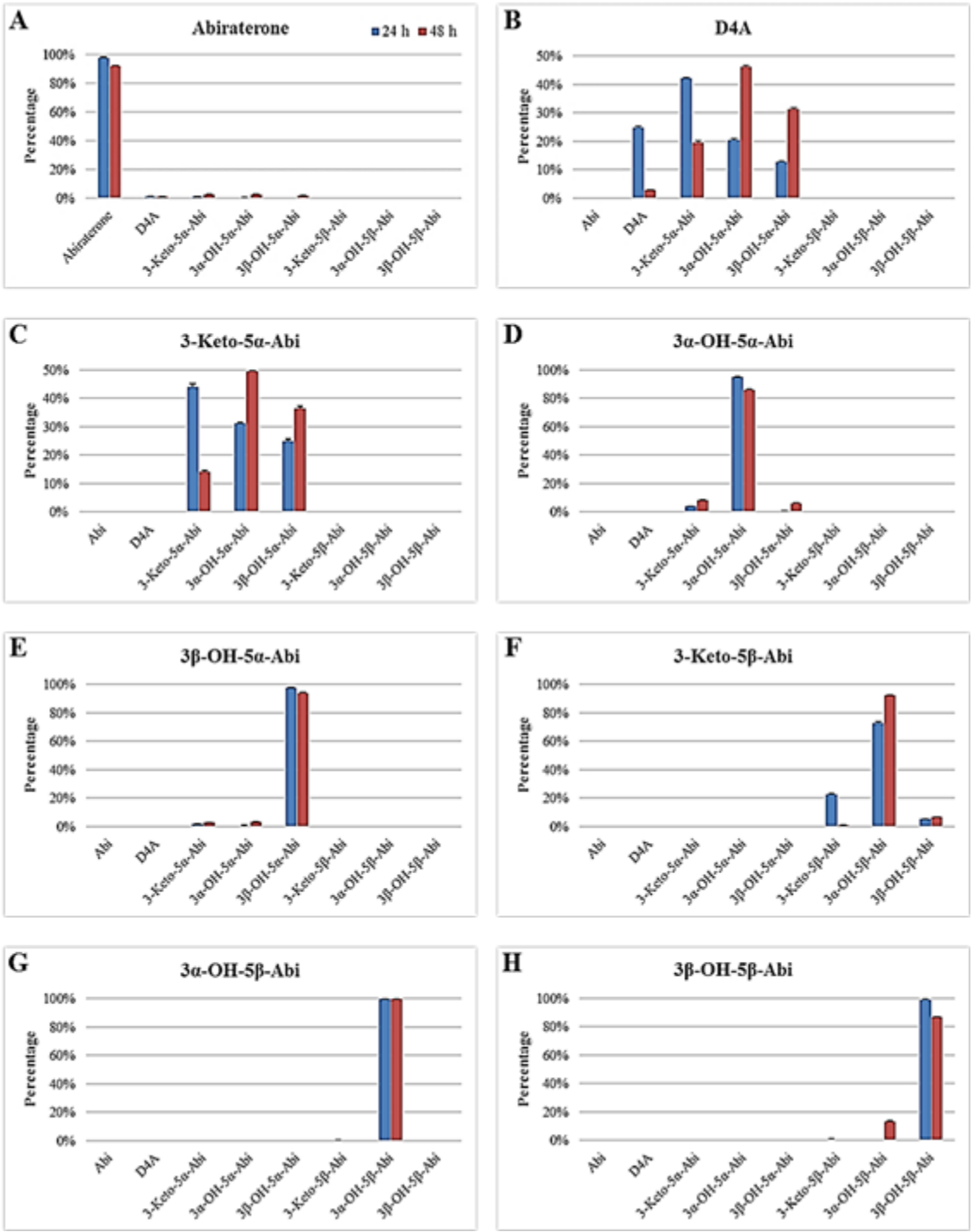

Figure 12. Metabolism of abiraterone and its metabolites in VCaP cells. A, Abi; B, D4A; C, 3-keto-5α-Abi; D, 3α-OH-5α-Abi; E, 3β-OH-5α-Abi; F, 3-keto-5β-Abi; G, 3α-OH-5β-Abi; and H, 3β-OH-5β-Abi.

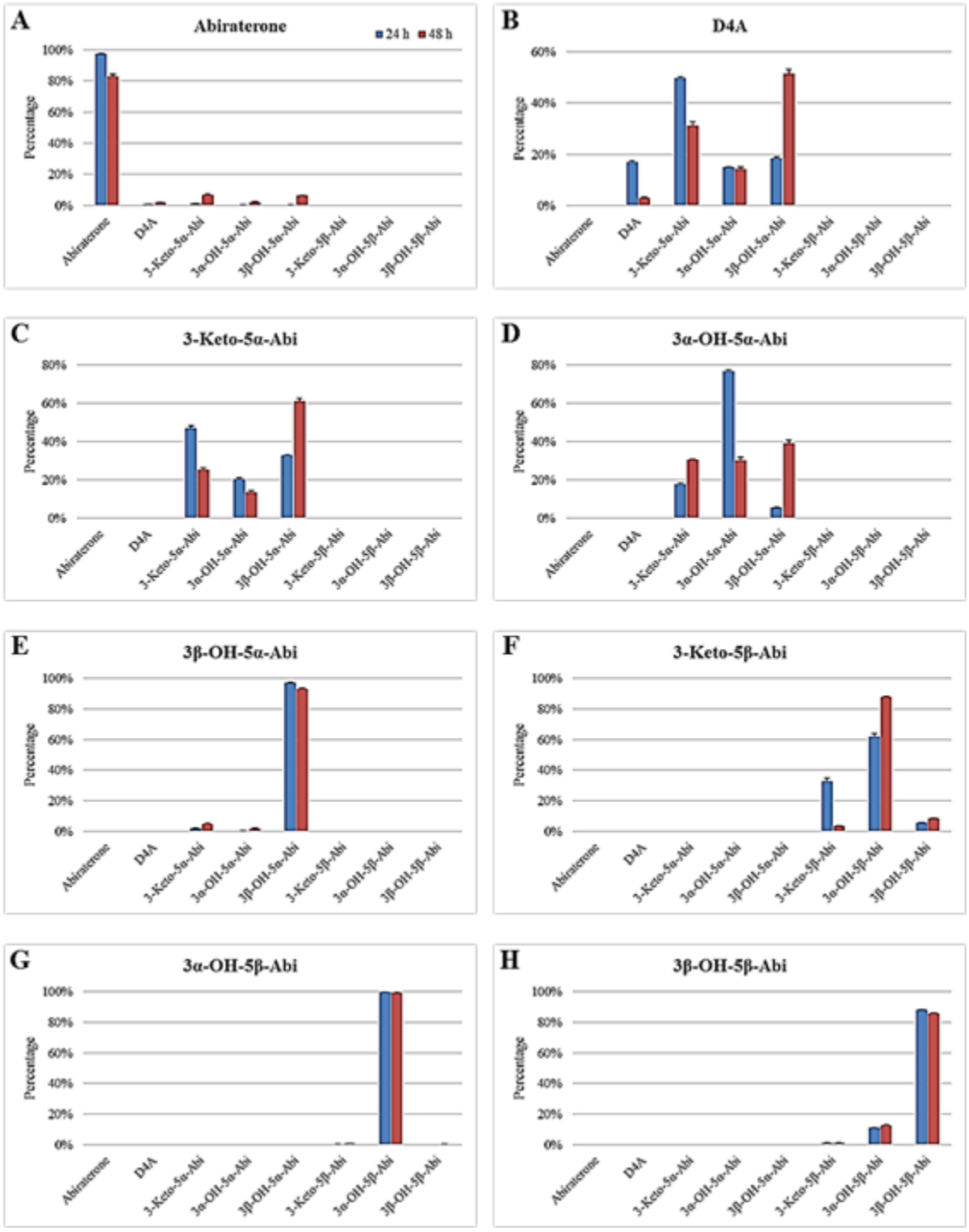

Figure 13. Metabolism of abiraterone and its metabolites in LAPC4 cells. A, Abi; B, D4A; C, 3-keto-5α-Abi; D, 3α-OH-5α-Abi; E, 3β-OH-5α-Abi; F, 3-keto-5β-Abi; G, 3α-OH-5β-Abi; and H, 3β-OH-5β-Abi.

3.3.2. Abiraterone *in vivo* metabolism

To confirm that the metabolism occurs in mice, a PK experiment was performed. Blood samples were collected 2 and 4 hr after the metabolite injection into NSG mice. The LC-MS analysis of mouse sera showed that abiraterone metabolism was fast: by 2 hrs after abiraterone injection, more than 40% was converted to the downstream metabolites, including the 5β-reduced metabolites (**Fig 14A**). In contrast, in the group of mice injected with D4A, the metabolism of D4A was not fast: only 20% was converted to the downstream metabolites after 4 hrs (**Fig 14B**). This could be due to the inhibitory effect of D4A on steroidogenic enzymes. Similar to the cell lines, conversion of the three 5α-reduced metabolites is reversible; injecting any of the 5α-reduced metabolites resulted in detecting all three of them but not abiraterone, D4A, or any of the 5β-reduced metabolites (**Fig 14C-E**). The favorite reduction pathway for 3-keto-5α-Abi is through 3α-HSD to produce 3α-OH-5α-Abi, as 45% of 3-keto-5α-Abi was converted (**Fig 14C**). In the other hand, the reversible reaction was slow: less than 10% of 3α-OH-5α-Abi was converted to 3-keto-5α-Abi. However, the 3β-OH-5α-Abi metabolite when injected into the mice resulted in the formation of both 3-keto-5α-Abi and 3α-OH-5α-Abi. All these results suggest that abiraterone metabolism occurs fast in mice and that none of the metabolites can generate abiraterone.

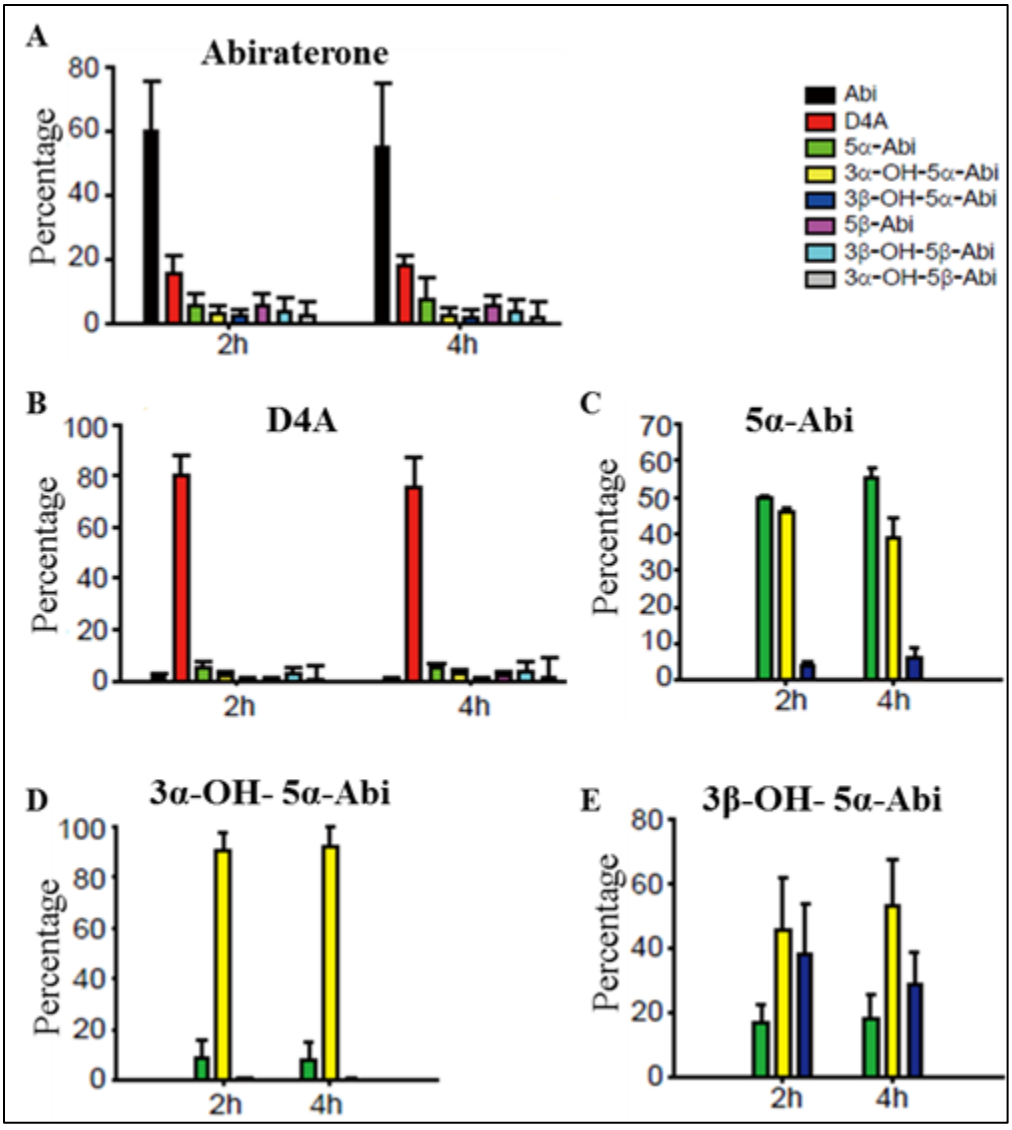

Figure 14. *In vivo* metabolism of abiraterone and its metabolites in NSG mice. A, Abi; B, D4A; C, 3-keto-5α-Abi; D, 3α-OH-5α-Abi; E, 3β-OH-5α-Abi.

3.3.3. Pharmacokinetics studies in humans

Abiraterone bioavailability was reported to be highly variable[14]. However, little is known about steroidal metabolites of abiraterone regarding the temporal nature of their formation and elimination that would inform the timing of metabolite sampling for biomarker studies. Analysis of pharmacokinetics samples from 15 healthy volunteers confirmed that not just abiraterone but its metabolites were also variable. All the metabolites were detected in the volunteers. The results in **Figure 15A-H** show the variability of the metabolite concentrations in the volunteers. The drop in the mean percentage of abiraterone over time is accompanied by a rise in the 5β-reduced metabolites (**Fig 16**). The pharmacokinetics analysis was performed assuming a non-compartmental model. The metabolite maximum concentration was achieved between 1.9-19.3 hours. The mean Tmax was 1.9 hr for abiraterone, 2.1 hr for D4A, and 2.7 hr for 3-keto-5α-Abi, and ranged between 3.2 and 19.3 hrs for the other metabolites (**Table 8**). The mean C_{max} was 90 ng/ml for abiraterone, 0.91 ng/ml for D4A, and 5.5 ng/ml for 3-keto-5α-Abi (**Table 9**). The mean AUC at 96 hrs ranged from 5.0 for 3β-OH-5α-Abi to 504 for abiraterone (**Table 10**). These data suggest that abiraterone metabolism via steroidogenic enzymes takes place rapidly and that D4A and 3-keto-5α-Abi are generated in rapid succession from the first abiraterone dose. This is the first study to evaluate the pharmacokinetics parameters of abiraterone and its seven steroidal metabolites in healthy volunteers, and these data will help in designing biomarker studies of abiraterone metabolite levels to enhance clinical treatment.

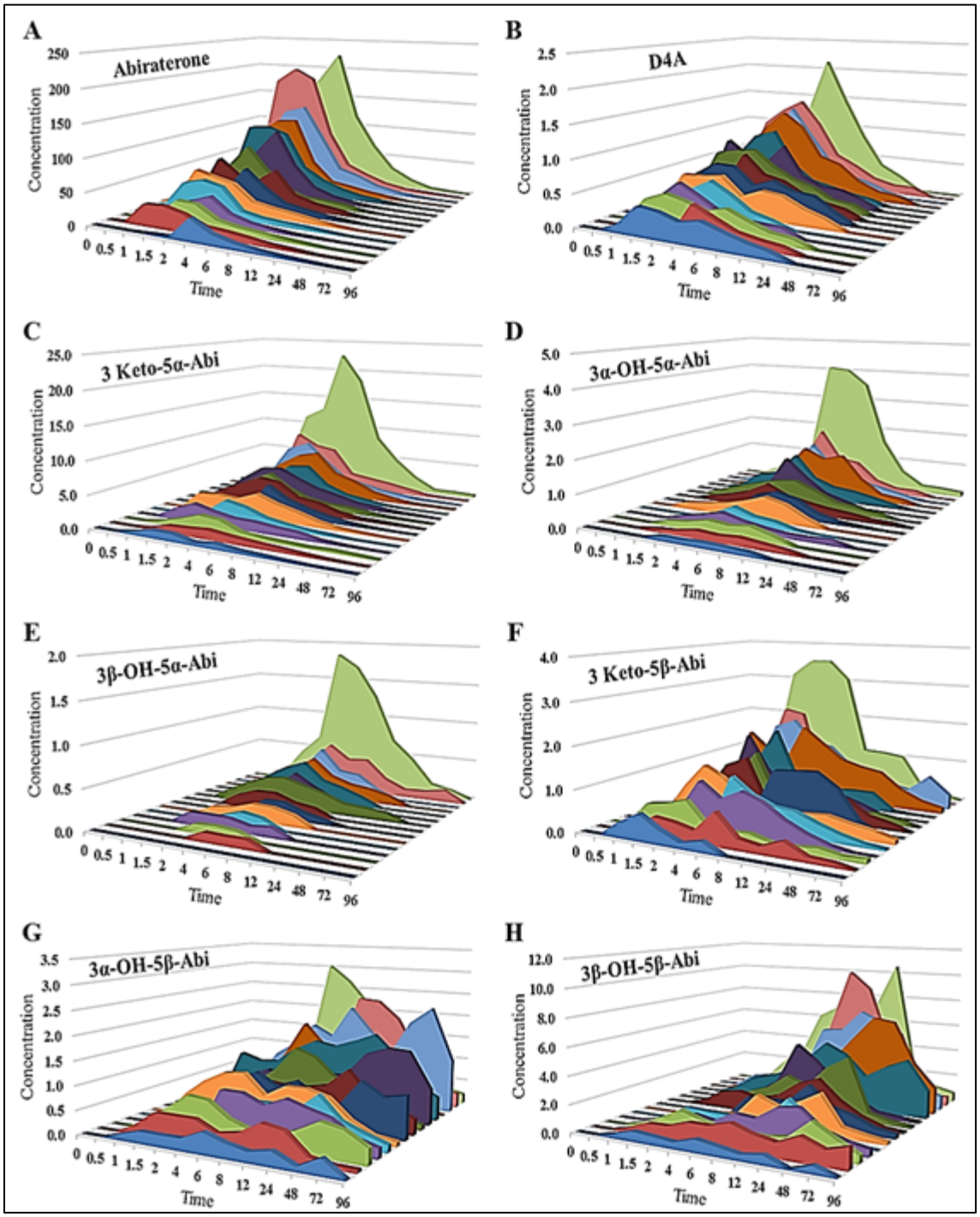

Figure 15. Pharmacokinetics of abiraterone metabolites in human serum. 15 healthy individual (color coded) draw blood up to 96 h after single dose of abiraterone acetate. A, Abi; B, D4A; C, 3-keto-5α-Abi; D, 3α-OH-5α-Abi; E, 3β-OH-5α-Abi; F, 3-keto-5β-Abi; G, 3α-OH-5β-Abi; and H, 3β-OH-5β-Abi.

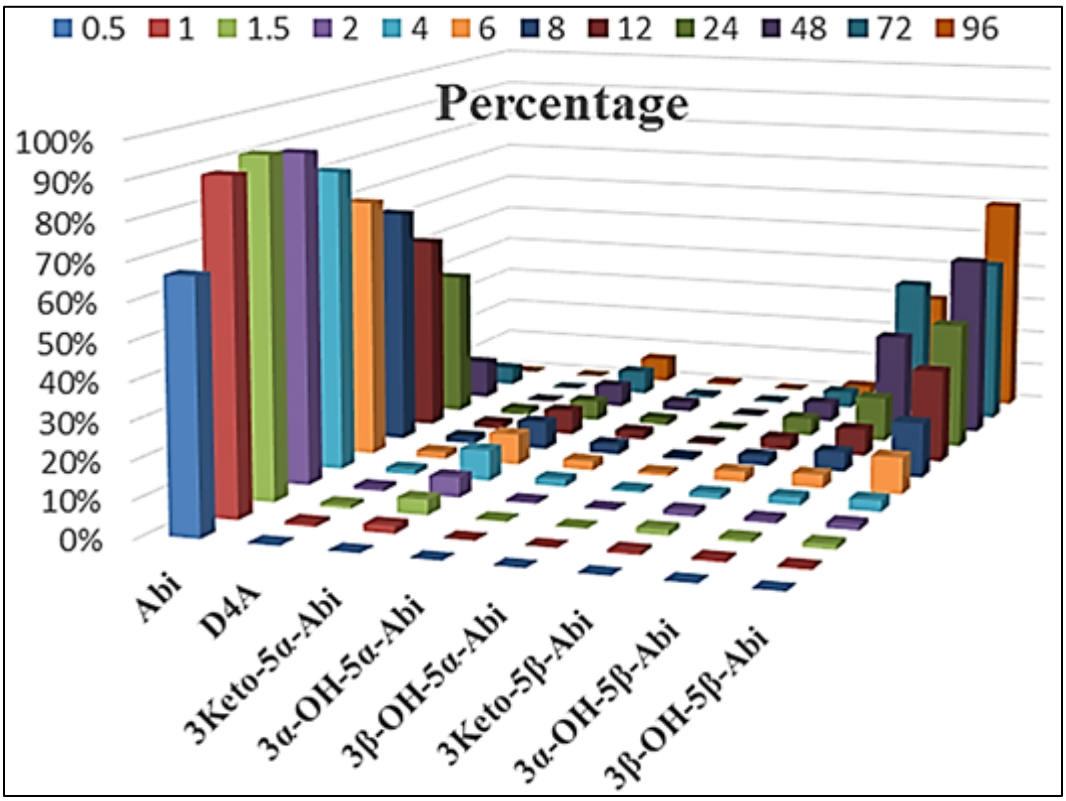

Figure 16. The mean percentage of abiraterone metabolites in human serum at 12 time points to cover the period (0.5-96 h)

Table 8. Tmax (hours) for abiraterone metabolites.

Analyte	Min	25th Percentile	Median	75th Percentile	Max	Mean	SEM
Abiraterone	1.0	1.5	1.5	2.0	4.0	1.9	0.23
D4A	1.0	1.5	2.0	2.0	4.0	2.1	0.22
3-keto-5α-Abi	1.5	2.0	2.0	4.0	4.0	2.7	0.28
3α-OH-5α-Abi	4.0	4.0	4.0	6.0	8.0	5.1	0.38
3β-OH-5α-Abi	0	4.0	4.0	4.0	6.0	3.7	0.33
3-keto-5β-Abi	1.5	1.5	2.0	4.0	12	3.2	0.72
3α-OH-5β-Abi	2.0	4.0	8.0	24	72	19.3	5.46
3β-OH-5β-Abi	6.0	8.0	12	24	48	16.8	2.92

Table 9. Cmax (ng/ml) for abiraterone metabolites.

Analyte	Min	25th Percentile	Median	75th Percentile	Max	Mean	SEM
Abiraterone	33.8	38.3	65.5	116.7	223.3	90.1	15.2
D4A	0.43	0.57	0.81	1.31	2.12	0.91	0.12
3-keto-5α-Abi	1.18	2.76	4.59	6.72	22.6	5.54	1.33
3α-OH-5α-Abi	0.16	0.44	0.76	1.47	4.07	1.06	0.25
3β-OH-5α-Abi	0.00	0.15	0.23	0.49	1.84	0.39	0.11
3-keto-5β-Abi	0.63	1.13	1.32	1.85	3.53	1.51	0.18
3α-OH-5β-Abi	0.44	0.90	1.19	1.77	3.02	1.41	0.18
3β-OH-5β-Abi	0.91	2.58	3.14	6.91	10.5	4.55	0.75

Table 10. AUC at 96 hours for abiraterone metabolites.

Analyte	Min	25th Percentile	Median	75th Percentile	Max	Mean	SEM
Abiraterone	165	233	322	596	1784	504	110
D4A	2.59	6.21	8.83	10.5	18.7	8.86	1.14
3-keto-5α-Abi	9.46	25.7	40.4	54.7	235	52.7	13.85
3α-OH-5α-Abi	1.99	4.98	8.81	16.8	63.4	14.3	3.88
3β-OH-5α-Abi	0.00	0.75	1.51	5.87	31.5	5.04	2.10
3-keto-5β-Abi	1.69	14.0	19.7	41.6	57.9	27.0	4.45
3α-OH-5β-Abi	20.1	44.2	52.1	103	162	70.6	10.21
3β-OH-5β-Abi	22.8	99.3	128	320	455	188	34.77

3.4. Conclusion

Until recently, very little was known about steroidogenic metabolism of abiraterone. The work presented here demonstrates that steroidogenic enzymes metabolize abiraterone to at least seven new compounds. The formation of the metabolites was fast as confirmed by *in vitro* and *in vivo* experiments. Conversion of abiraterone and D4A to downstream metabolites was irreversible. This was confirmed by showing that the accumulation of products did not drive flux to their precursors (in this case abiraterone and D4A). In healthy human subjects, the metabolism was also fast, and all the metabolites were detected from the first dose of abiraterone acetate. All these data confirmed the presence of a previously unappreciated novel pathway of abiraterone metabolism.

3.5. References

1 Barrie, S. E. *et al.* Pharmacology of novel steroidal inhibitors of cytochrome P450(17) alpha (17 alpha-hydroxylase/C17-20 lyase). *The Journal of steroid biochemistry and molecular biology* **50**, 267-273 (1994).

2 Potter, G. A., Barrie, S. E., Jarman, M. & Rowlands, M. G. Novel steroidal inhibitors of human cytochrome P45017 alpha (17 alpha-hydroxylase-C17,20-lyase): potential agents for the treatment of prostatic cancer. *Journal of medicinal chemistry* **38**, 2463-2471 (1995).

3 Jarman, M., Barrie, S. E. & Llera, J. M. The 16,17-double bond is needed for irreversible inhibition of human cytochrome p45017alpha by abiraterone (17-(3-pyridyl)androsta-5, 16-dien-3beta-ol) and related steroidal inhibitors. *J Med Chem* **41**, 5375-5381, doi:10.1021/jm981017j (1998).

4 DeVore, N. M. & Scott, E. E. Structures of cytochrome P450 17A1 with prostate cancer drugs abiraterone and TOK-001. *Nature* **482**, 116-119, doi:10.1038/nature10743 (2012).

5 Stover, J. T., Moore, R. A., Davis, K., Harrison, M. R. & Armstrong, A. J. Reversal of PSA progression on abiraterone acetate through the administration with food in men with metastatic castration-resistant prostate cancer. *Prostate cancer and prostatic diseases* **18**, 161-166, doi:10.1038/pcan.2015.7 (2015).

6 Li, R. *et al.* Abiraterone inhibits 3beta-hydroxysteroid dehydrogenase: a rationale for increasing drug exposure in castration-resistant prostate cancer. *Clinical cancer research : an official journal of the American Association for Cancer Research* **18**, 3571-3579, doi:10.1158/1078-0432.ccr-12-0908 (2012).

7 Kluetz, P. G. *et al.* Abiraterone acetate in combination with prednisone for the treatment of patients with metastatic castration-resistant prostate cancer: U.S. Food and Drug Administration drug approval summary. *Clin Cancer Res* **19**, 6650-6656, doi:10.1158/1078-0432.ccr-13-2134 (2013).

8 Auchus, R. J., Yu, M. K., Nguyen, S. & Mundle, S. D. Use of prednisone with abiraterone acetate in metastatic castration-resistant prostate cancer. *Oncologist* **19**, 1231-1240, doi:10.1634/theoncologist.2014-0167 (2014).

9 Ryan, C. J. *et al.* Abiraterone acetate plus prednisone versus placebo plus prednisone in chemotherapy-naive men with metastatic castration-resistant prostate cancer (COU-AA-302): final overall survival analysis of a randomised, double-blind, placebo-controlled phase 3 study. *The Lancet. Oncology* **16**, 152-160, doi:10.1016/s1470-2045(14)71205-7 (2015).

10 Acharya, M. *et al.* A phase I, open-label, single-dose, mass balance study of 14C-labeled abiraterone acetate in healthy male subjects. *Xenobiotica* **43**, 379-389, doi:10.3109/00498254.2012.721022 (2013).

11 Li, Z. *et al.* Conversion of abiraterone to D4A drives anti-tumour activity in prostate cancer. *Nature* **523**, 347-351, doi:10.1038/nature14406 (2015).

12 Li, Z. *et al.* Redirecting abiraterone metabolism to fine-tune prostate cancer anti-androgen therapy. *Nature* **533**, 547-551, doi:10.1038/nature17954 (2016).

13 Alyamani, M. *et al.* Development and validation of a novel LC-MS/MS method for simultaneous determination of abiraterone and its seven steroidal metabolites in human serum: Innovation in separation of diastereoisomers without use of a chiral column. *J Steroid Biochem Mol Biol*, doi:10.1016/j.jsbmb.2016.04.002 (2016).

14 Acharya, M. *et al.* Open-label, phase I, pharmacokinetic studies of abiraterone acetate in healthy men. *Cancer Chemotherapy and Pharmacology* **69**, 1583-1590, doi:10.1007/s00280-012-1865-3 (2012).

CHAPTER IV

ABIRATERONE METABOLISM IN PATIENTS WITH CASTRATION-RESISTANT PROSTATE CANCER

4.1. Background

Prior to its approval in 2011, abiraterone acetate went through several clinical trials to evaluate its efficacy, safety, and the dose. The first study, which was three small clinical trials, was reported in 2004 [1]. In these trials the major objective was to determine the dose that will result in maximum suppression of testosterone; the other objectives include safety and tolerability, pharmacokinetics, and evaluating some endocrine data. The second clinical trial was reported in 2008 [2]; it was a phase I/II clinical study with escalating dose of abiraterone acetate to evaluate drug safety, pharmacokinetics, and activity in chemotherapy-naive patients with CRPC. Based on the outcomes of this study, the selected dose for treatment in clinical practice was 1000 mg daily. The major side effects were associated with the blockade of CYP17A1 activity; which lowers glucocorticoid and

elevates mineralocorticoid levels. The side effects included hypertension, hypokalemia, and fluid retention, which were managed with a mineralocorticoid antagonist, and can be prevented when abiraterone acetate is administered with prednisone. Other clinical trials evaluated abiraterone acetate after ketoconazole[3] or in patients with prior treatment with chemotherapy[4,5]. Phase III trials were double-blind, placebo-controlled, multicenter designs for patients with prior chemotherapy (COU-AA-301)[6] or chemotherapy-naive CRPC patients (COU-AA-302) [7]. Based on the outcome of these two clinical trials for CRPC treatment, the US FDA approved abiraterone acetate in combination with prednisone to treat CRPC patients before or after chemotherapy. Since its approval, updated trial results have been published -- the median overall survival was 15.2 in abiraterone acetate plus prednisone arm, compared to 11.8 in the placebo plus prednisone arm for (COU-AA-301)[8]. Median overall survival was 34.7 months in the abiraterone group vs 30.3 months in the control group (COU-AA-302)[9].

As discussed in Chapter 3, abiraterone metabolism *in vitro* and *in vivo* generated at least seven metabolites through steroidogenic enzyme activity. The metabolites were also present in healthy humans in a clinical trial to evaluate the PK parameters after single dose of abiraterone acetate. Abiraterone metabolites play an important role in prostate cancer. D4A is the first downstream metabolite and inhibits the following steroidogenic enzymes: CYP17A1, 3βHSD1, and SRD5A1. It also inhibits expression of the AR-responsive genes: prostate-specific antigen (PSA), TMPRSS2, and FKBP5. *In vivo,* D4A inhibits tumor progression in xenograft mice when compared to abiraterone acetate[10]. However further metabolism of D4A will not only result in losing its effect, it will generate 3-keto-5α-Abi which stimulates the expression of AR-responsive genes and promotes tumor progression

in xenograft mice[11]. Thus, it was important to determine the metabolite levels in patients treated with abiraterone acetate.

This chapter focuses on determining abiraterone metabolites in several clinical trials that included investigation of the effect increasing the frequency of abiraterone acetate dose or adding steroidogenic enzyme inhibitors on abiraterone metabolism. In the first trial CRPC patients received a standard dose of abiraterone acetate (1 gm daily) with 5 mg twice daily of prednisone (a drug administered with abiraterone acetate to overcome adverse events). In the second study, 1 gm daily of abiraterone acetate was combined with leuprolide acetate (an LHRH agonist)[12]. The third study combined abiraterone acetate with prednisone and dutasteride (a SRD5A1 inhibitor that is used to treat benign prostate hyperplasia)[13]. The fourth and last trial was designed to study the effect of increasing the abiraterone acetate dose from 1 gm daily to 1 gm twice daily. Samples from the four trials were obtained and subjected to LC-MS analysis to measure the metabolite levels.

4.2. Determination of Abiraterone Metabolism in Clinical Trials

The common aim of these trials was to maximize the benefit of abiraterone treatment. None of these trials had a major objective to study abiraterone metabolism; however, one of the approaches to achieve the goals of these trials was through determining abiraterone metabolites and correlating them with clinical outcomes.

4.2.1. CRPC patients treated with standard dose of abiraterone acetate

In a clinical study held at the Cleveland Clinic under an Institutional Review Board – approved protocol (Case 7813), CRPC patients received a standard dose of abiraterone acetate (1gm daily) and 5mg twice daily of prednisone on an outpatient basis. The primary objective of this research study was to identify the biochemical mechanisms that underlie

resistance to hormonal therapies in advanced prostate cancer and to define the underlying mechanisms. One of the approaches was to determine abiraterone metabolites in the sera of the patients and correlate the levels with the clinical outcomes. The time from the daily dose to the blood draw was recorded. Blood was collected using Vacutainer Plus serum blood collection tubes (#BD367814, Becton Dickenson, Franklin Lakes, NJ). Blood was collected between 1 and 16 hours after the daily dose of abiraterone acetate was administered. Blood was allowed to clot and tubes were centrifuged at 2500 rpm for 10 minutes. Serum aliquots were frozen at -80°C until processing.

4.2.2. Neoadjuvant study of abiraterone in combination with an LHRH agonist

This clinical trial (NCT00924469) was a phase II open-label, randomized, multi-center study of neoadjuvant abiraterone acetate plus leuprolide acetate (an LHRH agonist) and prednisone versus leuprolide acetate alone in men with localized high-risk prostate cancer performed at Dana Farber Cancer Institute; and all patients provided written informed consent. The patients received the treatment for 24 weeks and then underwent surgery (prostatectomy). On the day of surgery, a blood sample also was drawn. The major aim of this trial was to evaluate the safety and efficacy of the combined treatment. However, for the purpose of this research, abiraterone and the metabolite levels were compared in both the prostate tissue and serum and were correlated with the clinical outcome.

4.2.3. Effect of increasing frequency to abiraterone acetate

This was a single arm, open–label, multicenter, phase II study conducted at the University of California San Francisco UCSF and Oregon Health and Science University OHSU. The study was approved by UCSF and OHSU Institutional Review Boards and all

patients provided written informed consent prior to participation. The trial aim was to evaluate the efficacy and safety of increasing abiraterone acetate dose in chemotherapy-naïve CRPC patients[3]. All patients started with the standard dose of abiraterone acetate and prednisone until the PSA concentration increased by 25% above nadir or until clinical or radiographic progression. At the time of disease progression, abiraterone acetate dose was increased to 1gm twice daily, and patients were monitored for a minimum of 12 weeks or until subsequent PSA, radiographic, or clinical progression.

4.2.4. Combining dutasteride with abiraterone acetate

This was a phase II, single-arm, multi-center, open-label study (NCT01393730) performed at Dana Farber Cancer Institute; all patients provided written informed consent. The main purpose of this research study was to determine the efficacy of adding dutasteride (SRD5A1 inhibitor) to abiraterone acetate and prednisone in patients with CRPC. Our purpose was to determine whether adding dutasteride would alter abiraterone metabolism by blocking D4A metabolism to the 5α-reduced metabolites, which may increase the levels of D4A and abiraterone, thus may be correlated with the clinical outcomes. Patients were treated with abiraterone acetate (1gm daily) and prednisone (5 mg daily) for two 4-week cycles. After this time, high-dose dutasteride (3.5 mg daily) was added (start of cycle 3). Patients continued on the 3-drug regimen until study withdrawal or radiographic disease progression. Blood samples were available from beginning of cycle 3, cycle 4, and cycle 7.

4.3. Results and Discussion

4.3.1. CRPC patients receiving standard dose of abiraterone acetate

This study is still recruiting patients in an ongoing basis. The patients included in the analysis were diagnosed with prostate cancer between January, 1994 and May, 2014 and began treatment with abiraterone acetate between December, 2011 and May, 2015. Samples from 34 patients were available for LC-MS analysis. All seven abiraterone metabolites were detected despite the treatment duration or time to blood draw (**Table 11**). Abiraterone as a percentage of the total metabolites was the greatest compared to all other metabolites, with a mean value of 43%. The lowest metabolite percentage was 3β-OH-5α-Abi at only 0.69% of the total metabolites. D4A has been reported to be more potent than abiraterone in inhibiting AR regulated gene expression. D4A levels never exceeded that of abiraterone in patients; the ratio of D4A: abiraterone ranged from 0.03-0.36 with a mean of 0.07. On the other hand, the ratio of 3-keto-5α-Abi:D4A ranged from 0.84-12.94 with a mean of 3.73. PSA concentration and *HSD3B1*genotype (a gene that can be mutated in CRPC patients) were evaluated for any correlation with the metabolite levels. However, due to the limited number of patients with a mutated gene (n=3) it was difficult to find correlations between the metabolite levels with the genotype and clinical outcomes.

4.3.2. Neoadjuvant study of abiraterone in combination with an LHRH agonist

Patients were enrolled from September 2009 through June 2011. Patients were randomized to treatment with abiraterone in combination with leuprolide and prednisone or leuprolide alone for 12 weeks. Then all patients received another 12 weeks of combination abiraterone, leuprolide and prednisone. After 24 weeks of neoadjuvant therapy, patients underwent surgery (prostatectomy). Abiraterone and leuprolide were able

to suppress tissue androgens more effectively compared to leuprolide alone. Samples from 15 patients were available for LC-MS analysis. Abiraterone metabolites were detected in both tissue and serum. In general, abiraterone levels in serum were lower than in tissue when calculated as percentage of all metabolites (**Fig 17A**). SRD5A activity is high in the prostate; thus, the D4A percentage was higher in serum than in the prostate (**Fig 17B**). Among all 5-reduced metabolites (**Fig 17C-H**), 3β-OH-5α-abi has higher tissue levels. For no metabolite did the concentration correlate with androgen levels in tissue or serum. However, the percentage of 3α-OH-5β-Abi and 3β-OH-5β-Abi in tissue and abiraterone in serum were correlated with baseline serum PSA when calculated using the Kruskal-Wallis test (**Table 12**).

4.3.3. Effect of increasing frequency to abiraterone acetate

Forty-one patients enrolled in the study from March 2013 to March 2014. In 14 of the 41 patients, the abiraterone dose was increased to 1 gm twice daily. When compared with the standard abiraterone acetate dose, abiraterone levels increased in 10 patients (**Fig 18A**), D4A levels increased in 8 (**Fig 18B**). Similar to abiraterone, 3-keto-5α-Abi levels increased in 10 patients (**Fig 18C**). 3α-OH-5α-Abi, 3β-OH-5α-Abi, and 3β-OH-5α-Abi had an increased levels in 9 patients (**Fig 18D,E&G**). 3-keto-5β-Abi and 3β-OH-5β-Abi increased in 12 of 14 patients (**Fig. 18F&H**). Overall, a non-significant increase in median abiraterone metabolite levels was observed in patients taking the increased dose, from 13.6 ng/mL at the time of progression on the standard daily abiraterone dose to 16.2 ng/mL on the increased dose (**Table 13**). Despite the escalated abiraterone dose, none of the patients had a 30% decline in PSA at study end.

Table 11. Concentration ng/ml of abiraterone metabolites in CRPC patients

Patient #	Time point hour, min	Abi	D4A	3-keto-5α-Abi	3α-OH-5α-Abi	3β-OH-5α-Abi	3-keto-5β-Abi	3α-OH-5β-Abi	3β-OH-5β-Abi
1	1,20	15.75	0.96	6.99	1.77	0.58	7.08	10.19	22.54
2	2,00	8.64	1.28	1.36	0.42	0.12	2.43	6.46	9.42
3	2,00	89.88	2.52	10.84	2.07	2.12	21.97	32.81	41.56
4	2,15	39.98	1.28	3.46	0.23	0.11	6.46	2.04	3.08
5	2,15	40.49	2.05	9.07	1.30	0.39	4.37	4.90	5.71
6	2,30	48.45	1.29	10.66	1.16	0.52	5.95	3.44	6.86
7	3,15	2.19	0.29	0.58	0.22	0.08	0.91	3.15	1.50
8	3,15	213.4	7.19	28.63	3.00	0.97	45.34	16.90	34.94
9	4,16	9.28	3.30	2.84	0.61	0.14	20.22	21.29	33.20
10	4,49	13.96	0.77	2.25	0.48	0.16	2.50	3.98	6.75
11	4,50	81.90	4.11	6.73	1.13	0.40	21.74	22.28	19.10
12	6,20	111.4	5.04	65.22	8.09	1.77	46.64	21.05	27.82
13	6,40	43.41	3.67	20.48	5.87	4.14	12.74	22.04	19.06
14	7,30	21.50	1.29	1.04	0.26	0.12	4.48	5.52	12.54
15	8,08	61.47	4.54	9.88	1.73	0.60	14.77	11.85	24.32
16	8,10	16.68	2.78	3.64	0.88	0.35	18.59	26.08	28.06
17	8,11	16.71	1.25	8.10	1.93	0.45	8.08	9.84	15.19
18	9,00	24.30	1.61	1.57	0.43	0.20	10.80	15.83	16.22
19	9,20	10.75	0.44	0.87	0.24	0.10	0.64	2.02	2.41
20	10,25	60.64	2.49	10.96	2.82	0.78	7.15	11.11	10.76
21	10,40	35.88	1.82	12.46	3.69	0.99	5.98	10.52	16.37
22	10,45	19.24	0.52	1.22	0.37	0.15	1.28	3.83	4.33
23	11,15	68.76	5.35	15.04	3.27	1.14	17.17	18.59	24.81
24	11,40	49.87	4.00	11.74	2.22	0.93	15.29	11.25	21.34
25	11,50	33.53	2.08	4.57	1.08	0.32	3.77	4.13	4.32
26	11,50	67.98	3.59	5.36	1.11	0.44	16.54	12.53	27.29
27	12,10	41.22	3.71	11.04	2.27	0.77	25.76	21.59	37.91
28	12,15	19.06	1.14	4.66	1.21	0.34	11.54	10.95	12.50
29	12,15	52.41	3.17	10.89	2.83	0.88	8.97	10.57	19.10
30	12,20	38.32	2.16	7.59	1.26	0.51	9.12	6.13	10.10
31	13,20	46.60	2.33	15.07	2.95	1.02	23.00	16.96	31.13
32	13,05	22.59	2.41	4.43	0.72	0.27	5.79	5.47	6.16
33	14,08	31.48	3.07	20.28	6.42	1.99	7.89	19.94	15.87
34	15,45	66.69	2.83	8.71	2.88	0.88	4.29	10.53	12.34

Table 12. Correlation between tissue and serum metabolites with baseline PSA

Analyte	**Tissue vs Baseline Serum PSA**		**Serum vs Baseline Serum PSA**	
	Coef	P	Coef	P
Abiraterone	-0.56*	0.03	-0.56	*0.03*
D4A	0.41	0.13	0.41	0.13
3-keto-5α-Abi	0.43	0.11	-0.01	0.96
3α-OH-5α-Abi	0.28	0.31	-0.09	0.74
3β-OH-5α-Abi	0.16	0.57	-0.05	0.87
3-keto-5β-Abi	0.41	0.13	-0.03	0.92
3α-OH-5β-Abi	0.54	*0.038*	-0.09	0.75
3β-OH-5β-Abi	0.53	*0.043*	0.09	0.75

*A negative coefficient indicates the values between metabolites and PSA were inversely correlated

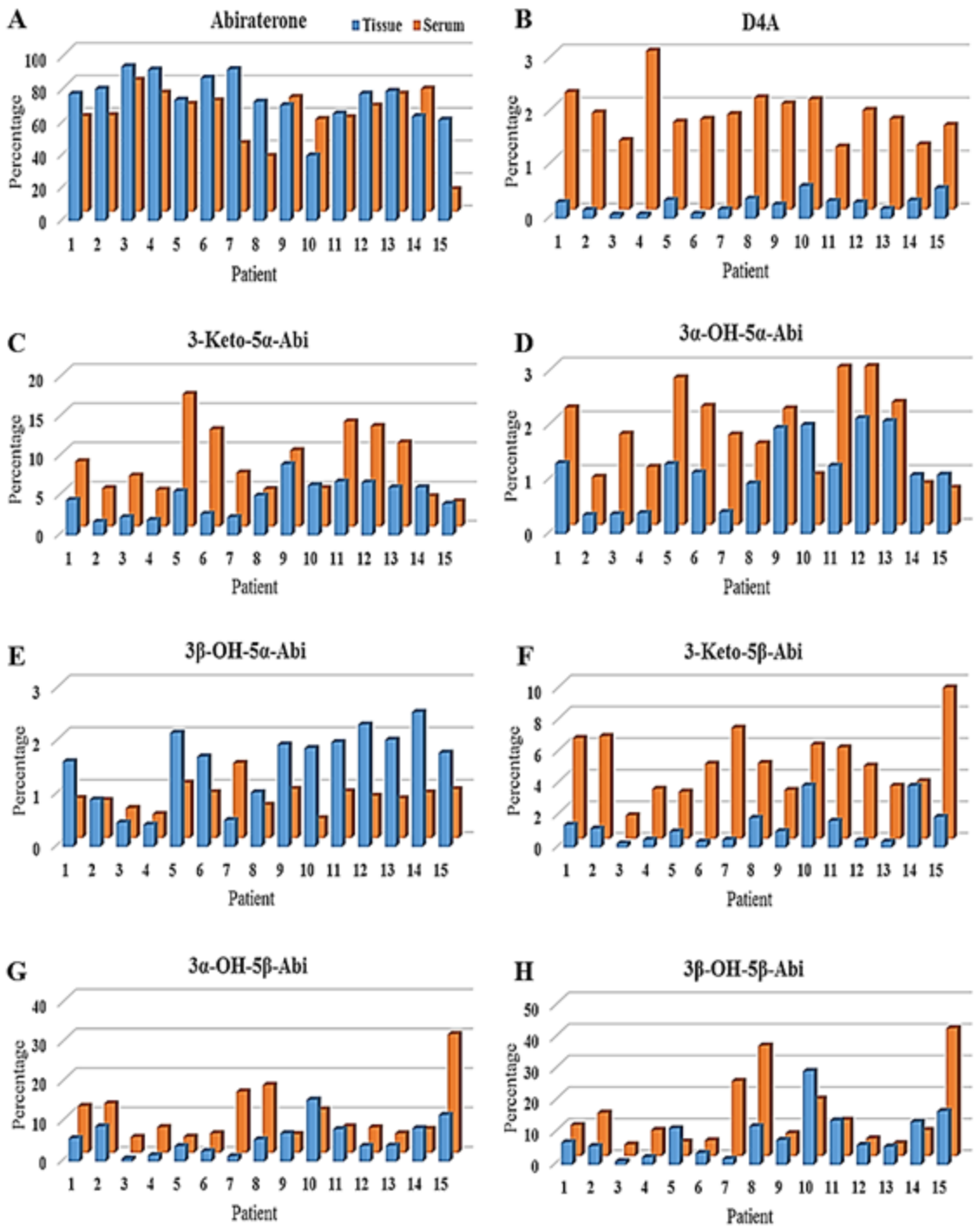

Figure 17. Abiraterone metabolites in human prostate and serum. A, Abi; B, D4A; C, 3-keto-5α-Abi; D, 3α-OH-5α-Abi; E, 3β-OH-5α-Abi; F, 3-keto-5β-Abi; G, 3α-OH-5β-Abi; and H, 3β-OH-5β-Abi.

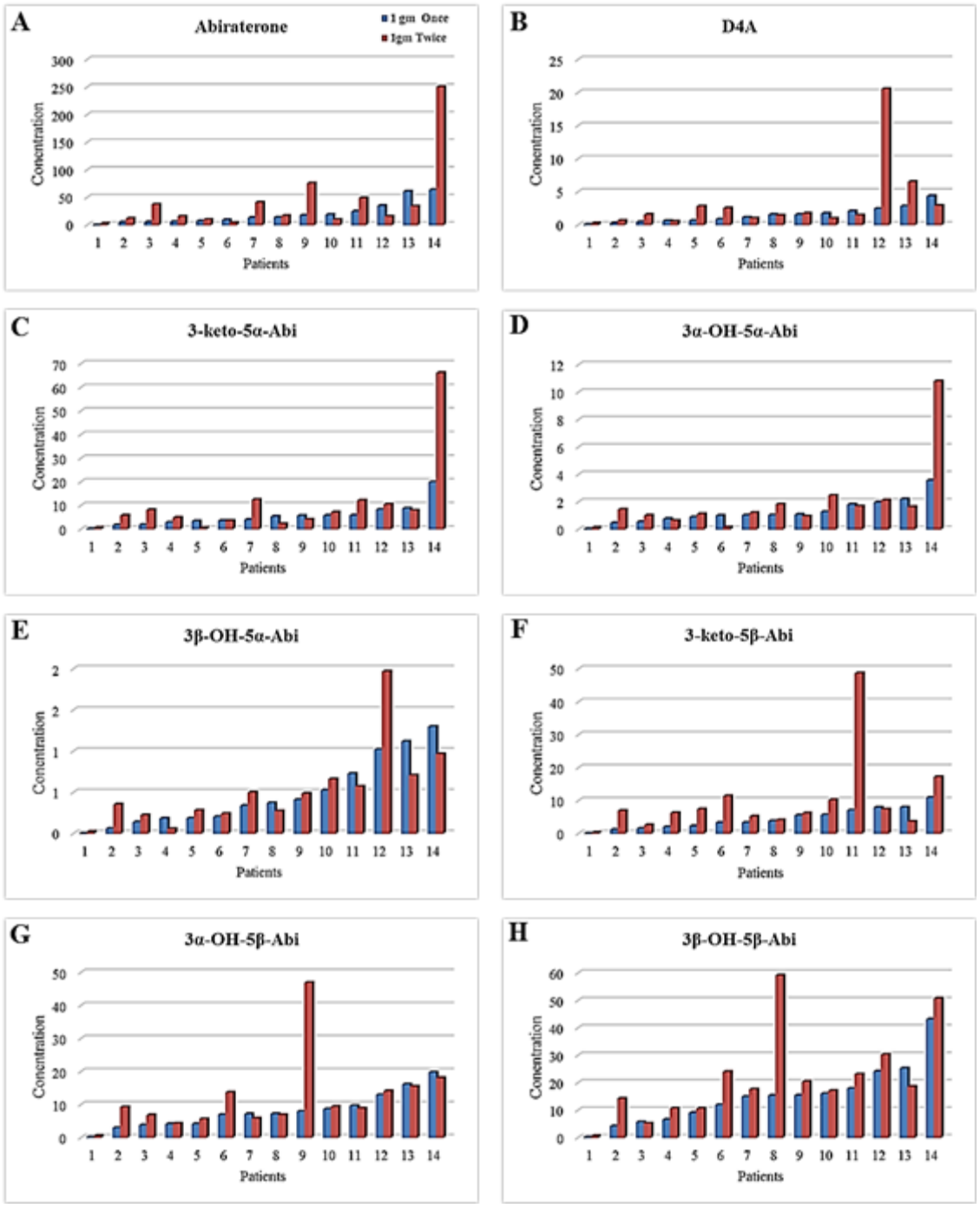

Figure 18. Metabolite concentration (ng/ml) after 1gm once vs. twice daily of abiraterone acetate. A, Abi; B, D4A; C, 3-keto-5α-Abi; D, 3α-OH-5α-Abi; E, 3β-OH-5α-Abi; F, 3-keto-5β-Abi; G, 3α-OH-5β-Abi; and H, 3β-OH-5β-Abi.

Table 13. Abiraterone dose dependent concentrations

Analyte	1gm/daily	1gm twice/daily	P
Abiraterone	13.57	16.21	0.25
D4A	1.36	1.53	0.24
3-keto-5α-Abi	4.69	6.45	0.29
3α-OH-5α-Abi	1.04	1.33	0.37
3β-OH-5α-Abi	0.36	0.42	0.76
3-keto-5β-Abi	3.55	6.62	0.12
3α-OH-5β-Abi	7.19	9.05	0.25
3β-OH-5β-Abi	15.14	18.12	0.21

4.3.4. Effect of adding dutasteride

Based on the analysis of the clinical trial with standard abiraterone acetate dose, (section 4.3.1.) 3-keto-5α-Abi:D4A ratio was 3.73. To test whether adding a SRD5A inhibitor will lower this ratio, samples from the clinical trial (NCT01393730) were analyzed. Patients enrolled between September 2011 and October 2012. Sixteen patients who had blood collected on abiraterone acetate alone (start of cycle 3) and after the addition of dutasteride (start of cycles 4 and 7) were included in the analysis (**Fig 19A**). Adding dutasteride doubled the mean concentrations of abiraterone and D4A (191.2 nM vs.372.4 nM and 9.9 nM vs. 18.2 nM ; respectively (**Table 14 and Fig 19B&C**).

On the other hand, adding dutasteride resulted in a dramatic decline in the 5α-reduced metabolites: 89% decline in the mean concentration of 3-keto-5α-Abi, 92% for 3α-OH-5α-Abi, and 73% for 3β-OH-5α-Abi (**Table 14 and Fig. 19D**). Concentrations of abiraterone, D4A, and 5α-Abi metabolites at cycle 7, the second time point after addition of dutasteride, were similar to cycle 4 (**Table 14**). Finally, the addition of dutasteride, did not decrease any of the 3 5β-reduced abiraterone metabolites, supporting a very specific biochemical effect of SRD5A inhibition on 5α-Abi metabolism (**Fig 19E**). The significance of adding dutasteride was evaluated between cycle 3 and 4 using a paired two-tailed t-test (**Table 14**). Together, these findings demonstrate that the elevated ratio of 5α-Abi:D4A in standard therapy can be lowered with dutasteride.

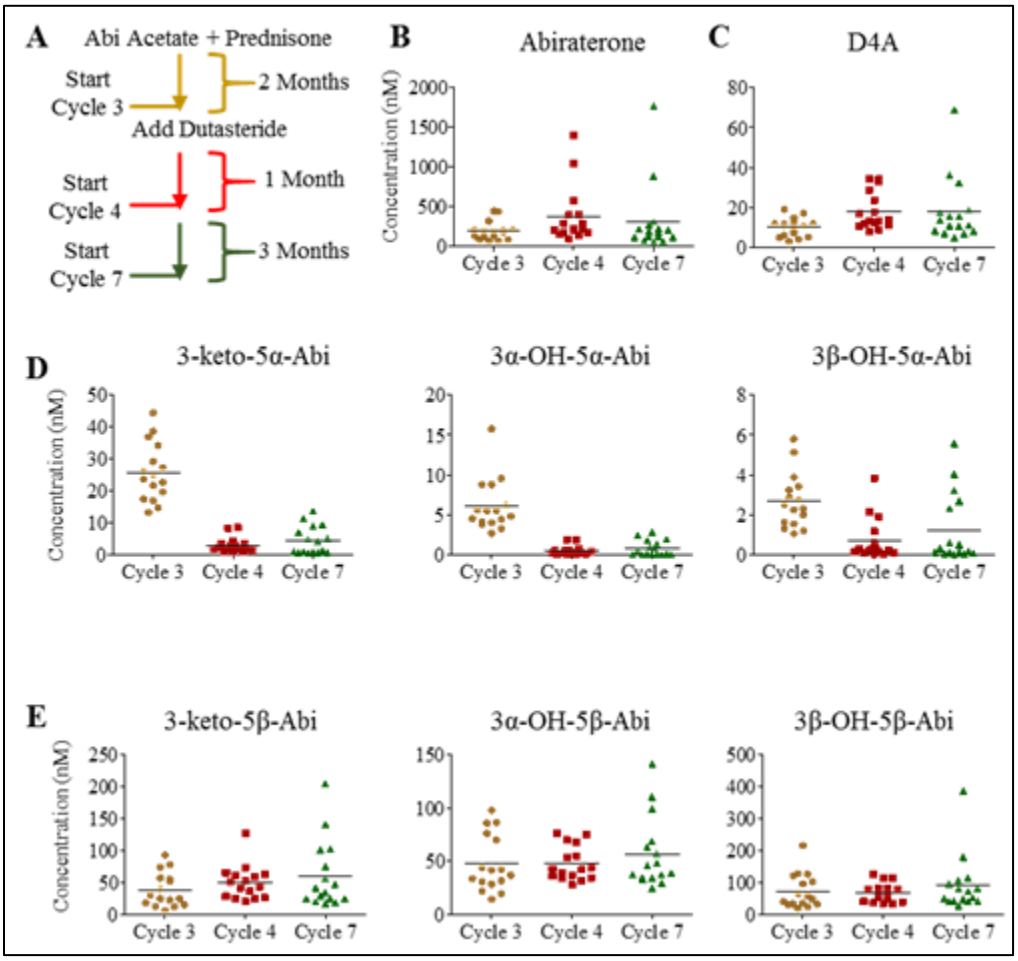

Figure 19. Effect of adding dutasteride to abiraterone; clinical trial (NCT01393730). A, Study design; B, Abi; C, D4A; D, 5α-reduced metabolites; E, 5β-reduced metabolites.

Table 14. Effect of dutasteride on abiraterone metabolites concentrations (nM)

Analyte	Cycle 3	Cycle 4	Cycle 4	P
Abiraterone	191.20	372.40	305.40	0.051
D4A	9.94	18.18	17.85	**0.002**
3-keto-5α-Abi	25.76	2.94	4.42	**<0.0001**
3α-OH-5α-Abi	6.09	0.50	0.80	**<0.0001**
3β-OH-5α-Abi	2.69	0.73	1.25	**<0.0001**
3-keto-5β-Abi	38.74	49.94	60.29	0.11
3α-OH-5β-Abi	47.78	48.00	56.59	0.97
3β-OH-5β-Abi	74.05	69.51	91.43	0.64

P value Cycle 3 vs Cycle 4

4.4. Conclusion

Abiraterone was approved in 2012 based on the outcome of the clinical trial where it showed an increase in overall survival. Since then, improving the drug is an ongoing aim for many researchers. Although the clinical trials described in this chapter were not designed to study abiraterone metabolites, we were able to detect abiraterone metabolites in order to determine whether the levels of the metabolites can be used as a potential biomarker and be correlated with clinical outcomes. None of the studies gave a clear correlation between the metabolite levels and the clinical outcomes but this is something that researchers need to take into consideration in future designs. In the abiraterone plus LHRH agonist leuprolide (neoadjuvant) study, the 5α-reduced metabolites were present in serum and the tissue at higher levels than D4A. The increased dose of abiraterone did lower PSA but it did not achieve the study goal of a 50% decline, and although the increased dose also raised the D4A level, the ratio D4A:3-Keto-5α-Abi remained the same. However, combining abiraterone acetate with dutasteride can reverse the ratio by leading to higher D4A.

4.5. References

1 O'Donnell, A. *et al.* Hormonal impact of the 17alpha-hydroxylase/C(17,20)-lyase inhibitor abiraterone acetate (CB7630) in patients with prostate cancer. *British journal of cancer* **90**, 2317-2325, doi:10.1038/sj.bjc.6601879 (2004).

2 Attard, G. *et al.* Phase I clinical trial of a selective inhibitor of CYP17, abiraterone acetate, confirms that castration-resistant prostate cancer commonly remains hormone driven. *Journal of clinical oncology : official journal of the American Society of Clinical Oncology* **26**, 4563-4571, doi:10.1200/jco.2007.15.9749 (2008).

3 Ryan, C. J. *et al.* Phase I clinical trial of the CYP17 inhibitor abiraterone acetate demonstrating clinical activity in patients with castration-resistant prostate cancer who received prior ketoconazole therapy. *Journal of clinical oncology : official journal of the American Society of Clinical Oncology* **28**, 1481-1488, doi:10.1200/jco.2009.24.1281 (2010).

4 Danila, D. C. *et al.* Phase II multicenter study of abiraterone acetate plus prednisone therapy in patients with docetaxel-treated castration-resistant prostate cancer. *Journal of clinical oncology : official journal of the American Society of Clinical Oncology* **28**, 1496-1501, doi:10.1200/jco.2009.25.9259 (2010).

5 Reid, A. H. *et al.* Significant and sustained antitumor activity in post-docetaxel, castration-resistant prostate cancer with the CYP17 inhibitor abiraterone acetate. *Journal of clinical oncology : official journal of the American Society of Clinical Oncology* **28**, 1489-1495, doi:10.1200/jco.2009.24.6819 (2010).

6 Fizazi, K. *et al.* Abiraterone acetate for treatment of metastatic castration-resistant prostate cancer: final overall survival analysis of the COU-AA-301 randomised, double-blind, placebo-controlled phase 3 study. *The Lancet. Oncology* **13**, 983-992, doi:10.1016/s1470-2045(12)70379-0 (2012).

7 Ryan, C. J. *et al.* Abiraterone in metastatic prostate cancer without previous chemotherapy. *The New England journal of medicine* **368**, 138-148, doi:10.1056/NEJMoa1209096 (2013).

8 Sternberg, C. N. *et al.* Abiraterone acetate for patients with metastatic castration-resistant prostate cancer progressing after chemotherapy: final analysis of a

multicentre, open-label, early-access protocol trial. *The Lancet. Oncology* **15**, 1263-1268, doi:10.1016/s1470-2045(14)70417-6 (2014).

9 Ryan, C. J. *et al.* Abiraterone acetate plus prednisone versus placebo plus prednisone in chemotherapy-naive men with metastatic castration-resistant prostate cancer (COU-AA-302): final overall survival analysis of a randomised, double-blind, placebo-controlled phase 3 study. *The Lancet. Oncology* **16**, 152-160, doi:10.1016/s1470-2045(14)71205-7 (2015).

10 Li, Z. *et al.* Conversion of abiraterone to D4A drives anti-tumour activity in prostate cancer. *Nature* **523**, 347-351, doi:10.1038/nature14406 (2015).

11 Li, Z. *et al.* Redirecting abiraterone metabolism to fine-tune prostate cancer anti-androgen therapy. *Nature* **533**, 547-551, doi:10.1038/nature17954 (2016).

12 Taplin, M. E. *et al.* Intense androgen-deprivation therapy with abiraterone acetate plus leuprolide acetate in patients with localized high-risk prostate cancer: results of a randomized phase II neoadjuvant study. *Journal of clinical oncology : official journal of the American Society of Clinical Oncology* **32**, 3705-3715, doi:10.1200/jco.2013.53.4578 (2014).

13 McKay, R. R. *et al.* A Phase II Trial of Abiraterone Combined with Dutasteride for Men with Metastatic Castration-Resistant Prostate Cancer. *Clinical cancer research : an official journal of the American Association for Cancer Research*, doi:10.1158/1078-0432.ccr-16-0987 (2016).

CHAPTER V

BIOCHEMICAL ACTIVITIES OF GALETERONE STEROIDAL METABOLITES

5.1. Introduction

In an effort to overcome drug resistance in prostate cancer, several approaches were taken into consideration when designing new agents, specifically, targeting androgen biosynthesis by inhibiting steroidogenic enzymes or direct targeting and antagonizing the AR. Abiraterone and enzalutamide are FDA-approved for treatment of CRPC. Abiraterone inhibits the enzyme 17α-hydroxylase/17,20-lyase (CYP17A1) [1,2], whereas enzalutamide directly antagonizes the AR[3,4]. Unfortunately, tumor resistance eventually develops against both of these agents and some evidence suggests that resistance to abiraterone is yet again engendered by a reinstatement of AR signaling[5,6]

Currently under clinical development, galeterone (Gal), 17-(1H-benzimidazol-1-yl) androsta-5,16-dien-3β-ol, is a steroidal 17-azole compound that inhibits CYP17A1,

directly competes with androgens to bind and antagonize AR, promotes AR protein degradation, and had clinical activity in a phase I/II clinical trial[7-11]. Galeterone shares its Δ^5, 3β-hydroxyl structure with abiraterone. The two drugs are distinguished by their C17 moieties – the benzamidazole ring of galeterone – and the 3-pyridyl structure of abiraterone. These differences may explain why galeterone has been reported to have more direct effects on AR

However, abiraterone is metabolized *in vivo* to Δ^4-abiraterone (D4A), which more potently than abiraterone inhibits the androgen axis[12], and 5α-abiraterone, which in contrast is an AR agonist that promotes tumor progression[13]. The differing activities of abiraterone and galeterone may be due to their respective steroidal metabolites that interact with steroidogenic enzymes and AR, which in turn may thus far have led to an incomplete accounting of the context and activities of the parent drugs. However, metabolites of galeterone along steroidogenic pathways have not yet been identified (**Fig. 20**).

The aim of this chapter is to describe *in vitro* and *in vivo* galeterone metabolism by steroidogenic enzymes and to evaluate galeterone metabolite activity in prostate cancer.

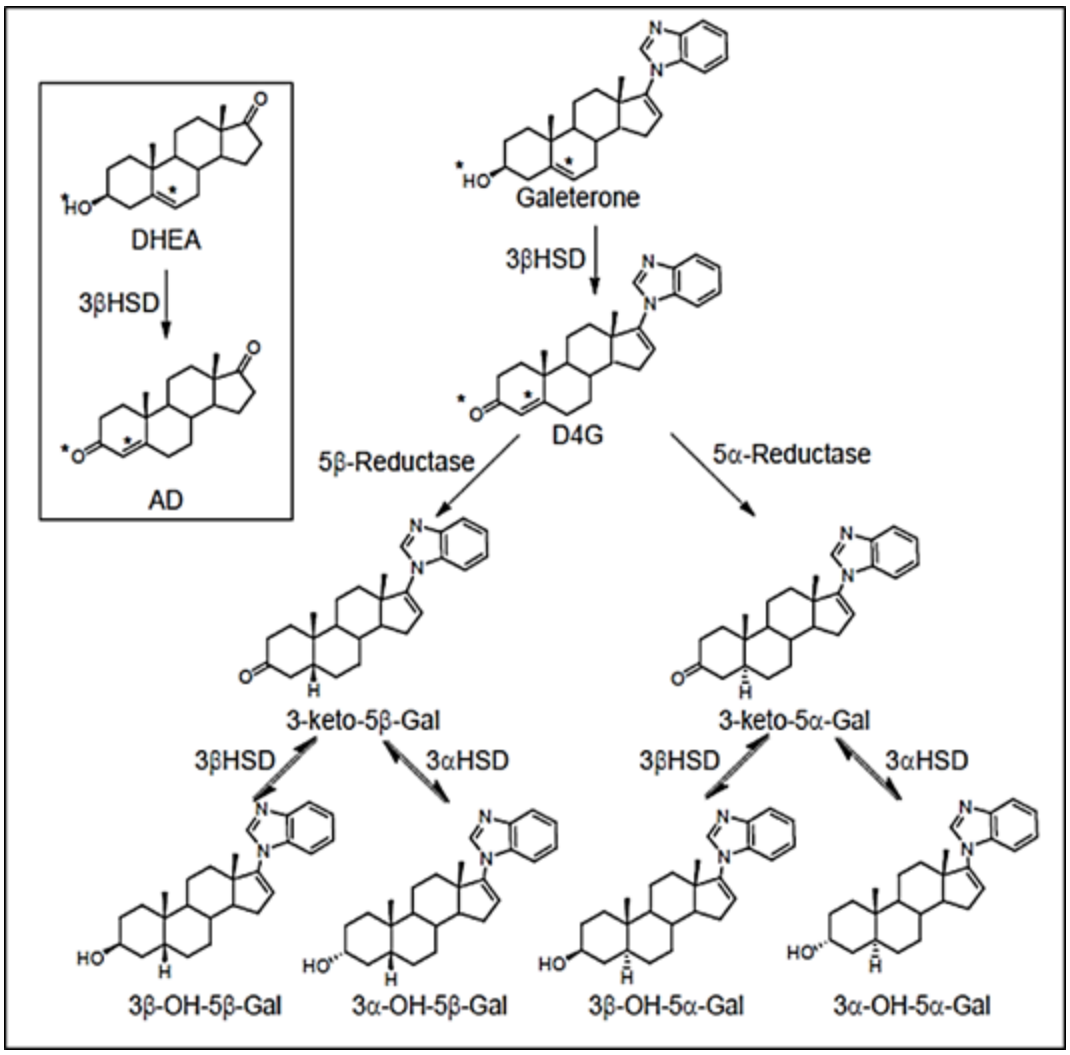

Figure 20. Steroidogenic metabolism of galeterone

5.2. Experimental Section

5.2.1. Cell lines and chemicals

LNCaP, 293T and VCaP cells were purchased from the American Type Culture Collection (Manassas, VA) and maintained in RPMI-1640 (LNCaP) or DMEM (293T and VCaP) with 10% FBS. LAPC4 cells were kindly provided by Dr. Charles Sawyers (Memorial Sloan Kettering Cancer Center, New York, NY) and grown in Iscove's Modified Dulbecco's Medium with 10% FBS. All experiments with LNCaP and VCaP cells were done in plates coated with poly-DL-ornithine (Sigma-Aldrich, St. Louis, MO). A 293T cell line stably expressing human CYP17A1 was generated by transfection with plasmid pcDNA3-c17 (a generous gift of Dr. Walter Miller, University of California, San Francisco) and selection with G418 as described[14]. Cell lines were authenticated by DDC Medical (Fairfield, OH) and determined to be mycoplasma-free using the following primers:

5'-ACACCATGGGAGCTGGTAAT-3' and

5'-GTTCATCGACTTTCAGACCCAAGGCAT3'.

Dutasteride was purchased from Medkoo Biosciences (Chapel Hill, NC). Methanol, acetonitrile, water, and formic acid were LC–MS grade and all were from Fisher Scientific (Fair Lawn, NJ). Double charcoal-stripped human serum was from Golden West Biological Inc. (Temecula, CA). Galeterone and D4G were purchased from Shanghai Forever Synthesis Co., Ltd. (Shanghai, China). 3-keto-5α-galeterone, 3α-OH-5α-galeterone, 3β-OH-5α-galeterone, 3-keto-5β-galeterone, 3α-OH-5β-galeterone, and 3β-OH-5β-galeterone were synthesized in the laboratory of Dr. Richard Auchus, University of Michigan Medical School.

5.2.2. Cell line metabolism

To test the hypothesis that galeterone would be metabolized by steroidogenic enzymes to D4G, and 6 metabolites downstream of D4G, two prostate cancer cell lines, LNCaP (which expresses mutant 3βHSD1 with high enzyme activity) [15] and LAPC4 (which expresses wild-type 3βHSD1 with low enzyme activity) [15], were used. Cells were seeded and incubated in 12-well plates with 0.2 million cells/well for ~24 h and then incubated with 0.1μM of either galeterone, D4G or 3-keto-5α-Gal (5αG) for 24 and 48 hr. Media were collected at the two time points and were subjected to LC-MS analysis. This experiments was performed in triplicate for each drug and was repeated in three biological repeats.

To confirm that steroidogenic enzymes directly metabolize galeterone, 3βHSD1, SRD5A1, or AKR1C2 was overexpressed in HEK-293 cells, which were then treated with galeterone, D4G, or 5αG respectively. Media were collected 3 and 6 hours after the treatment and were subject to LC-MS analysis.

To study the effect of blocking SRD5A1 on D4G metabolism, LAPC4 cells (which express SRD5A1) were incubated with D4G with and without SRD5A1 inhibitors (dutasteride and LY191704) or short hairpin RNAs targeting SRD5A1. Media samples were collected 3 and 6 hours and were subjected to LC-MS analysis.

5.2.3. *In vivo* metabolism

To study the metabolism of galeterone *in vivo*, male NSG mice, 6 to 8 weeks of age were obtained from the Cleveland Clinic Biological Resources Unit. All mouse studies were conducted under a protocol approved by the Cleveland Clinic Institutional Animal Care and Use Committee. Mice (n = 3 mice/group) were injected intraperitoneally with

100 μL solution containing 0.15 mmol/kg of either galeterone, D4G, 3-keto-5α-Gal 3α-OH-5α-Gal, or 3β-OH-5α-Gal. Blood was collected 2 and 4 hrs after injection, centrifuged at 10,000 rpm, and the sera were stored at -80ºC for LC-MS analysis.

5.2.4. Effects of galeterone metabolites on steroidogenic enzyme activity

To study the effect of galeterone metabolites on steroidogenic enzymes, three cell lines were used: HEK-293, LNCaP, and LAPC4. HEK-293 cells overexpressing CYP17A1 were treated with [^{3}H]-pregnenolone in the presence of D4A (0.1, 1 and 10 nM), or galeterone and its metabolites (1, 10 and 100 nM), for 3 and 6 h, and conversion to DHEA was assessed by HPLC. LNCaP cells were treated with [^{3}H]-DHEA and the indicated drugs at 0.1, 1.0, and 10 μM for 24 and 48 h, and the conversion to AD was assessed by HPLC. LAPC4 cells were treated with [^{3}H]-AD and 1, 5 and 10 μM of the indicated drugs for 8 and 24 h, and flux to 5α-dione was assessed by HPLC. All experiments went through the same protocol as follows: 12-well plates with 0.2 million cells/well for ~24 h and then incubated with indicated drugs or a mixture of radioactive ([^{3}H]-labeled) and non-radioactive steroids (final concentration, 100 nM; ~1,000,000 cpm/well; PerkinElmer, Waltham, MA) at 37ºC. Aliquots of medium were collected at the indicated times.

5.2.5. AR competition assay

The affinity of galeterone and its metabolites for mutated or wild-type AR were assessed as follows: LNCaP (mutated AR) or LAPC4 (wild-type AR) were cultured in serum-free medium for 48 h and then incubated with [^{3}H]-R1881 with or without the drugs (D4A, galeterone, D4G, 5α-Gal) for 30 min. Cells were washed with 1X PBS 4 times and 0.9% NaCl solution twice before lysis with RIPA buffer. Intracellular radioactivity was measured with a Beckman Coulter LS60001C liquid scintillation counter and normalized

to the protein concentration as detected with a Wallac Victor2 1420 Multilabel counter (Perkin Elmer).

5.2.6. Effects of galeterone metabolite on AR-regulated gene expression

To study the effect of galeterone metabolites on AR target gene expression. LNCaP and LAPC4 cells were serum starved for 48 h before treatment with DHT (0.5 or 0.1 nM, respectively) and 1 μM of galeterone, D4G, 5α-Gal, D4A or 5α-Abi for 24 h. Cells were starved with phenol red-free and serum-free medium. RNA was extracted with a GenElute Mammalian Total RNA miniprep kit (Sigma-Aldrich). cDNA was synthesized from 1 μg RNA in a reverse transcription reaction using the iScript cDNA Synthesis Kit (Bio-Rad, Hercules, CA). Quantitative PCR (qPCR) analysis was conducted in triplicate with primers for PSA, TMPRSS2, and RPLPO (housekeeping gene) in an ABI 7500 Real-Time PCR machine (Applied Biosystems) using iTaq Fast SYBR Green Supermix with ROX (Bio-Rad) in 96-well plates at a final reaction volume of 20 μL. Accurate quantitation of each mRNA was achieved by normalizing the sample values to RPLPO and to vehicle-treated cells.

5.2.7. Mouse xenograft studies

All mouse studies were conducted under a protocol approved by the Cleveland Clinic Institutional Animal Care and Use Committee. Male NSG mice, 6 to 8 weeks of age were obtained from the Cleveland Clinic Biological Resources Unit.

In order to study the efficacy of D4G as a tumor suppresser, D4G was compared with galeterone. 10^7 VCaP cells were injected subcutaneously with Matrigel into surgically orchiectomized NSG mice that were implanted with 5 mg 90-day sustained-release DHEA pellets (Innovative Research of American, Sarasota, FL) to mimic human physiology. Once

tumors reached 300 mm^3 (length × width × width × 0.52), the mice were arbitrarily assigned to vehicle (n=11), galeterone (n=11), or D4G (n=11) treatment groups. Galeterone and D4G (0.15 mmol/kg in 0.10 mL 15% ethyl alcohol in safflower oil) were administered via 5 mL/kg intraperitoneal injection twice daily, 5 days per week for up to 20 days. Control groups were administered 0.10 mL of a solution of 15% ethyl alcohol in safflower oil. Once the treatment was started, tumor volume was measured with calipers three times per week, and time to increase in tumor volume by 20% was determined. Mice were sacrificed at treatment day 20. The significance of the difference between treatment groups was assessed by Kaplan-Meier survival analysis using a log-rank test in SigmaStat 3.5. Student's t-test was used to determine significance between different treatments.

To evaluate whether 3-keto-5α-Gal enhances tumor growth, it was compared with 3-keto-5α-Abi which has been shown previously to enhance tumor growth in mice[13]. 10^7 VCaP cells were injected subcutaneously with matrigel. Once tumors reached 100 mm^3 (length × width × width height × 0.52), mice were surgically orchiectomized and arbitrarily assigned to vehicle (n=9), 3keto-5α-Abi (n=9), or 3keto-5α-Gal (n=9) treatment groups. 3keto-5α-Abi and 3keto-5α-Gal (0.15 mmol/kg in 0.10 mL 15% ethyl alcohol in safflower oil) were administered via 7.55 mL/kg intraperitoneal injection once daily, 5 days per week for 24 days. Control groups were administered 0.1 mL of a solution of 15% ethyl alcohol in safflower oil. Tumor volume was measured every other day, and time to increase in tumor volume by 30% was determined. Mice were sacrificed at treatment day 24. The significance of the difference between treatment groups was assessed by Kaplan-Meier survival analysis using a log-rank test in SigmaStat 3.5. Student's t-test was used to determine significance.

5.2.8. High-performance liquid chromatography (HPLC)

Collected medium from the experiments in section 5.2.4. was treated with 1,000 units of β-glucuronidase (Helix pomatia; Sigma-Aldrich) at 37°C for 2 h, extracted with 860 µL ethyl acetate:isooctane (1:1), and concentrated under nitrogen gas. HPLC analysis was performed on a Waters 717 Plus HPLC or an Agilent 1260 HPLC. Dried samples were reconstituted in 100 µl 50% methanol and injected into the instrument. Steroids were separated on a Kinetex 100 × 2.1 mm, 2.6 µm particle size C_{18} reverse-phase column (Phenomenex, Torrance, CA) using a methanol/water gradient at 30°C. The column effluent was analyzed using a dual-wavelength UV-visible detector set at 254 nm or β-RAM model 3 in-line radioactivity detector (IN/US Systems, Inc.) and Liquiscint scintillation cocktail (National Diagnostics, Atlanta, GA). All HPLC studies were conducted in triplicate and repeated at least 3 times in independent experiments.

5.2.9. Mass spectrometry

Galeterone and its seven steroidal metabolites were determined using the validated LC-MS method for the determination of abiraterone and its seven structurally related metabolites[16] with slight modifications. The mobile phase consisted of 30% A (0.2% formic acid in water) and 70% B (0.2% formic acid in methanol:acetonitrile, 60:40). Separation of the metabolites was achieved using a Zorbax Eclipse plus 150 x 2.1 mm, 3.5µm C18 column (Agilent, Santa Clara, CA) at a flow rate of 0.2 ml/min. Drug metabolites were ionized using electrospray ionization in positive ion mode.

The LC-MS method was applied to analyze cell media and mouse serum samples. To 200 µL media, 40 µL internal standard (abiraterone) was added, then the analytes were extracted with 2 ml TMBE (Sigma Aldrich, St. Louis, MO), the TMBE was evaporated,

and the sample reconstituted with 200 µL (methanol:H_2O; 1:1). The standard curves were prepared in media. The metabolites were extracted from 20 µl mouse serum by adding 280 µl methanol containing the internal standard. The samples were then vortexed and centrifuged at 12,000 rpm for 10 min, and 200 µl supernatant was transferred to the HPLC vial.

To extract the metabolites from the tumor, tumor (28.3-63.3 mg) was homogenized with 750 µl LC-MS grade water. Then 75 µl internal standard (abiraterone) was added to the mixture, the metabolites were extracted from the homogenate using 2.5 ml TMBE, the organic layer was then evaporated, and the samples were reconstituted with 300 µl methanol: water (50:50).

5.3. Results and Discussion

5.3.1. Galeterone metabolite separation by LC-MS/MS

The modifications of abiraterone validated LC-MS/MS method resolved all galeterone metabolites (**Fig 21**). The method was applied to detect galeterone metabolites in cell media, mouse serum, and mouse tumor

5.3.2. *In vitro* metabolism of galeterone by steroidogenic enzymes

After treating LNCaP and LAPC4 cells with galeterone for 24 or 48h, galeterone metabolites including D4G, 5αG, 3α-OH-5αG and 3β-OH-5αG were detected by LC-MS. Metabolism of galeterone to D4G and to subsequent 5α-reduced metabolites was more robust in LNCaP than LAPC4 cells (**Fig. 22A&B**), consistent with the known high 3βHSD enzyme activity in LNCaP cells. D4G was converted to 5αG, 3α-OH-5αG, and 3β-OH-5αG but not back to galeterone, indicating that conversion from galeterone to D4G is irreversible. 5αG treatment led to the production of 3α-OH-5αG and 3β-OH-5αG but not

D4G or galeterone. No 5β-reduced metabolites were detectable, consistent with the absence of 5β-reductase activity in prostate cancer cell lines.

Expression of 3βHSD1 in HEK-293 cells permitted the conversion from galeterone to D4G (**Fig. 23A**). Similarly, expression of SRD5A1 or SRD5A2 resulted in the conversion of D4G to 5αG (**Fig. 23B**). Expression of AKR1C2, the major enzyme that converts endogenous 3-keto steroids such as DHT to their 3α-OH metabolites, enabled the conversion from 5αG to 3α-OH-5α-Gal in a time- and concentration-dependent manner (**Fig. 23C**). In LAPC4 cells with endogenous SRD5A1 activity, the SRD5A inhibitor LY191704 or dutasteride blocked the conversion from D4G to 5αG (**Fig. 24A**). Stable SRD5A1 knockdown with short hairpin RNAs similarly ablated metabolism from D4G to 5αG (**Fig. 24B**). Together, these data support the hypothesis that galeterone undergoes direct metabolism by steroidogenic enzymes, similar to endogenous steroids and the structurally related drug, abiraterone.

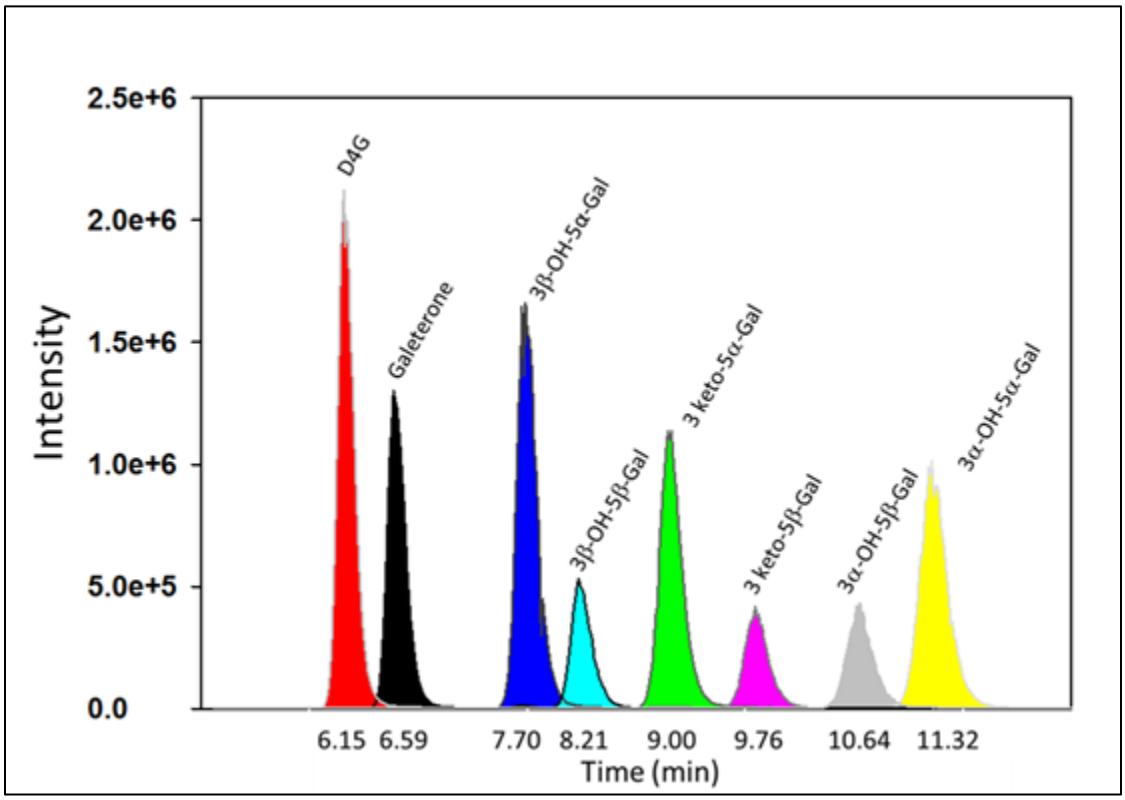

Figure 21. LC-MS separation of all galeterone metabolites. The results were obtained by injecting 10 µL of 50 ng/mL standard mixture of galeterone and its metabolites.

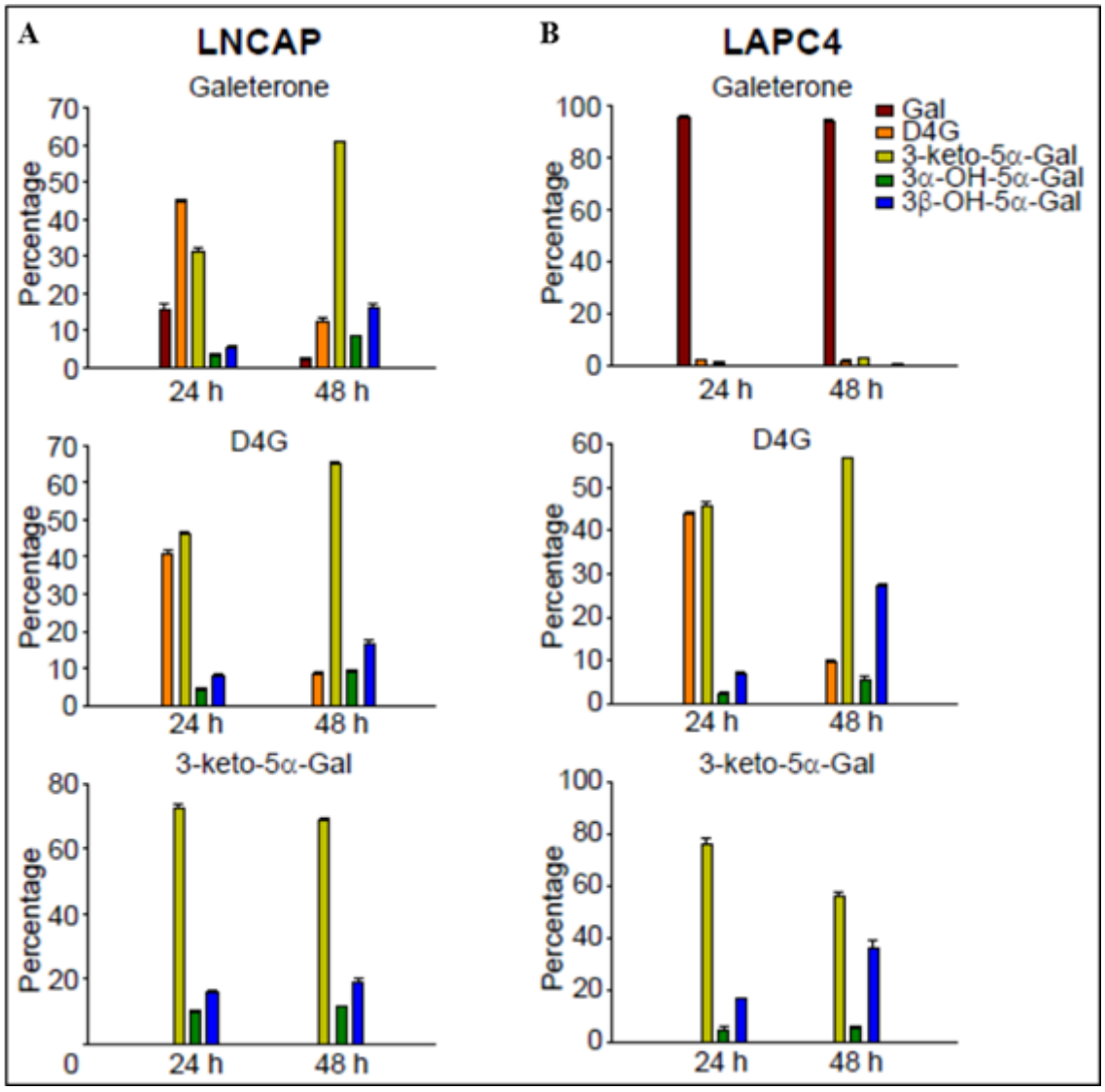

Figure 22. Metabolism of galeterone and its metabolites in A, LNCAP and B, LAPC4 cells

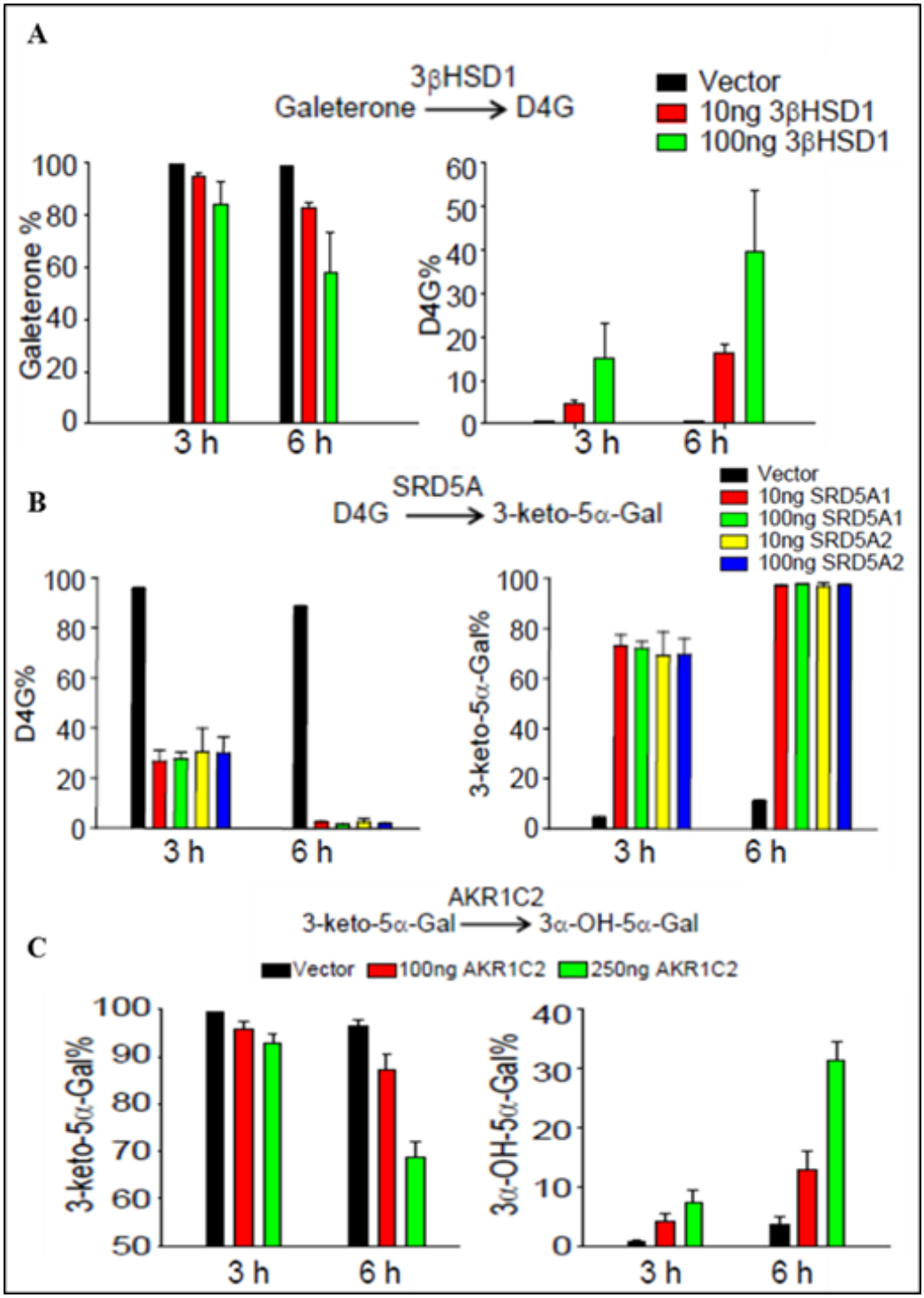

Figure 23. Steroidogenic enzymes required for galeterone metabolism. Overexpressing of A, 3βHSD1; B, SRD5A; and C, AKR1C2 resulted in converting the precursors.

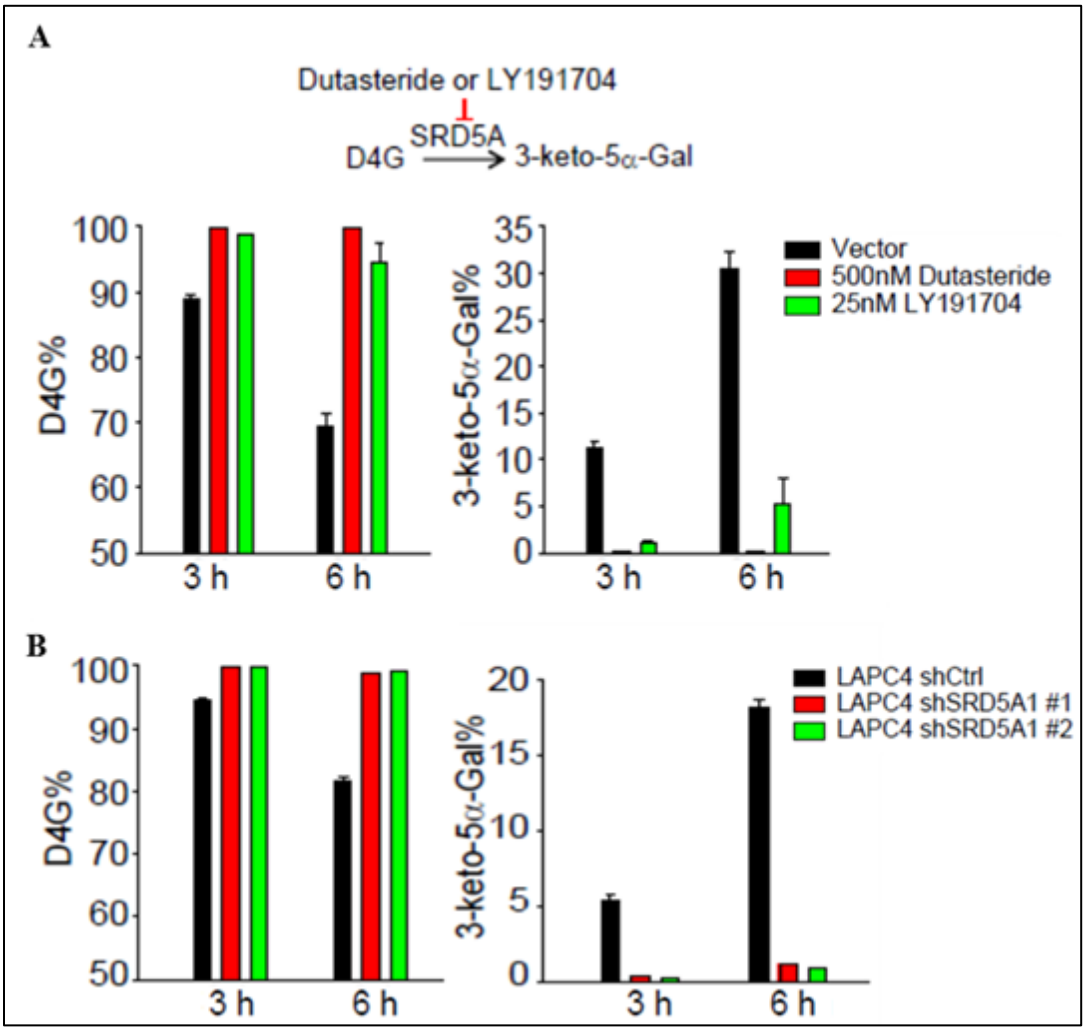

Figure 24. Effect of blocking SRD5A1 on D4G metabolism. D4G conversion was blocked A, Pharmacologically or B, genetically.

5.3.3. *In vivo* metabolism

Galeterone and its metabolites were injected into NSG mice to determine its metabolism *in vivo* (**Fig. 25**). In addition to D4G and the three 5α-reduced metabolites, three 5β-reduced metabolites – 5βG, 3α-OH-5βG and 3β-OH-5βG – were detected in mouse serum after galeterone injection. Furthermore, injecting any one 5αG-compound led to detection of all three 5α-reduced metabolites, which indicates that 5αG, 3α-OH-5α-G and 3β-OH-5α-G are interconvertible *in vivo*. In subsequent studies, we focused on D4G and the 5α-reduced metabolites because 5α-reduction leads to the formation of a planar structure, as occurs with the most potent endogenous androgen, DHT[17,18]. On the other hand, 5β-reduction of 3-keto steroids introduces a 90° bend, which generally inactivates steroid hormones and facilitates their clearance.

5.3.4. Effects of galeterone metabolites on steroidogenic enzyme activity

Galeterone was reported to be more potent than abiraterone against CYP17A1 expressed in *E. coli*[7,19]. However, the comparative effects of their respective metabolites on steroidogenic enzymes is not known. D4A, the abiraterone metabolite that most potently inhibits steroidogenesis, was compared with galeterone and its metabolites[12]. In HEK-293 cells stably expressing CYP17A1, D4A, at a concentration of 10 nM, completely blocked CYP17A1-catalyzed conversion of [3H]-pregnenolone to DHEA. Galeterone and its metabolites were approximately 100-fold weaker in blocking the production of DHEA (**Fig. 26A**). This result indicated that galeterone and its metabolites are 100-fold less potent than D4A in blocking CYP17A1 activity. In LNCaP cells, which possess high 3βHSD enzyme activity, galeterone inhibited the conversion of [3H]-DHEA to Δ^4-androstenedione (AD), comparably to D4G and D4A (**Fig. 26B**). Conversion from D4G to 5αG slightly

reduces the capacity to inhibit 3βHSD1 activity. D4G was more potent than galeterone and comparable to D4A in inhibiting SRD5A activity, as assessed with the conversion of [3H]-AD to 5α-dione in LAPC4 cells (**Fig. 26C**).

5.3.5. The effect of galeterone and its metabolites on AR and AR signaling

Galeterone has been reported to directly bind to and enhance the degradation of AR[10]. To determine the affinity of galeterone and its metabolites for AR, a competition assay was performed. The affinity of D4G for mutant AR (expressed in LNCaP, T877A) and wild-type AR (expressed in LAPC4 cells) was greater than that of galeterone, comparable to that of D4A, and comparable to or slightly greater than that of 5αG (**Fig. 27A&B).** To assess the functional consequences of galeterone and its metabolites, their effects on expression of androgen-responsive genes were investigated. Galeterone and D4G inhibited DHT-induced AR-target gene expression in LNCaP and LAPC4 cells, comparable to D4A (**Fig. 27C&D**). To a lesser extent, 5αG also suppressed DHT-induced gene expression. Notably, however, 5αG somewhat increased basal *PSA* expression in the absence of DHT in LNCaP cells. Compared with 3-keto-5α-abiraterone (5α-Abi), a weak AR agonist, 5αG is an even weaker agonist (**Fig. 27C&D**). Taken together, these data indicate that the conversion from galeterone and D4G by SRD5A to 5αG may lead to a diminished effect on AR stability and AR-responsive gene expression.

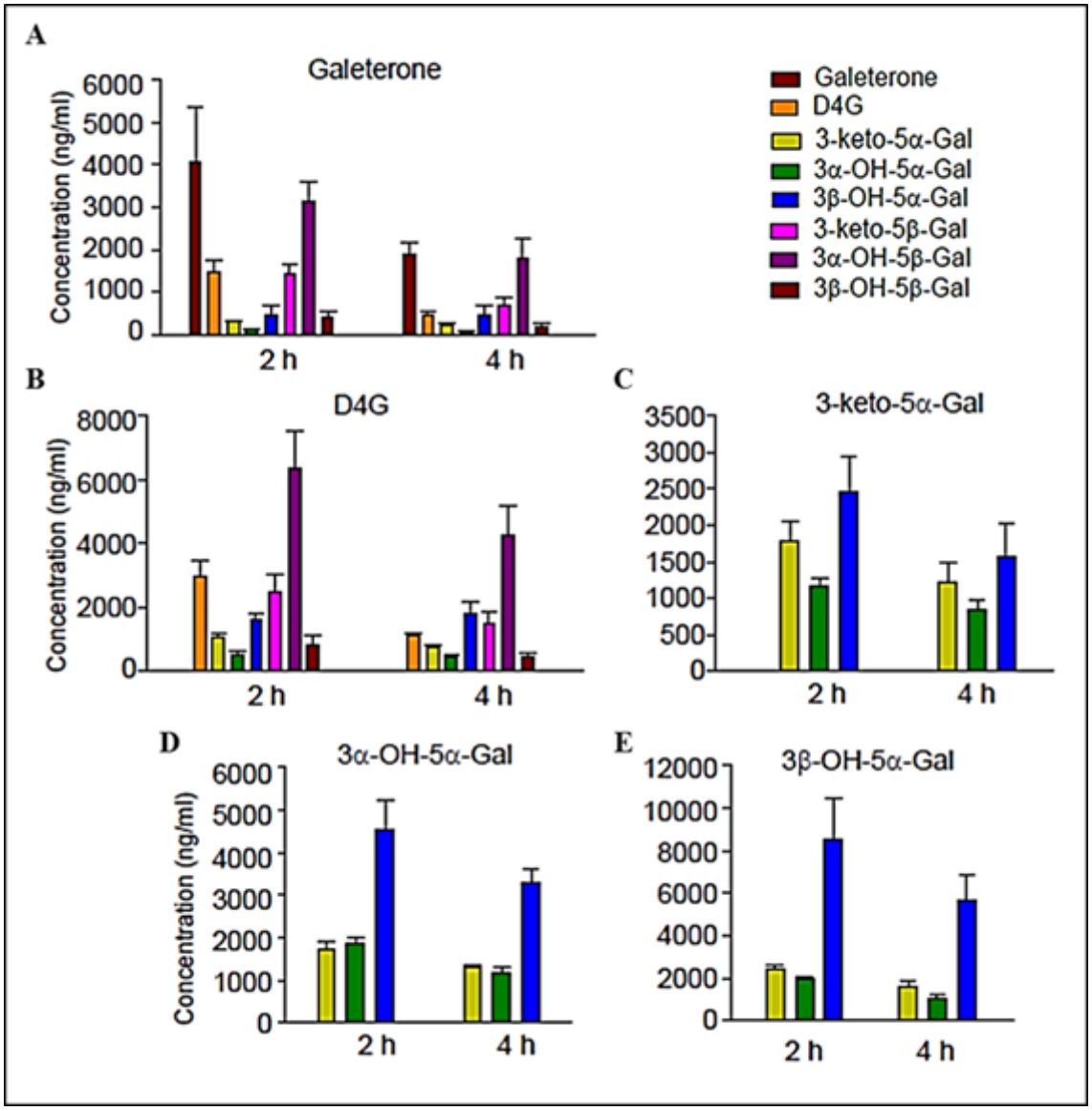

Figure 25. Galeterone metabolism *in vivo*. A, Galeterone; B, D4G; C, 3-keto-5α-Gal; D, 3α-OH-5α-Gal; E, 3β-OH-5α-Gal.

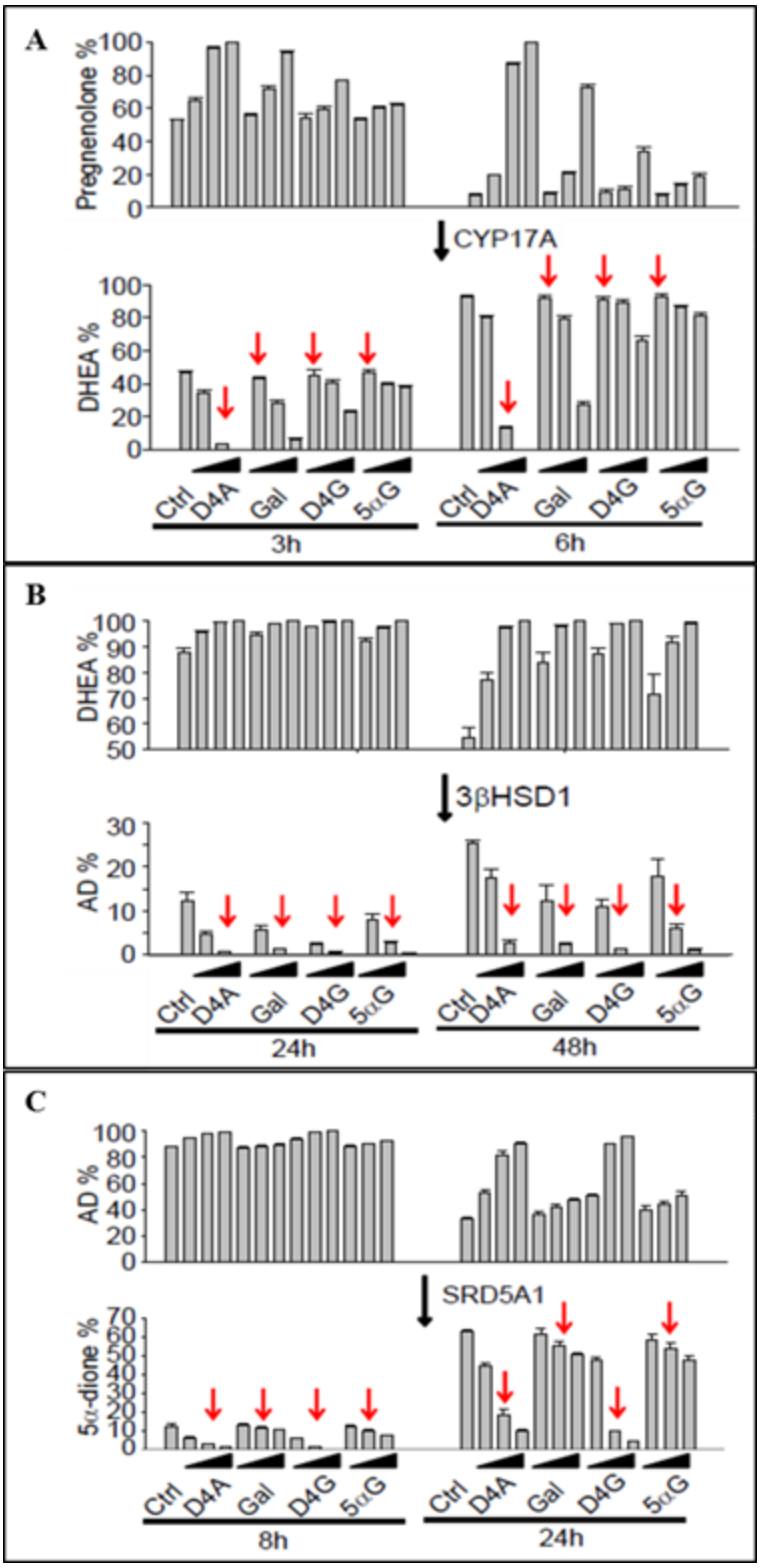

Figure 26. Effect of galeterone metabolites on steroidogenic enzyme activity. A, effect on CYP17A; B, 3βHSD1; and C, SRD5A1

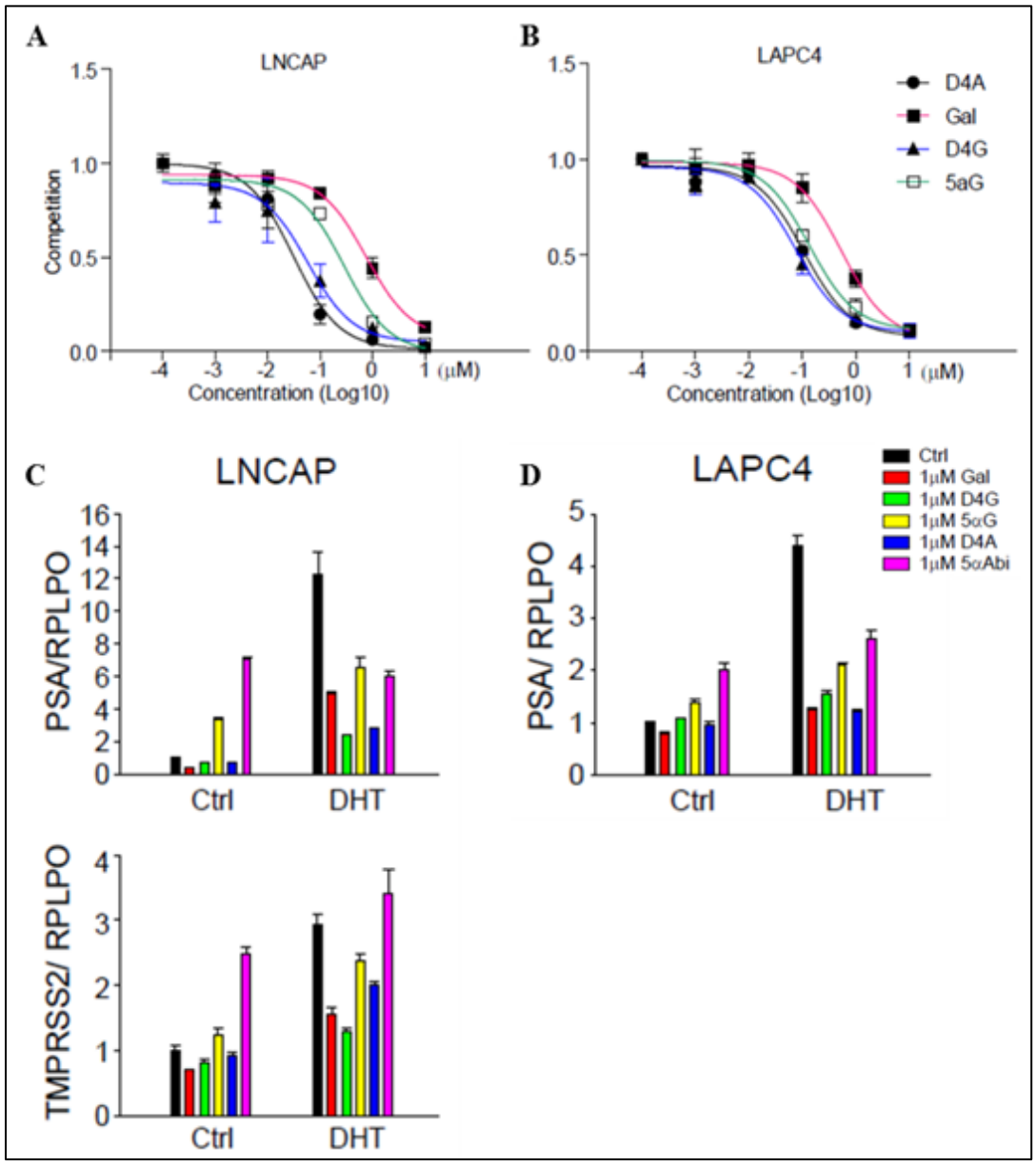

Figure 27. Effect of galeterone metabolites on AR signaling. Affinity of the metabolites to AR in A, LNCAP and B, LAPC4 cells. The effect of the metabolites on AR regulated gene expression in C, LNCAP and D, LAPC4 cells.

5.3.6. Galeterone metabolite effects on tumor progression in a mouse xenograft model

The effect of D4G on tumor growth in a xenograft mouse model was studied because D4G was comparable to or slightly better than galeterone in blocking steroidogenesis and suppressing AR regulated gene expression. VCaP xenografts were grown subcutaneously in orchiectomized mice with DHEA pellet implantation to mimic human adrenal androgen physiology. Time from initiation of treatment with D4G, galeterone, or vehicle to tumor progression (>20% increase in tumor volume) was assessed by generating Kaplan–Meier survival curves, and comparing treatment groups with the log-rank test. Galeterone inhibited xenograft growth (vehicle vs. galeterone, p=0.01). Xenograft progression was also significantly delayed in the D4G group compared with the vehicle group (p=0.02) and was no different when compared to the galeterone group (D4G vs galeterone, p=0.98) (**Fig. 28**). LC-MS analysis for galeterone and its metabolites in serum and tumors collected at the study end confirmed that conversion to downstream galeterone steroidal metabolites is detectable in both xenografts and serum (**Fig. 29A&B**).

Due to 3-keto-5α-Gal ability to stimulate AR regulated gene expression, the effect of 3-keto-5α-Gal activity on xenograft tumor progression was studied in orchiectomized mice injected subcutaneously with VCaP xenografts. The mice were assigned to vehicle, 3-keto-5α-Gal, or 5α-Abi. Time from initiation of treatment to tumor progression (>30% increase in tumor volume) was assessed by generating Kaplan–Meier survival curves and comparing treatment groups with the log-rank test (**Fig 30**). Tumors from vehicle-treated mice did not differ from those receiving 3-keto-5α-Gal (P=0.125), nor did tumors from mice receiving 3-keto-5α-Gal treatment differ from those receiving 5α-Abi (P=0.20).

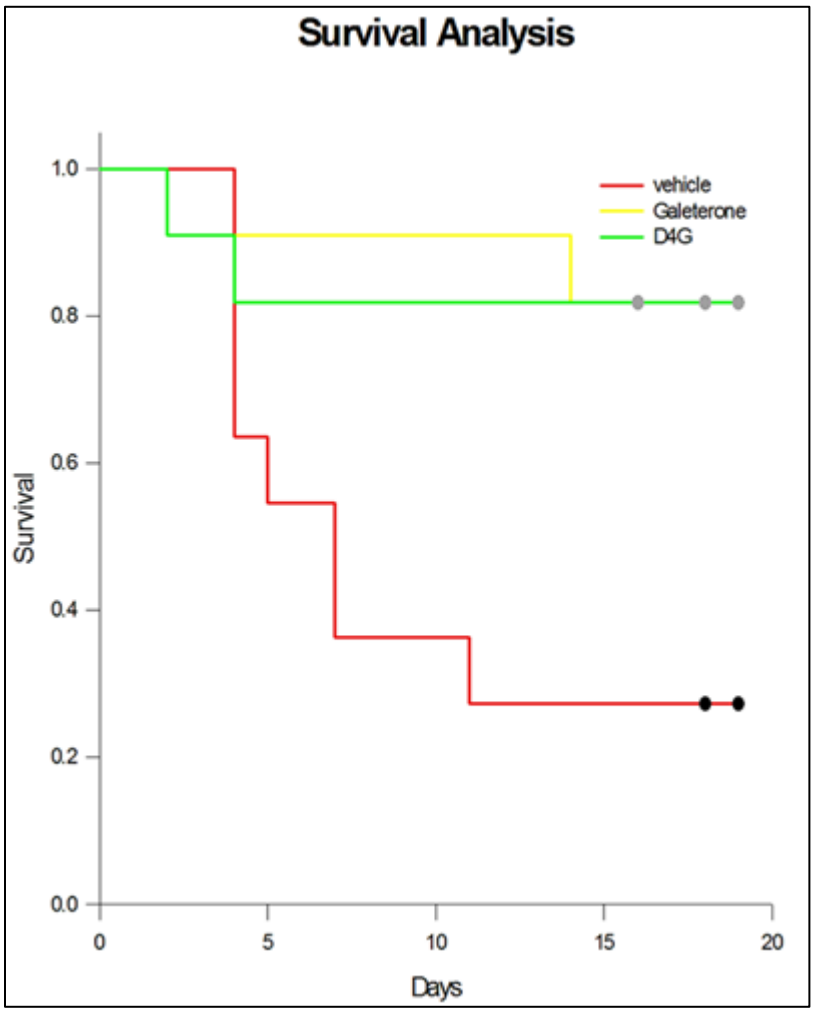

Figure 28. Survival curve of mice treated with galeterone or D4G. Galeterone and D4G will delay the growth of mouse xenograft compared to vehicle.

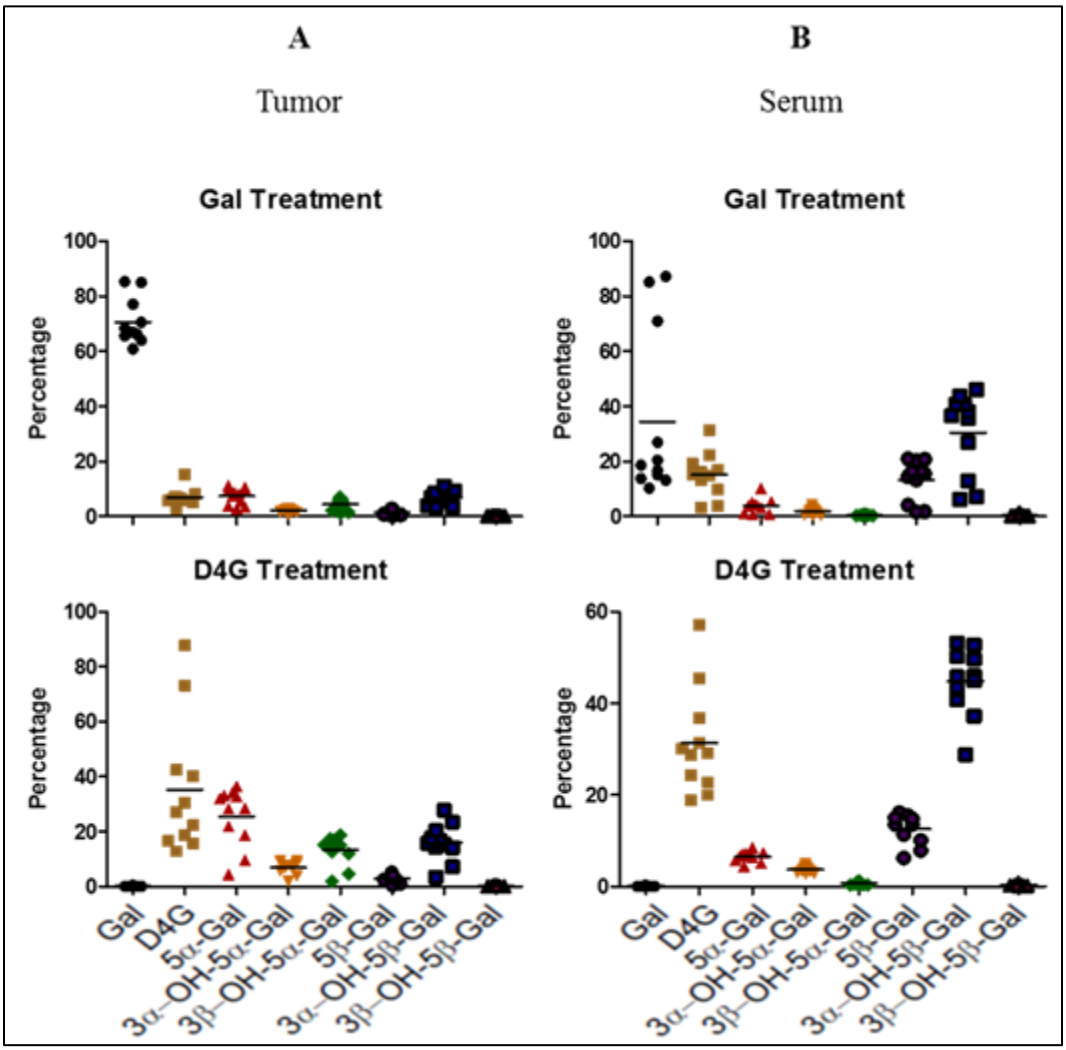

Figure 29. Metabolite percentages in tumor and serum. The results were obtained from LC-MS analysis for A, tumor samples and B, serum samples.

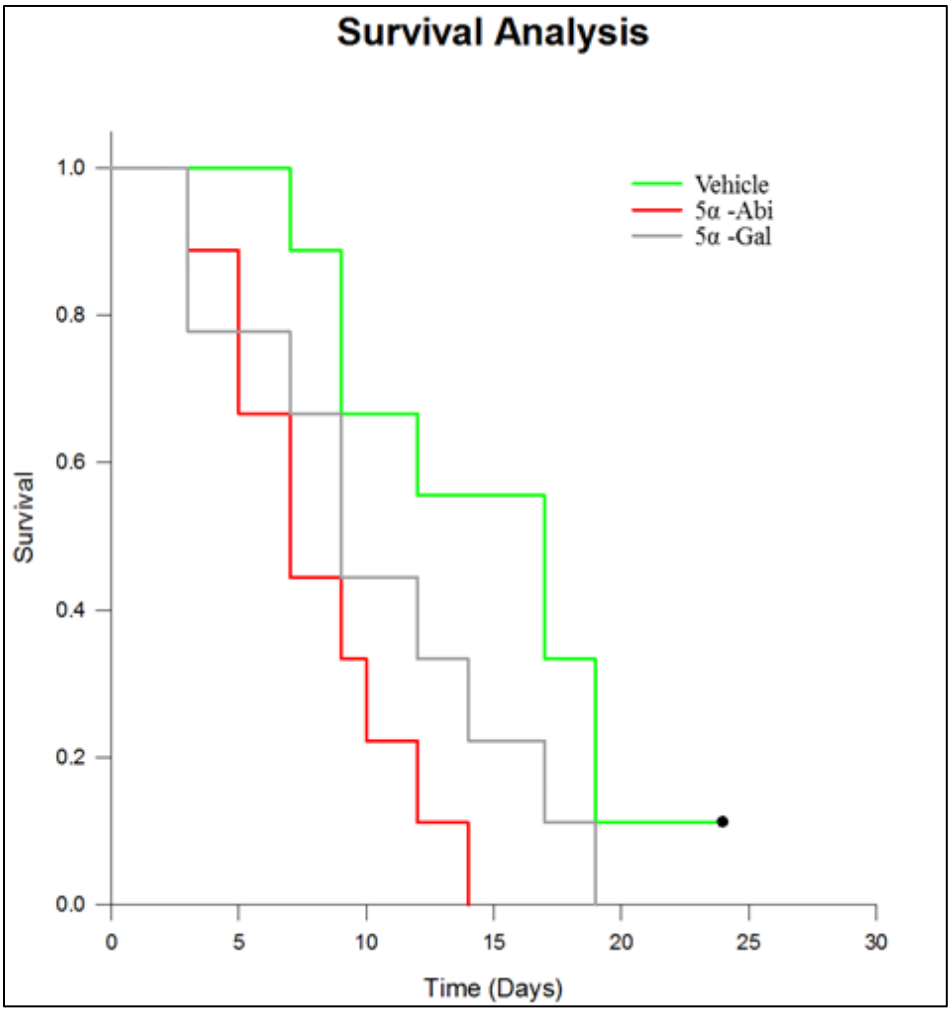

Figure 30. Effect of 5α-galeterone on tumor growth. 5α-Abi and 5α-Gal promote tumor progression in mouse xenograft.

5.4. Conclusions

Galeterone undergoes steroidogenic metabolism to generate D4G, 3-keto-5α-Gal, 3-keto-5β-Gal and 4 other steroidal metabolites. This pathway was confirmed both *in vitro* and *in vivo*. Galeterone metabolites had opposing effects on prostate tumors in the xenograft models. Whereas D4G inhibits steroidogenic enzymes, AR-regulated gene expression, and tumor progression, its conversion resulted in loss of activity and generation of 3-keto-5α-Gal, which promoted AR target gene expression and enhanced tumor growth. Galeterone follows the same steroidogenic metabolism as abiraterone, which suggests a novel pathway for metabolism of steroidal 3β-OH Δ^5 analogues, which should be considered in future drug design.

5.5. References

1 Ryan, C. J. *et al.* Abiraterone in Metastatic Prostate Cancer without Previous Chemotherapy. *The New England journal of medicine*, doi:10.1056/NEJMoa1209096 (2012).

2 de Bono, J. S. *et al.* Abiraterone and increased survival in metastatic prostate cancer. *The New England journal of medicine* **364**, 1995-2005, doi:10.1056/NEJMoa1014618 (2011).

3 Scher, H. I. *et al.* Increased survival with enzalutamide in prostate cancer after chemotherapy. *The New England journal of medicine* **367**, 1187-1197, doi:10.1056/NEJMoa1207506 (2012).

4 Beer, T. M. *et al.* Enzalutamide in metastatic prostate cancer before chemotherapy. *The New England journal of medicine* **371**, 424-433, doi:10.1056/NEJMoa1405095 (2014).

5 Carreira, S. *et al.* Tumor clone dynamics in lethal prostate cancer. *Science translational medicine* **6**, 254ra125, doi:10.1126/scitranslmed.3009448 (2014).

6 Attard, G. *et al.* Clinical and biochemical consequences of CYP17A1 inhibition with abiraterone given with and without exogenous glucocorticoids in castrate men with advanced prostate cancer. *The Journal of clinical endocrinology and metabolism* **97**, 507-516, doi:10.1210/jc.2011-2189 (2012).

7 Njar, V. C. & Brodie, A. M. Discovery and development of Galeterone (TOK-001 or VN/124-1) for the treatment of all stages of prostate cancer. *J Med Chem* **58**, 2077-2087, doi:10.1021/jm501239f (2015).

8 Purushottamachar, P. *et al.* Systematic structure modifications of multitarget prostate cancer drug candidate galeterone to produce novel androgen receptor down-regulating agents as an approach to treatment of advanced prostate cancer. *Journal of medicinal chemistry* **56**, 4880-4898, doi:10.1021/jm400048v (2013).

9 Kwegyir-Afful, A. K., Ramalingam, S., Purushottamachar, P., Ramamurthy, V. P. & Njar, V. C. Galeterone and VNPT55 induce proteasomal degradation of AR/AR-V7, induce significant apoptosis via cytochrome c release and suppress growth of castration resistant prostate cancer xenografts in vivo. *Oncotarget* **6**, 27440-27460, doi:10.18632/oncotarget.4578 (2015).

10 Yu, Z. *et al.* Galeterone prevents androgen receptor binding to chromatin and enhances degradation of mutant androgen receptor. *Clinical cancer research : an official journal of the American Association for Cancer Research* **20**, 4075-4085, doi:10.1158/1078-0432.ccr-14-0292 (2014).

11 Montgomery, B. *et al.* Androgen Receptor Modulation Optimized for Response (ARMOR) Phase I and II Studies: Galeterone for the Treatment of Castration-Resistant Prostate Cancer. *Clinical cancer research : an official journal of the American Association for Cancer Research* **22**, 1356-1363, doi:10.1158/1078-0432.CCR-15-1432 (2016).

12 Li, Z. *et al.* Conversion of abiraterone to D4A drives anti-tumour activity in prostate cancer. *Nature* **523**, 347-351, doi:10.1038/nature14406 (2015).

13 Li, Z. *et al.* Redirecting abiraterone metabolism to fine-tune prostate cancer anti-androgen therapy. *Nature* **533**, 547-551, doi:10.1038/nature17954 (2016).

14 Papari-Zareei, M., Brandmaier, A. & Auchus, R. J. Arginine 276 controls the directional preference of AKR1C9 (rat liver 3alpha-hydroxysteroid dehydrogenase) in human embryonic kidney 293 cells. *Endocrinology* **147**, 1591-1597, doi:10.1210/en.2005-1141 (2006).

15 Chang, K. H. *et al.* A gain-of-function mutation in DHT synthesis in castration-resistant prostate cancer. *Cell* **154**, 1074-1084, doi:10.1016/j.cell.2013.07.029 (2013).

16 Alyamani, M. *et al.* Development and validation of a novel LC-MS/MS method for simultaneous determination of abiraterone and its seven steroidal metabolites in human serum: Innovation in separation of diastereoisomers without use of a chiral column. *The Journal of steroid biochemistry and molecular biology*, doi:10.1016/j.jsbmb.2016.04.002 (2016).

17 Bruchovsky, N. & Wilson, J. D. The conversion of testosterone to 5-alpha-androstan-17-beta-ol-3-one by rat prostate *in vivo* and in vitro. *The Journal of biological chemistry* **243**, 2012-2021 (1968).

18 Mostaghel, E. A. *et al.* Variability in the androgen response of prostate epithelium to 5alpha-reductase inhibition: implications for prostate cancer chemoprevention. *Cancer research* **70**, 1286-1295, doi:0008-5472.CAN-09-2509 [pii]

10.1158/0008-5472.CAN-09-2509 (2010).

19 Yin, L. & Hu, Q. CYP17 inhibitors--abiraterone, C17,20-lyase inhibitors and multi-targeting agents. *Nat Rev Urol* **11**, 32-42, doi:10.1038/nrurol.2013.274 (2014).

CHAPTER VI

PROJECT CONCLUSIONS AND FUTURE DIRECTIONS

CYP17A1 is a clinically validated target for the treatment of CRPC[1-3]. Non-steroidal and steroidal CYP17A1 inhibitors are both undergoing pharmacologic and clinical development; however, the consequences of using steroidal vs. non-steroidal drugs are not well understood. Here, I determined that abiraterone and galaterone, Δ^5, 3β-hydroxyl steroidal drugs, are converted to at least seven steroidal metabolites that are either 3-keto Δ^4, (1 metabolite) 5α-reduced (3 metabolites), or 5β -reduced (3 metabolites) *in vitro* and *in vivo,* and have important downstream consequences on the androgen axis. Therefore, steroidogenic metabolism of drugs with the Δ^5, 3β-hydroxyl structure appears to be a class effect, instead of being a property that is unique to a single drug. The activity of these metabolites is a critical issue with broad consequences for drug development across steroid-dependent diseases.

The development of the LC-MS/MS method that distinguished the metabolites gave a clear picture and understanding of abiraterone and galeterone metabolism. Despite its

novelty in separating all the diasteroisomers, the method did not require any sophisticated techniques and was developed using materials that are available in any analytical lab.

An important property that distinguishes galeterone from abiraterone is that galeterone has been reported to have direct properties as an AR antagonist and degrader, while CYP17A1 is generally thought to be the main direct target of abiraterone. However, conversion of galeterone by 3βHSD and SRD5A to other metabolites that are formed *in vitro* and *in vivo*, with varying biochemical activities, clearly has consequences on steroidogenic enzymes and direct effects on AR. Importantly, D4G and 5αG bind AR more potently than galeterone, although both of these metabolites downstream of 3βHSD have divergent effects on AR. Interestingly, despite the increased affinity for AR and maintaining AR enhanced degradation activity, the activity of D4G in a xenograft model of CRPC was no better than that of galeterone. It is possible that any increased anti-tumor xenograft activity by D4G was reversed because it is one metabolic step closer to 5αG, resulting in higher intratumoral concentrations of the latter. This result raises the possibility that SRD5A inhibition to block 5αG synthesis might be beneficial.

These findings also suggest that the design and use of steroid-based drugs for prostate cancer should consider the relative activities of steroidogenic enzymes in prostate cancer. For example, abiraterone and galeterone are rapidly converted to their steroidal metabolites in cells that have high, but not low, 3βHSD1 activity. A published head-to-head comparison of galeterone vs. abiraterone in LAPC4 xenografts demonstrated galeterone to have superior activity[4]. However, 3βHSD1 activity is low in LAPC4 cells, and therefore this comparison likely was more selectively focused on galeterone and abiraterone. The consequences of downstream galeterone metabolites are more likely to

be seen in cancer models and patients that have the 3βHSD1 N367T missense that accumulates and results in high activity[5].

The presence of steroidal abiraterone metabolites in patients was confirmed by analyzing samples from patients who underwent treatment with abiraterone acetate[6,7]. The metabolite levels can be altered by combining abiraterone acetate with other drugs like SRD5A inhibitors which may maximize the benefits of the treatments. Although increasing the standard dose of abiraterone acetate resulted in increasing D4A levels, it also increased 5α-Abi and therefore maintained the percentage of both the good and the bad metabolites. In prostate tissue, which expressed high SRD5A1activity, the D4A level was lower than the 5α-Abi level. All these results indicate that new strategies are critically needed in treatment options that involve abiraterone acetate.

Galeterone is under study in clinical trials; therefore, this work was limited by patient sample availability; as a result it was not possible to assess the metabolites in clinical samples. However, given the similar metabolic behavior of galeterone and abiraterone in prostate cancer models, *in vivo* and with specific steroidogenic enzymes, it is highly likely that the concentrations of galeterone metabolites are significant and similar to abiraterone metabolites in patients.

In summary, our results provide a more complete picture of abiraterone and galeterone metabolism and activity. These findings demonstrate that metabolism by steroidogenic enzymes is a class effect of Δ^5, 3β-hydroxyl drugs that should be accounted for in preclinical and clinical drug development and distinguishes these agents from non-steroidal inhibitors. The levels of these metabolites and their respective activities are determined by the expression and activity of endogenous steroidogenic enzymes, including

3βHSD and SRD5A. These findings must be considered for the development of better treatment strategies.

6.1. References

1 Alex, A. B., Pal, S. K. & Agarwal, N. CYP17 inhibitors in prostate cancer: latest evidence and clinical potential. *Ther Adv Med Oncol* **8**, 267-275, doi:10.1177/1758834016642370 (2016).

2 Bambury, R. M. & Rathkopf, D. E. Novel and next-generation androgen receptor-directed therapies for prostate cancer: Beyond abiraterone and enzalutamide. *Urol Oncol* **34**, 348-355, doi:10.1016/j.urolonc.2015.05.025 (2016).

3 Yoshimoto, F. K. & Auchus, R. J. The diverse chemistry of cytochrome P450 17A1 (P450c17, CYP17A1). *The Journal of steroid biochemistry and molecular biology* **151**, 52-65, doi:10.1016/j.jsbmb.2014.11.026 (2015).

4 Bruno, R. D. *et al.* Synthesis and biological evaluations of putative metabolically stable analogs of VN/124-1 (TOK-001): head to head anti-tumor efficacy evaluation of VN/124-1 (TOK-001) and abiraterone in LAPC-4 human prostate cancer xenograft model. *Steroids* **76**, 1268-1279, doi:10.1016/j.steroids.2011.06.002 (2011).

5 Hearn, J. W. *et al.* HSD3B1 and resistance to androgen-deprivation therapy in prostate cancer: a retrospective, multicohort study. *The Lancet. Oncology* **17**, 1435-1444, doi:10.1016/S1470-2045(16)30227-3 (2016).

6 Li, Z. *et al.* Conversion of abiraterone to D4A drives anti-tumour activity in prostate cancer. *Nature* **523**, 347-351, doi:10.1038/nature14406 (2015).

7 Li, Z. *et al.* Redirecting abiraterone metabolism to fine-tune prostate cancer anti-androgen therapy. *Nature* **533**, 547-551, doi:10.1038/nature17954 (2016).